



**UNIVERSITA' DEGLI STUDI DI NAPOLI  
"FEDERICO II"**

**FACOLTA' DI INGEGNERIA**

DIPARTIMENTO DI INGEGNERIA DEI MATERIALI E DELLA PRODUZIONE

---

**DOTTORATO IN INGEGNERIA DEI MATERIALI E DELLE  
STRUTTURE XXII CICLO**

**MULTISCALE DESIGN AND MANUFACTURING OF  
ADVANCED COMPOSITES INTEGRATING  
DAMPING FEATURES**

**Ph.D. Dissertation  
by  
Alfonso Martone**

TUTOR: DR. MICHELE GIORDANO  
COORDINATORE: CH.MO PROF. DOMENICO ACIERNO

December 2009



# Acknowledgements

This dissertation would not have been possible without the help and support of a great number of people.

The personality to whom I am most obliged, perhaps, is Michele Giordano, who has been, apart from my Tutor, the definitive source of support throughout my years of PhD studies. His compliance and willingness to develop the understanding of the topic in my study is greatly appreciated.

The activities were performed in the framework of the project “ARCA” granted to IMAST Scarl by Italian Ministry M.I.U.R. I would like to be grateful to each of the partner of this research program, in particular Alenia Aeronautica for the damping test on material.

Above all I would like to thanks Prof. Domenico Acierno, his support and interest was essential to let me conclude my PhD study.

I am grateful to prof. Lecce for the opportunity that I had.

I would also like to thank Dr. Cantoni and Ing. Paonessa for their input and suggestions throughout this project.

I am grateful for the financial support and interaction with CNR-IMCB researcher, particularly Dr. Mauro Zarrelli, his continuous encouragement, his enthusiasm in spur Vesuvius, and the many conversations, as enlightening as always.

I am grateful for the contribution of Massimo and Pasquale, which wisdom have fed my desire for knowledge.

The last but not the least I would thank to the members of Giordano research group for their patience and resignation to my humour, when I enter the lab and meet Gabriella, Antonietta, Angelo, Daniele, Mauro, and all the other members I feel at home.

I would also thank to my parents Patrizio e Virginia for their unconditional support as I pursued this goal.



# TABLE OF CONTENTS

## MULTISCALE DESIGN AND MANUFACTURING OF ADVANCED COMPOSITES INTEGRATING DAMPING FEATURES

<b>ACKNOWLEDGEMENTS</b>	3
<b>LIST OF FIGURES</b>	8
<b>LIST OF TABLES</b>	12
<b>DISSERTATION ABSTRACT</b>	13
<b>CHAPTER I</b>	
<b>MULTI-SCALE DESIGN OF COMPOSITE STRUCTURES</b>	16
1.1 Introduction	16
1.2 Multi-disciplinary design of composite structure	18
1.3 Multi-scale design of a composite fuselage	21
1.4 Research outline	24
1.5 References	28
<b>CHAPTER II</b>	
<b>ENERGY METHODS FOR DAMPING EVALUATION</b>	30
2.1 Summary	30
2.2 Loss factor of composite materials	31
2.2.1 Loss factor prediction by the strain energy method	32
2.3 Layered composites analysis	33
2.3.1 Micro scale-Unified approach for unidirectional fiber reinforced composites <sup>[6]</sup>	33
2.3.2 Macro scale - Damping of angled plies composites	37
2.4 Nano scale – Damping of nanocomposites	44
2.5 References	47
<b>CHAPTER III</b>	
<b>MEASURING COMPOSITE DAMPING</b>	48
3.1 Summary	48
3.2 Damping mechanisms	49
3.2.1 Viscoelastic materials	50
3.3 Measuring damping of materials	55
3.3.1 Vibration damping	55
3.3.2 Dynamical mechanical analysis	59
3.4 References	64
<b>CHAPTER IV</b>	
<b>HYBRID COMPOSITES EMBEDDING DAMPING FEATURES</b>	65
4.1 Summary	65
4.2 Enhancement of damping in polymer composites	66
4.3 Macro scale: Interleaved visco-elastic layer	68
4.3.1 Experimental proof of concept	68

4.3.2	Macro-mechanics for hybrid laminates	72
4.4	Micro scale: hybrid layers	74
4.4.1	Visco-elastic modelling for hybrid fiber layers	76
4.5	Increment of dissipation energy by nano-fillers	78
4.6	References	80

## **CHAPTER V**

<b>MULTI-SCALE MODELLING OF HYBRID COMPOSITES</b>	82	
5.1	Summary	82
5.2	Nano scale: hybrid matrices integrating carbon nanotubes	83
5.2.1	Transversely isotropic lamina	86
5.3	Micro scale: Hybrid dry preform	86
5.3.1	Viscoelastic definition set for hybrid dry preform composites	88
5.4	Macro scale: Damping of hybrid laminates	91
5.4.1	Damping of angle-ply laminates	91
5.5	Multi-scale analysis of hybrid laminates	95
5.6	The HYLAN.m code	98
5.7	References	102

## **CHAPTER VI**

<b>MANUFACTURING AND TESTING OF HYBRID COMPOSITES</b>	103	
6.1	Summary	103
6.2	Manufacturing of hybrid multi-scale laminates	104
6.2.1	The VARTM process	106
6.2.2	Materials	107
6.3	Set-up hybrid dry preform technology	111
6.3.1	Textile geometry	111
6.3.2	Manufacturing hybrid dry preform	113
6.4	Hybrid nano-loaded epoxy system	115
6.4.1	Dispersion of nanotubes	115
6.4.2	Characterization of hybrid nano-scale hosting matrix	117
6.5	Coupons for testing	120
6.5.1	Hybrid matrix- RTM6 + MWCNT Unidirectional laminates	120
6.5.2	Unidirectional laminates integrating hybrid dry preform	123
6.5.3	Hybrid laminates- Angle ply laminates embedding viscoelastic sheets	128
6.6	Conclusions and Discussions	132
6.6.1	Macro-scale analysis of hybrid composites.	132
6.6.2	Micro-scale analysis of hybrid composites.	133
6.6.3	Nano-scale analysis of hybrid composites	134
6.7	References	137

## **CHAPTER VII**

<b>HYBRID COMPOSITE STIFFENED PLATE</b>	138	
7.1	Summary	138
7.2	Manufacturing and testing of multi-scale plane plate	139
7.2.1	Material architecture	139
7.2.2	Mechanical testing	143
7.3	Design and Manufacturing of Stiffened plate	145

7.3.1	Large scale component specification	145
7.3.2	Manufacturing	147
7.4	Conclusions	151
7.5	References	153

## **CHAPTER VIII**

<b>CONCLUSIONS</b>		154
8.1	Final discussion	154
8.2	Contributions	155
8.3	Future Work	157
8.4	Academic publications	158

# LIST OF FIGURES

Figure 1- 1: Airlines continue to adapt to the realities of the market. From The Boeing Company.	16
Figure 1- 2: Aircraft market projections. From The Boeing Company.	17
Figure 1- 3: Design requirements for fuselage structures. From Van Tooren [1].	18
Figure 1- 4: Typical aeronautical fuselage barrel and a stiffened plate.	19
Figure 1- 5: Multiscale analysis of a composite fuselage barrel. From ARCA [3]	21
Figure 1- 6: Through the scale analysis of a composite structure.	24
Figure 1- 7: Multi-level analysis of composite structures.	26
Figure 2- 1: Compliance matrix elements dependences. From [3]	33
Figure 2- 2: Unidirectional composite material	34
Figure 2- 3: Plate deformation according to Kirchoff-Love assumptions	39
Figure 2- 4: Thickness and boundary affecting solution	40
Figure 3- 1: Temperature effects on complex modulus and loss factor material properties.	52
Figure 3- 2: Frequency effects on complex modulus and loss factor material properties.	54
Figure 3- 3: Damping test set-up.	56
Figure 3- 4: Typical frequency response of a vibrating cantilever beam.	56
Figure 3- 5: System with one degree of freedom. From Beranek, Noise and Vibration Control [1].	57
Figure 3- 6: Time variation of displacement of mass-spring-dashpot system released by initial position $X_0$ .	58
Figure 3- 7: Stress-strain phase shift for a sinusoidally excited material.	59
Figure 3- 8: Three point bending testing set-up	60
Figure 3- 9: Typical master curve for a viscoelastic material	61
Figure 4- 1- A) Contribution of interlaminar damping as function of fibres orientation. B) Variation of total loss factor with fibres orientation under uniaxial extension. From Hwang and Gibson [2]	67
Figure 4- 2: Hybrid laminate, Interleaved viscoelastic layer architecture	68
Figure 4- 3: Dynamic visco-elastic properties of thermoplastic elastomers considered as interleaf films, measured at the frequency of 10 Hz. From Kishi et al. [4]	69
Figure 4- 4: Damping properties of thermoplastic polyurethane interleaved laminates and non interleaved laminate, depending on the lay-up sequences. From Kishi et al. [4]	69
Figure 4- 5: Two different laminates with interleaved visco elastic layers. a) a layer interleaved in the mid-plane and b) two layers interleaved away from the mid-plane	70
Figure 4- 6: Experimental results in the case of glass fiber composites with a single viscoelastic layer of thickness of 200 $\mu\text{m}$ interleaved in the middle plane and for three lengths of the test specimens. a) laminate damping as function of the fiber orientation and b) laminate damping as function of the modal frequency. From Berthelot and Sefrani [10].	71
Figure 4- 7: Experimental laminate damping as function of the fiber orientation for three lengths of the test specimens. a) laminate with a single viscoelastic layer of thickness 400 $\mu\text{m}$ interleaved at middle plane, b) laminate with two viscoelastic layers of 200 $\mu\text{m}$ interleaved away from the middle plane. From Berthelot and Sefrani [10].	71
Figure 4- 8: Damping ratio vs normalised bending stiffness, from [10]	74



Figure 4- 9: Allocation of dissipation components vs fiber orientation in a composite beam [11].	75
Figure 4- 10: Proposed hybrid lamina architecture	75
Figure 4- 11: Two ideal hybrid models: a) regular triangle model b) regular quadrilateral model.	77
Figure 4- 12: Stick-slip mechanism.	78
Figure 4- 13: percent increment of passive damping changing dimension. From Rajora [20].	79
Figure 4- 14: Effect of filler content in damping ratio. From Rajora [20].	79
Figure 5- 1: Effective reinforcement modulus vs filler aspect ratio	84
Figure 5- 2: Longitudinal loss factor vs filler aspect ratio	85
Figure 5- 3: Transverse loss factor vs filler aspect ratio	85
Figure 5- 4: Schematic of composite hierarchy for computation of viscoelastic properties of hybrid composites	86
Figure 5- 5: Schematic of composite hierarchy for computation of viscoelastic properties of hybrid dry preform composites	87
Figure 5- 6: Different diameter fibres arrangement	87
Figure 5- 7: Hybrid composite elastic domain	89
Figure 5- 8: Hybrid composite dissipative domain	90
Figure 5- 9: The matlab tool developed was integrate in the multi-objective platform, modeFRONTIER.	92
Figure 5- 10: Beam subjected to three point bending load scheme	92
Figure 5- 11: Static stress distribution within the laminate thickness at the section $x=L/4$ . A)Longitudinal normal stress, B)Transverse shear stress.	93
Figure 5- 12: Laminate loss factor in function of the distance between supports	94
Figure 5- 13: Schematic representation for the integrated analysis of hybrid laminates	95
Figure 6- 1: Hybrid laminate hierarchy	104
Figure 6- 2: Process flow for Resin Transfer Molding	105
Figure 6- 3: Typical VARTM process set-up	106
Figure 6- 4: Dynamic viscosity profiles at three different heating rate 1-2.5-10°C/min	107
Figure 6- 5: Dynamical mechanical analysis of the Hexcel RTM6	108
Figure 6- 6: Nomograph Nisshimbo Mobilon® Film	108
Figure 6- 7: Thermoplastic Polyurethane Thermogravimetric analysis. Lycra® does not release flier substances at temperature of curing cycle for the epoxy system used.	109
Figure 6- 8: Dynamical mechanical analysis of the MOBILON®	110
Figure 6- 9: Dynamical mechanical analysis of the Lycra®	110
Figure 6- 10: Pristine dry perform datasheet	112
Figure 6- 11: Suitable preform micro-architectures. a) viscoelastic fibres are arranged alongside of carbon yarn. b) viscoelastic fibres are arranged to form an independent yarn in the preform.	113
Figure 6- 12: Phases of reeling in process for Lycra® fibres in roll compatibles with the weaving creel	113
Figure 6- 13: Arrangement of yarns on the weaving creel.	114
Figure 6- 14: Weaving phases. a) the carbon hybrid yarns input in the loom. b) weft yarn positioning.	114
Figure 6- 15: The final hybrid preform is automatically reel in cardboard cylinder by the loom.	115
Figure 6- 16: Bending modulus of nanocomposites processed by sonication at three different temperatures with a MWCNT content of 0.1 % wt	116

Figure 6- 17: Electrical conductivity measurement. Data are plotted against the ratio of actual filler content and the statistical critical value.	118
Figure 6- 18: Effect of the aspect ratio in the increment of bending modulus. At higher nanotubi content in each case a decrement in the effect of introducing nanotubes in the matrix is present.	119
Figure 6- 19: Effect of the aspect ratio in the increment of $\tan\delta$ . The filler with aspect ratio 50 granted a stepwise increment in $\tan\delta$ .	119
Figure 6- 20: Viscosity measurements for the nano-loaded matrix at different nanotubes content. Hybrid system consists of the RTM6 epoxy resin mixed with MWNT having aspect ratio of 55.	121
Figure 6- 21: Optical microscopy for the hybrid 1%wt nano-composite. Image is magnified at 50X.	121
Figure 6- 22: Manufacturing of hybrid unidirectional multiscale composite.	122
Figure 6- 23: Damping test for the unidirectional composite used as baseline.	122
Figure 6- 24: Damping test for the unidirectional composite containing 1% wt of CNTs.	123
Figure 6- 25: Composite manufacturing via vacuum infusion process. The relevant phases of the process are: the stacking upon the tool a), vacuum bag preparation b), resin infusion c), cure of the system, d) demoulding of composite plate.	124
Figure 6- 26: Micrograph of hybrid laminate including 5 % vol. of viscoelastic fibres, picture is magnified at 20X. The thermoplastic elastomeric fibres are visible contiguous to carbon tow according to the textile architecture defined.	125
Figure 6- 27: Hybrid dry preform containing 10 % vol. of viscoelastic fibres exhibits important manufacturing problems. a) shrinkage due to the contact with the heat tool b) composite plate after demoulding,	125
Figure 6- 28: DMA analysis of TCU260+RTM6 composites, unidirectional 0° samples	126
Figure 6- 29: DMA analysis of TCU260+RTM6 composites, unidirectional 90° samples	126
Figure 6- 30: DMA analysis of Hybrid 5%+RTM6 composites, Unidirectional 0° samples.	127
Figure 6- 31: DMA analysis of Hybrid 5% +RTM6 composites, Unidirectional 90° samples.	127
Figure 6- 32: DMA analysis of Hybrid 10%+RTM6 composites, unidirectional 0° samples	128
Figure 6- 33: DMA analysis of Hybrid 10%+RTM6 composites, unidirectional 0° samples	128
Figure 6- 34: Manufacturing of hybrid interleaved layer architecture composites. Baseline plate and laminate with the viscoelastic layer at the middle C0 have been fabricated together a), e). The hybrid laminates with viscoelastic layer moved away from middle plane have fabricated below a common vacuum bag.	129
Figure 6- 35: DMA test for the reference angle ply laminate	130
Figure 6- 36: DMA test for the interleaved layer configuration	130
Figure 6- 37: DMA test for the C1 configuration	131
Figure 6- 38: DMA test for the C2 configurations	131
Figure 6- 39: Comparison of mechanical data for interleaved layer architectures	132
Figure 6- 40: Comparison of dissipative data for interleaved layer architectures	133
Figure 6- 41: Comparison of the mechanical and the dynamic properties of the hybrid unidirectional composites. The data have been extrapolated from previous tests at the temperature of -30 °C in fiber direction.	134
Figure 6- 42: Comparison of the mechanical and the dynamic properties of the hybrid unidirectional composites. The data have been extrapolated from previous tests at the temperature of -30 °C orthogonal to fiber direction.	134

Figure 6- 43: Effective reinforcement modulus, $E_{\eta}$ , as a function of normalised volume content of nanotubes for the different aspect ratios fillers.	135
Figure 6- 44: Damping test for unidirectional hybrid multi scale unidirectional composite.	136
Figure 7- 1: Complex viscosity measurement for the 1% CNTs+ RTM6 system. The isothermal measure at the infusion temperature of 90°C shows the increment of the system viscosity	140
Figure 7- 2: Vacuum bag preparation. a) the reinforcement preform is stacked upon the tool, b) pelply application, c) vacuum bag application, d) the plate after the curing process	141
Figure 7- 3: Specimens for mechanical testing	142
Figure 7- 4: Ultrasonic analysis of coupons before testing. a) scanning on the fiber reinforced plate manufactured as baseline in testing, b) scanning on the multiscale fiber reinforced plate	142
Figure 7- 5: Mechanical test set-up. a) Short beam test fixture (SBS), b) Un-notched tensile fixture (UNT), c) Uniaxial compression fixture (CLC), d) Four point bending fixture (FPB).	143
Figure 7- 6: Mechanical test results. Loading the matrix by carbon nanotubes does not modify sensibly the mechanical properties of the laminate, only tensile and interlaminar strength decreases.	144
Figure 7- 7: Composite stiffened plate specifications	146
Figure 7- 8: Tool parts assembly	148
Figure 7- 9: Tool control system. a) A series of electrical resistances control the temperature, b) Thermocouples “J” monitor the tool temperature during the infusion process.	148
Figure 7- 10: Manufacturing of the hybrid stiffened plate. a) stacking of the preform upon the tool, b) vacuum bag, c) resin progression within bag, d) final composite.	149
Figure 7- 11: Stringers manufacturing. a) Stacking of the preform, b) Vacuum bag	149
Figure 7- 12: Final stiffened composite plate- baseline plate	150
Figure 7- 13: Final multiscale composite plate	150
Figure 7- 14: Multilevel composite structure	152

# LIST OF TABLES

Table 5- 1: Properties of the three different phases constituent the hybrid laminate	88
Table 5- 2: Mechanical and dissipative properties of PEKK-IM7 unidirectional prepreg at -20°C	92
Table 5- 3: Predicted laminate properties	93
Table 5- 4: Comparison for architecture	96
Table 6- 1: Optical microscopy of final nano-composites (Nanocyl N7000) with different CNT content: 0.05 %wt (a); 0.1 %wt (b); 0.2 %wt (c); 0.3 %wt (d); 0.5 %wt (e) MWCNT content.	117
Table 6- 2: Interleaved layer fabricated panels	129
Table 6- 3: Multi-scale composite properties for 1%wt plate	135
Table 7- 1: Properties of CNTs used	139
Table 7- 2: Manufactured hybrid plates	141

## DISSERTATION ABSTRACT

# **MULTISCALE DESIGN AND MANUFACTURING OF ADVANCED COMPOSITES INTEGRATING DAMPING FEATURES**

Alfonso Martone

Doctor of Philosophy, December 2009

Multi-functionality is a current issue in materials design, in particular, the fast growing application of advanced composites in commercial aeronautic is raising the need to design primary structures with composite material that perform multiple functions: i.e. able to fulfil not only mechanical allowable but also functional requirement such as vibroacoustic and fire reaction.

The development of multifunctional design tools integrating structural and damping features enables a next step toward the exploitation of the composite materials benefits. It is worth noting that the structural damping in the case of a composite fuselage is a multiscale problem. The fuselage vibroacoustic requirement is determined by the behaviour of stringers reinforced skin, that is determined by the panel damping behaviour which owns its damping features to its laminate architecture and constituents materials.

The requirement chain for a composite structure is formulated by a top-down approach determined by the behaviour of sub-structures which compose the final structural component. Aim of this work is to individuate and implement a design procedure able to describe a composite structure starting from its constituents, moreover for each dimensional scales the behaviour have to be modelled. The through dimensional scales model proposed for describing composite materials use the formulation of constitutive equation for describe the material behaviour at each sub-component. From the homogenization of fibres and hosting matrix it is possible to formulate a micro-scale constitutive matrix describing mechanical and dissipative lamina behaviour, with analogous approach the laminate behaviour is described by the homogenization of the constituents layers.

The potential of describe mechanical and dissipative feature for a laminate starting from its elementary constituents gives the chance of imagine hybrid architecture able to improve a desired feature. Keeping in mind the passive damping feature, three possible hybrid architecture have been proposed for suit the requirement of increment material performance, moreover the composite have to maintain its mechanical properties above a defined level to preserve structural safety. The insertion of a viscoelastic layer within the laminate has been individuuated as promising architecture for increase damping performance although this configuration is susceptible to interlaminar stress and prone to de-bonding. From theoretically study on the energy allocation within the laminate is formulated the novel idea of an hybrid laminate where the viscoelastic material is embedded as long fiber in the reinforcement preform, this architecture contribute to increment the damping properties withstand the mechanical properties but enhancement level is less than an interleaved containing the same volume of added material. Rather than modifying the fiber arrangement the lamina passive damping could be increased by means of introducing high damping nano-fillers within the hosting matrix. For the prediction of the overall laminate properties an hierarchical procedure has proposed accounting the hybridization at each laminate level. Considering elementary structures, such as a beam, subjected to boundary condition which induce that energy is allocated in only one component, the damping predicted is the overall damping capacity for the considered energy component.

A valuable technology for manufacturing composite materials have to be flexible in changing constituents properties as well as the insertion of a softer material as lamina or the use of hybrid layer stacking the fibres or the use of a pre-hybridised hosting matrix. Process technologies allowing the listed item are based on the liquid moulding, in particular the VARTM process is selected as this process could be easily extended on large scale fabrication.

Unidirectional composites of the proposed lamina architecture were manufactured and tested. In each case a valuable increment in passive damping were measured. Both the interleaved layer and the hybrid preform lead to a loss in mechanical performances, whilst the hybrid laminates manufactured by the nanofilled hosting matrix kept the its mechanical features leading to an enhancement of loss factor until 40% at temperatures suitable for aeronautical applications.

The most promising architecture selected from experimental study was the *multiscale* laminate, as they are reinforced by microscale long fibres and nanoscale nanotubes. As proof of the industrial feasibility of this solution a simple typical aeronautical component has manufactured. A stiffened composite plate is designed and manufactured for further acoustical testing. In addition the angle ply laminate has fabricated and mechanical tested.

*Keywords:* Hybrid composites, Multiscale modelling, Damping , Viscoelastic, Carbon nanotubes.

# 1

## Multi-scale design of composite structures

### 1.1 Introduction

In recent years, the global slump required the reorganization of the main airline company in terms of better resource management, i.e. air routes have been re-arranged, and the global efficiency of aeronautical system has been improving through the adaptation of the airport and aircraft efficiency as well as maintenance cost and fuel consumption or fatigue life. A key parameter for the aerospace industry is to anticipate customers exigencies, in fact, as The Boeing Company reports, although the uneven economic recovery, in the next two decades the projections indicate the need of about thirty thousand new aircrafts above all in the range of single aisle commercial liner, where market will absorb twenty thousand vehicles.



COPYRIGHT © 2009 THE BOEING COMPANY

Figure 1- 1: Airlines continue to adapt to the realities of the market. From The Boeing Company.



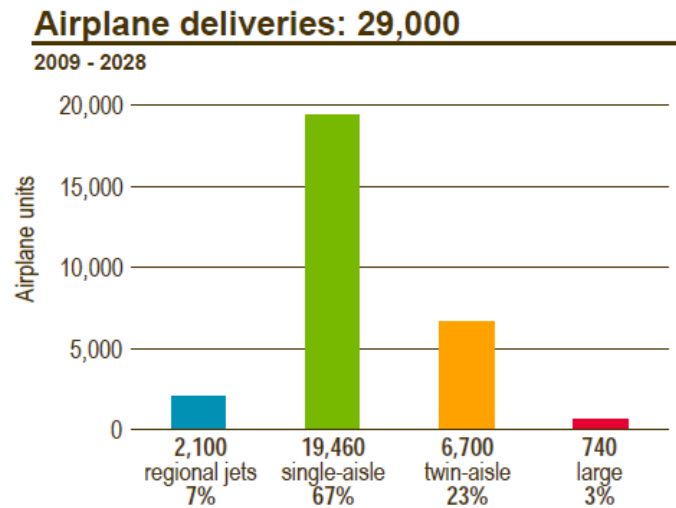


**Figure 1- 2: Aircraft market projections. From The Boeing Company.**

The aerospace industry challenge, therefore, is to meet the more exigent requirement of more efficient aircrafts, as the volatile fuel price engraves fleet handling, furthermore the new environmental rules have to be satisfied.

The introduction of composite materials thanks to their versatility as well as the material adjustable architecture and the high strength to weight ratio offers themselves as base technology for next aircraft generation. Composite materials were employed in aeronautical industry since the late 70's, but always in secondary structural components. Often the main advantage accounted to the use of composites is the weight saving estimated about 30% of the final weight, but this gain, which implies less than 10% in terms of the directing operational costs, is a not convincing argument for the industry change. However, if the improvement in the flight performance is attempted in a more general sense, the composite technology represents the more attractive evolution for the new aircraft generation. Both the actual biggest aerospace companies individuate the composite application for the aircraft primary structural part as a strategical manufacturing technology. A more realistic estimation of weight reduction would be guessed in 10%, but if the weight is saved on primary structures, as fuselage, wings or empennage the reduction in operating costs will be proportional.

A main aircraft structure, such as a fuselage barrel have to obey, beyond the essential structural performances, even to acoustical or damage tolerance features. Moreover, the use of composite materials allows to geometrically define components to improve aerodynamic efficiency, in particular the overlapping of more than one component represents a critical point for the classic metallic fuselages.

The improving study for the final structure may be focused not only on the final component but also on the composite material itself and on the manufacturing process which could be not independent of the final component.

## 1.2 Multi-disciplinary design of composite structure

The necessity of a multidisciplinary design approach addressing the transition from the metallic to the composite fuselage aircraft that includes not only mechanical issues but also the vibration suppression and thermal insulation aspects has been illustrated by a series of papers from Van Tooren et al. [1].

The starting point individuated for the choice of a new combination of materials, structural concepts and manufacturing technology is the improvement of the efficiency by integration of functions. They schematically represented the problem of the requirements which have to be fulfilled during the development of an aircraft fuselage crossing the most important material and structural design criteria, the horizontal axis in the figure 1-3, with the level of fulfilment of design requirements, the vertical axis.

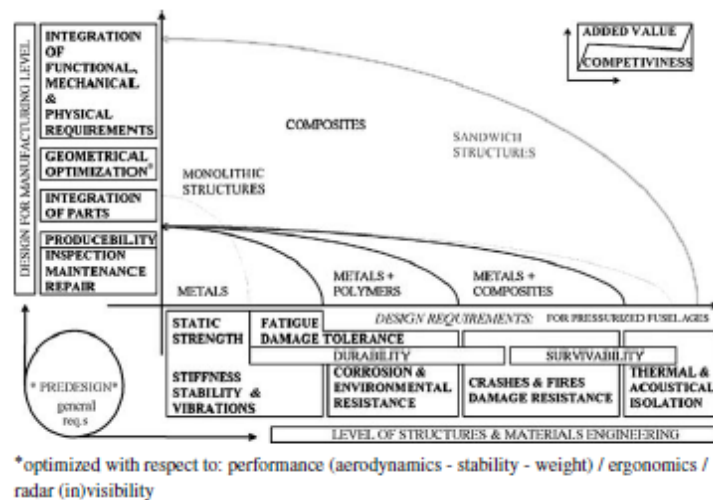


Figure 1- 3: Design requirements for fuselage structures. From Van Tooren [1].

Current design practise is characterized by a sequential methodology and structural optimization is only done with respect of stiffness and strength. The respect of physical requirements such as thermal and acoustical insulation is done at the end with additional weight and costs.

The use of composite material implies the possibility to integrate within a single system all needed features to fulfil physical requirements, i.e. thermal insulation or damping material, moreover they allow a freedom in the shape valuable for structure efficiency. Composites necessitate more attention during the design phase, these materials show a brittle behaviour and they are sensitive to the presence of flaws, therefore attention should be paid to avoid stress concentration and load conditions may be carefully predicted. It becomes clear that the combination of materials, structural concepts and manufacturing technologies are strictly related to final component and to all the requirements that should be satisfied.

Van Tooren examined, as case study, the integrate design for a fuselage panel; in its study the decisive feature is the material technology, metallic or composite, addressing the analysis both to structural and to sound insulation requirements.

A simple example of integrated design is represented by the analysis of a fuselage barrel. The introduction of composite material, in fact, undoubtedly lead to the decreasing of final weight of the structure.

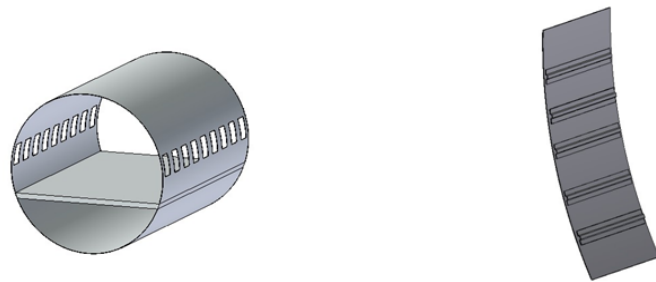


**Figure 1- 4: Typical aeronautical fuselage barrel and a stiffened plate.**

The buckling stress of the stringer-skin panel is determined by the Euler stress for columns

$$\sigma = E \frac{\pi^2}{L^2} \frac{(EI)_{\text{panel}}}{(EA)_{\text{panel}}}$$

It needs to be remarked that this formula could be applied for composite structure in term of its equivalent isotropic material. Composite fuselage demands thinner skin panels that could influence the damage tolerance feature of the system, furthermore the sound insulation properties could be changed. The sound insulation of a fuselage depends on many variables, the noise spectrum of the source incident, the resonances frequencies of the structure, the pressure difference from the inside and the outside.

$$TL = 10 \log \left( \frac{P_{in}}{P_{tr}} \right)$$

The improvement in transmission loss for a stiffened plate related to the frames and stiffeners pitch can be expressed as follows:

$$\Delta TL = 10 \log \left( \frac{\left( \frac{1}{b} + \frac{1}{L} \right)_{old}}{\left( \frac{1}{b} + \frac{1}{L} \right)_{new}} \right)$$

From this equation it can be concluded that an increment of the stiffener pitch (normally the lower) gives a large increment in TL. An increasing of the skin thickness leads to two separated effects: a direct increment in TL as the mass of the fuselage panel increase and a panel stiffness increase which in turn moves panel natural frequency potentially depressing the TL value.

Considering the structure loss factor as a damping constant an increment in structure loss factor will approximately result in a TL improvement defined as

$$\Delta TL \approx 10 \log \left( \frac{\eta_{new}}{\eta_{old}} \right)$$

A method to improve the structure loss factor is to modify material architecture embedding high loss factor materials within laminate stacking. In particular, the local addition of the viscoelastic materials to the vibrating structure has been the standard procedure to control vibration amplitude for composite fuselage panels. The detrimental effect on the structural efficiency resulting by the application of a viscoelastic layer to the fuselage skin panel for the improvement of the acoustical insulation has been discussed in latest papers leaving room to further improvement.

Through the reported examples, two key parameters for the study of a composite structure could be individuated, firstly the importance of the overall material architecture on the final response of the structure, in fact both mechanical performances (stiffness and strength) and sound insulation (transmission loss and loss factor) could be controlled by a proper definition of the material architecture; moreover this feature could lead to contrasting requests needing an optimization process accounting the multiple disciplinary aspects.

### 1.3 Multi-scale design of a composite fuselage

As matter of fact, the flexibility of composite materials architectures gives the chance to design and manufacture materials that are simultaneously compliant for both the structural and the vibroacoustic requirements of a primary structure.

The development of multifunctional design tools integrating structural and damping features enables a next step toward the exploitation of the composite materials benefits. It is worth noting that the structural damping in the case of a composite fuselage is a multiscale problem. As illustrated in the Figure 1- 5 the fuselage structure vibroacoustic requirement is top-down determined by the behaviour of the stringers reinforced skin, that is, in turn, determined by the panel damping behaviour, that owns its damping features to its laminate architecture and constituent materials.

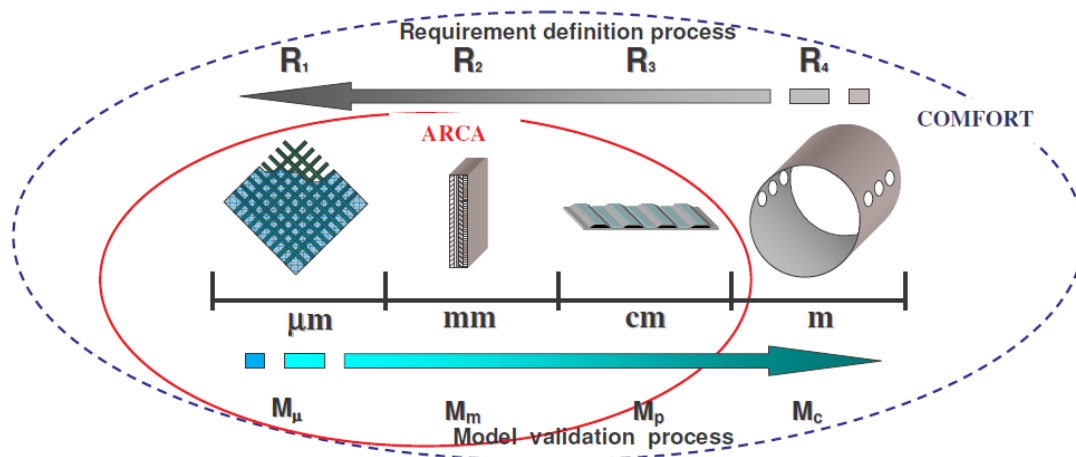


Figure 1- 5: Multiscale analysis of a composite fuselage barrel. From ARCA [3]

Different technical disciplines are in charge to develop design tools for the different dimensional scales. From the bottom-up perspective, robust constitutive equations for the structural and viscoelastic behaviour of constituents materials to be passed through the different dimensional scales at the laminate level are needed to perform reliable dynamical structural analysis of proper bounded sub elements and, in turn, to be implemented into the whole fuselage barrel design.

In particular, the insertion of viscoelastic layer within the laminate has been individuated as the most promising architecture for increasing damping performance of plane structures. The dynamical behaviour of elementary structures (beam, plates) based on the interleaved viscoelastic layer architecture has been intensely investigated and a plenty of models have

been proposed for the evaluation of the damping loss factor at the structure mechanical resonances (modal analysis).

The pioneering works of Ross, Kerwin and Ungar, RKU [5], have been investigated the constrained layer configuration where a metallic plate have been added with a viscoelastic layer upper constrained by a thin metallic layer. They have been focused on the evaluation of the flexural modal damping properties of the hybridised plate structure where mechanical energy dissipation has been assigned only at the viscoelastic layer. Based on the RKU method, Cupial and Nizioł [7] have been later developed a method for calculating the modal in-plane flexural loss factor of a composite panel with a viscoelastic interleaved layer by the use of first order shear deformation theory where the composite layers have been considered orthotropic. A considerable effort has been made by the group of Saravanos that in a series of paper introduced a real multiscale model for the modal behaviour of an interleaved hybrid composite starting from constituent materials. In particular, Saravanos and Pereira [8] have been demonstrated the increasing in damping properties of composite plates by embedding viscoelastic layers in the material stacking sequence. A semi-analytical method has been further proposed by Saravanos [9] for solving the dynamical motion of the hybrid interleaved laminate that involves high-order and discrete layer theories to include transverse shear effects in laminates. Finally, Berthelot [10] has been proposed a generalised method for modal damping calculation in the case of composite plates and beam that has been based on the Ritz method where the transverse shear effects are introduced through equilibrium condition on laminate thickness.

Modelling the composite materials viscoelasticity has led to two alternative approaches: the correspondence principle and Strain Energy Method (see Chandra et al., [11]). In particular the latter method, relates the total damping of a composite material or a composite structure to the damping of each constituent phase and the fraction of the total strain energy stored in that phase. The method states that for any system of linear viscoelastic elements the loss factor can be expressed as a ratio of summation of the product of individual element loss factor and strain energy stored in each element to the total strain energy.

The potential application of Strain Energy Method formalism to different dimensional scales has driven the present work. Ni and Adams [4] have been first developed a model for flexural damping behaviour of a composite laminate based on the classical plate theory by using the “Strain Energy Method”. Saravanos proposed later in 1989 a micromechanics treatment for calculation of the lamina loss factor including the out-of-plane effects

through high order thick laminate theory. Yim and Gillespie [12] have been used the equilibrium equations to account for the transverse shear stresses in predicting the modal loss factor. Only recently, Radford and Mèlo [13] proposed the use of the Dynamical Mechanical Analysis method to characterize the composite lamina constitutive equation based on the Strain Energy Method by the introduction of only four viscoelastic independent parameters for lamina.

An alternative to insert viscoelastic layer within the laminate is to engineer the damping feature into the structure by introducing at lamina level filler capable to increment the passive damping. A number of hybrid solution could be imagined by the modification of the lamina basic constituents: the fibres and the hosting matrix.

The presence of viscoelastic sheet within a laminate make the material prone to de-bonding induced by high shear stress reached, however if the viscoelastic material would be embedded in fibres preform the final damping could be incremented [14], the arrangement of viscoelastic fibres in warp or weft direction induces, for effect of stiffness gradient, a deformation field enhancing energy stored in material and hence the dissipated energy.

Rather than modifying fiber arrangement, that certainly introduces technological efforts in the final manufacturing process due to the handling of different stiffness fibres, the lamina damping could be improved by introducing nanoscale fillers (such as carbon nanotubes) into the host structure matrix. For such nano-composites [15], [16], the combination of extremely large interfacial contact area and low mass density of the filler materials implies that frictional sliding of nanoscale fibres within the polymer matrix has the potential to cause significant dissipation of energy with minimal weight penalty. Another attractive feature of this concept is that the nanoscale additives could be seamlessly integrated [17] into composite systems without sacrificing mechanical properties or structural integrity.

The damping behaviour of nanocomposites has modelled from Finegan and Gibson applying the correspondence principles at Halpin-Tsai model for short fiber composites, their predictions show that composites having very low fiber aspect ratios should have higher damping than those having high fiber aspect ratios [18]. Multi-walled nanotubes have observed to be a better reinforcement than single-walled, moreover are more effective in enhancing damping characteristic of the composites [19].

The reinforcement effect of carbon nanotube in polymeric matrix depends not only by their content within the hosting system according to traditional micro-mechanics of composites but also by the level of dispersion within the final nano-composite [20]-[21].

Percolation theory [22] can be suitably considered to describe these boundaries. The percolation phenomenon represents a well-known and studied topic for many filler matrix systems, mainly for electrical properties. In fact, the first evidence of percolation threshold to model electrical behaviour of CNT/polymer nano-composite is due to Coleman et al. back in 1998 [23].

## 1.4 Research outline

This work is ideally divided in four parts. In the first part, constituted by chapters I, II and III, the analytical solution for damping predictions and experimental methods for measuring it are presented. The second part, chapters IV and V, reports the proposed material architectures for enhancement passive damping for a material at each dimensional scale,, furthermore, the numerical procedure for simulating multiscale behaviour of composite structure is described. The third part, chapter VI, reports all the experimental activities on the hybrid unidirectional composites; while in the fourth part chapter VII the feasibility of the selected architecture on large scale components.

Each chapter is arranged by following the dimensional path, as illustrated in the following Figure 1- 6, both the modelling analysis of hybrid composites and the experimental manufacturing and testing have covered item starting from nanocomposites to the final structural component.

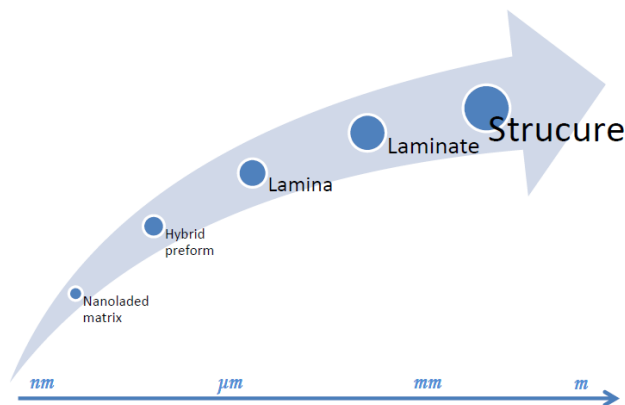


Figure 1- 6: Through the scale analysis of a composite structure.



In the chapter II the problem of material damping is presented with the aim of understanding dissipation mechanisms within the composites. The proposed approach analyse material dissipative properties by the strain energy method which allows to keep the same formalism over different dimensional scales.

Composite damping depends on many aspect of material architecture, this phenomenon is analysed at three different dimensional scale. At laminate levels the dissipation mechanism is explained by the evaluation of each energy components, introducing the calculation of out of the plane stress components. At micro-level a complete description of dissipative component for transversely isotropic material is proposed following Saravanos unified approach. Then the analysis of nano-composites is proposed extending short fiber composite theories for nano-dimensional fillers.

The purpose of the chapter III is to introduce the fundamental of damping by means of viscoelastic material and measuring the relevant parameters for any specific polymer. Damping is an important parameters related to the study of dynamic behaviour of fiber-reinforced composite structures and the successful characterization of dynamic response of viscoelastically damped composite materials is essential to verify the effectiveness of analytical methods based upon its constituents. The main damping mechanisms are described and attention is focused on the viscoelastic materials which are characterized by high ratio between the dissipative and elastic features. The measuring techniques are also described. Structural damping is based on the analysis of a vibrating structure and damping feature is measured at system's resonance, this is usually indicated as modal damping. Moreover the dynamical mechanical approach is reported, in that case the material damping is expressed in terms of the phase shift form exiting sinusoid force and the material response.

The chapter IV describes hybrid laminate architectures able to improve the passive damping. The well known interleaved solution is examined by literature works of Berthelot, moreover based on the principle of maximize stored energy a novel hybrid architecture for the lamina has been proposed. The passive damping of a composite lamina could be enhanced by imaging an hybrid fiber preform which includes viscoelastic material or by means of a lamina consisting in an high damping matrix. Passive damping of the hosting matrix could be improved by dispersing carbon nanotubes within the resin before the lamina infusion.

The numerical tool based on the model developed in the previous chapter is described in the chapter V, the matlab code developed has been embedded in the multi-objective

platform, called modeFRONTIER, which integrate optimization and statistical procedure that would be used for the individuation of the optimal hybrid architecture related to the specific boundary conditions.

First the numerical analysis on the mechanical and dissipative behaviour of hybrid unidirectional laminae are presented, i.e. the hierarchical procedure for the evaluation of mechanical properties of multiscale unidirectional composites is discussed.

The integrated multi-level procedure, Figure 1- 7, for the analysis of hybrid composited is explained and as application the analysis of two possible hybrid laminate including 3% in volume of damping material is led accounting the final engineering constants of material and the final dissipative constant describing overall material dissipation are evaluated.

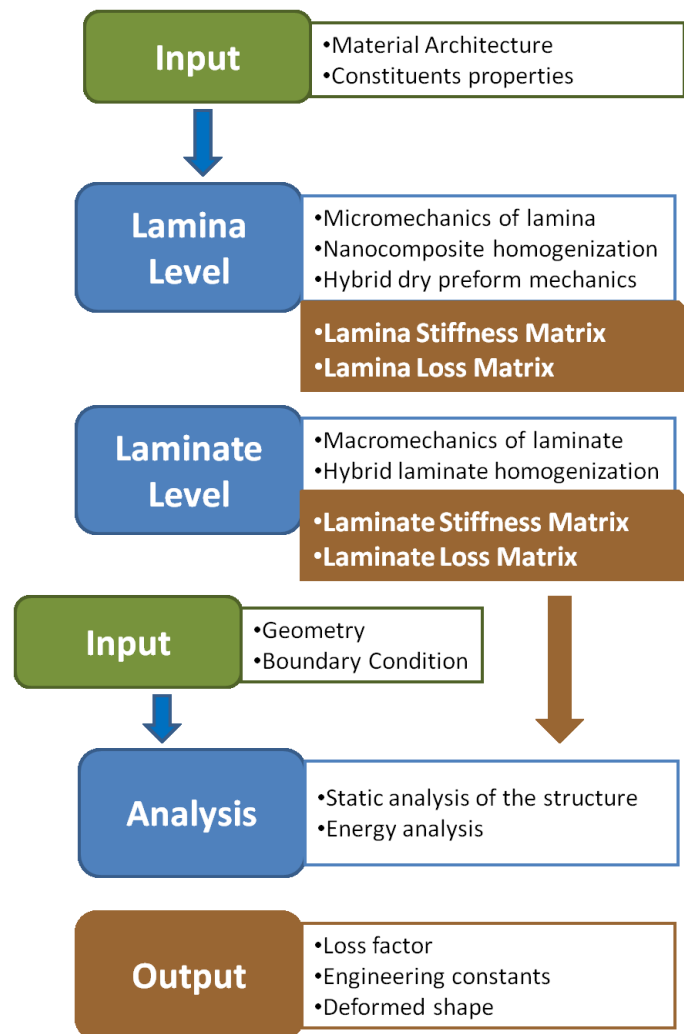


Figure 1- 7: Multi-level analysis of composite structures.

In the chapter VI the experimental analysis of the proposed hybrid architecture have been presented. For each proposed architecture, unidirectional coupons have been tested to verify the increment in loss factor. The hybridization of the laminate was experimentally studied over all dimensional scales. On the macro scale laminates with macroscopically integrated viscoelastic layer have fabricated and tested. Moreover the concept of hybrid lamina is examined in terms of hybrid preforms, where viscoelastic material is integrated as fiber along carbon tow direction, and in terms of laminae infused by a nanoloaded epoxy system. In each case a valuable increment in passive damping were measured, mainly at the requirement temperature, i.e. the cruise condition in the case of an aeronautical application. Both the interleaved layer and the hybrid dry preform lead to a loss in mechanical performances for the considered material, although the material damping is enhanced at each testing temperature. In the case of nano loaded matrix composites, mechanical performances are kept over all test conditions, but the enhancement in material damping is sensible only at temperatures below zero degrees.

Among the hybrid architectures examined in the course of this study the most promising, capable of enhance the damping response of a composite structure withstand the mechanical performance, was found to be the ***“multiscale” laminate***.

A multiscale laminate is a fiber reinforced polymer modified with CNTs, is indicated as *“multiscale”* as they are reinforced with microscale fibres and nanoscale nanotubes. High energy sonication has been widely used to disperse the CNT load in the resin before the infusion, however more recently calendaring has gained popularity as a means to disperse CNTs due to its efficiency and scalability which make it the suitable for high volume and high rate production.

The chapter VII address to describe the design and the manufacturing of a typical composite structure for aeronautical application. A stiffened composite plate is manufactured by VARTM for further acoustical testing, moreover large scale panel were manufactured in order to mechanically characterize the hybrid laminate.

## 1.5 References

- [1] Tinseth R, 2009. Middle east market update. *Oral presentation, Dubai airshow 2009*.
- [2] Beukers A, Van Tooren MJL, De Jong Th, 2005. Multi-disciplinary design philosophy for aircraft fuselages: Part I-V. *Applied Composite Materials 12*.
- [3] ARCA, Optimization of acoustical characteristics for advanced composite material. Italian research program 2005.
- [4] Ni RG, Adams RD, 1984. A rational method for obtaining the dynamic mechanical properties of laminate for predicting the stiffness and damping of laminated plates and beams. *Composites 15*.
- [5] Jones DIG, 2001. Handbook of vibration damping. *John Wiley & Sons*.
- [6] Saravanos DA, Chamis CC 1989. Unified micromechanics of damping for unidirectional fiber reinforced composites. *NASA Technical Memorandum 102107*.
- [7] Cupial P, Nizioł J, 1995. Vibration and damping analysis of three-layer composite plate with viscoelastic mid-layer. *Journal of Sound and Vibration 183*.
- [8] Saravanos DA, Pereira JM, 1992. Effects of interply damping layers on the dynamic characteristics of composite plates. *ALAA Journal 30*.
- [9] Saravanos DA, 1994. Integrated damping mechanics for thick composite laminates. *Journal of Applied Mechanics, 61*.
- [10] Berthelot JM, Sefrani Y, 2006. Damping analysis of unidirectional glass fiber composites with interleaved viscoelastic layers: Experimental investigation and discussion. *Journal of Composite Materials Vol. 40*.
- [11] Chandra R, Singh SP, Gupta K 1999. Damping studies in fiber-reinforced composites a review. *Composite Structures 46*.
- [12] Yim JH, Gillespie JW, 2000. Damping characteristics of 0° and 90° AS4/3501-6 unidirectional laminates including the transverse shear effect. *Composite Structures 50*.
- [13] Melo JDD, Radford DW, 2004. Time and temperature dependence of the viscoelastic properties of PEEK/IM7. *Journal of Composite Materials Vol. 38*.
- [14] Martone A, Zarrelli M, Antonucci V, Giordano M, 2009. Manufacturing and testing of an hybrid composite integrating viscoelastic fibres. *Proceeding of ICCM 17<sup>th</sup>-International Conference on Composite Materials*.
- [15] Qian D, Dickey EC, Andrews R, Rantell T, 2000. Load transfer and deformation mechanisms in carbon nanotubes-polystyrene composites. *Applied Physics Letters 76*.
- [16] Allaoui A, Bai S, Cheng HM, Bai JB, 2002. Mechanical and electrical properties of a MWNT/epoxy composite. *Composites Science and Technology 62*.

- [17]Ajayan PM, Schadler LS, Giannaris C, Rubio A, 2000. Single Walled carbon nanotube-polymer composites: strength and weakness. *Advanced Materials* 12.
- [18]Finegan IC, Tibbetts GG, Gibson RF, 2003. Modelling and characterization of damping in carbon nanofiber/polypropylene composites. *Composites Science and Technology* 63.
- [19]Rajora H, Jalili N, 2005. Passive vibration damping enhancement using carbon nanotubes-epoxy reinforced composites. *Composites Science and Technology* 65.
- [20]Song YS, You JR, 2005. Influence of dispersion state of carbon nanotubes on physical properties of epoxy nanocomposites. *Carbon* 43.
- [21]Breton Y, Desarmot G, Salvétat JP, Delpoux S, Sinturel C, Beguin F, 2004. Mechanical properties of multiwall carbon nanotubes/ epoxy composites: influence of network morphology. *Carbon* 42.
- [22]Coniglio R, Baker DR, Paul G, Stanley HE, 2003. Continuum percolation thresholds for mixtures of spheres of different sizes. *Physica A* 319.
- [23]Coleman JN, Curran S, Dalton AB, Davey AP, McCarty B, Blau W, Barklie RC, 1998. Percolation-dominated conductivity in a conjugated-polymer-carbon-nanotube composite. *Physical Review B* 58.
- [24]Baluch HA, van Tooren MJL, Schut EJ, 2008. Design tradeoff for fiber composite fuselages under dynamic loads using structural optimization. *49<sup>th</sup> AIAA Structures, Structural Dynamics and Materials*.
- [25]Rao MD, 2003. Recent Applications of Viscoelastic Damping for Noise Control in Automobiles and Commercial Airplanes. *Journal of Sound and Vibration* 262.

# Energy methods for damping evaluation

## 2.1 Summary

In this chapter the problem of material damping is presented with the aim of understanding dissipation mechanism within the composites.

Specific damping capacity is evaluated as the ratio of dissipated energy and the overall stored energy in the structure. In the proposed approach material dissipative properties are analysed by the strain energy method which allows to keep the same formalism over different dimensional scales.

Composite damping depends on many aspect of material architecture, this phenomenon is analysed at three different dimensional scale. At *laminate level* the dissipation mechanism is explained by the evaluation of each energy components, introducing the calculation of out of the plane stress components. At *micro level* a complete description of dissipative component for transversely isotropic material is proposed following Saravanos unified approach. Then the analysis of nanocomposites is proposed extending the short fiber composite theories for nano-dimensional fillers, the nano-loaded material could be described in the lamina analogy by a stiffness and loss matrices formulated according to dispersion state assumed within hosting matrix.

## 2.2 Loss factor of composite materials

Damping is an important parameter for vibration control, fatigue endurance, impact resistance, etc... Although the damping of composite materials is not very high, it is significantly higher than that measured for most usual metallic materials. Unfortunately structures composed of composite materials lose this distinctive feature while typically are built as monolithic elements in order to enhance the mechanical behaviour of the overall structure, instead in metallic structures an important contribution to structural damping is the aerodynamic bump effect near structural joints.

The lack of passive damping in composite structures lead to the need of proper treatments to improve system dynamic response which could waste part of the weight gain. Moreover, composites offer the capability of tailoring material behaviour through opportune functionalization, consequently combining the characteristic of composite materials, as high specific strength, specific stiffness, viscoelastic properties, it is possible to recover the damping feature.

The successful characterization of dynamic response of damped composite materials depends upon the use of appropriate analytical models/methods describing properties of composites based upon its constituents and their interaction. Essentially, mechanics of material and elasticity approaches have been utilised for elastic solution of moduli and the damping is further predicted using two different methods (a) Correspondence Principle and (b) Strain Energy Method.

The Correspondence Principle states [2] that the linear elastostatic analysis can be converted to dynamic linear visco-elastic analysis by replacing elastic moduli or compliances with complex moduli and compliances, respectively. The loss factor has been expressed as a ratio of the imaginary stiffness to the real stiffness, whereas the strain energy method relates the total damping in the material or structure to the damping of each element and the fraction of the total strain energy stored in that element. In the strain energy method for any system of linear viscoelastic elements the loss factor can be expressed as a ratio of summation of the product of individual element loss factor and strain energy stored in each element to the total strain energy. Applying these methods to composites, the material is seen as a system and whether the analysis is micromechanical or macromechanical is dependent on the nature of the elements.

In micromechanical analysis, the elements include the constituents such as fibres, matrix and void content, on the other hand for macromechanical analysis the individual lamina are

the elements whose strain and dissipation energies combine to give the overall loss factor of the laminate.

### 2.2.1 Loss factor prediction by the strain energy method

Each of these approaches has its own scope and limitations, with regards to damping prediction in composites, since the strain energy method allows the use of the same symbolism over different dimensional scales makes this approach the more suitable in this work where an unified approach to composite damping prediction is proposed.

Strain energy is stored within an elastic solid when the solid is deformed under load. In the absence of energy losses the strain energy is equal to the work done by external loads. When the elastic solid carries the load it deforms with strains ( $\epsilon$ ,  $\gamma$ ) and the material is stressed ( $\sigma$ ,  $\tau$ ). The work of external forces is stored as strain energy  $U$  within the elastic solid.

$$U = \frac{1}{2} \int_V \boldsymbol{\sigma} \boldsymbol{\epsilon} dV = \frac{1}{2} \int_V (\sigma_{11} \epsilon_{11} + \sigma_{22} \epsilon_{22} + \sigma_{33} \epsilon_{33} + \tau_{12} \gamma_{12} + \tau_{13} \gamma_{13} + \tau_{23} \gamma_{23}) dV$$

The total energy stored within the material is the sum of the energy stored in all the phases constituent the elastic body,

$$U = \frac{1}{2} \sum_{V_i} \int_{V_i} \boldsymbol{\sigma} \boldsymbol{\epsilon} dV$$

The specific damping capacity (SDC) is commonly used as a measure of the mechanical energy dissipated by a material per cycle. The SDC of a material system is

$$\psi = \frac{\Delta U}{U} = 2\pi \tan \delta = 2\pi \eta$$

Where  $\Delta U$  is the dissipated energy and  $U$  is the maximum strain energy per cycle,  $\tan \delta$  is the ratio of the storage material property over the dissipative terms,  $\eta$  is the loss factor. Damping is indeed calculated as the summation over the different mechanical energies dissipated by the material due to different stress components. The dissipated energy is

$$\Delta U = \frac{1}{2} \int_V \boldsymbol{\psi} \boldsymbol{\sigma} \boldsymbol{\epsilon} dV = \frac{1}{2} \int_V \left( \sum_{ij} \psi_{ij} \sigma_{ij} \epsilon_{ij} \right) dV$$

where  $\psi$  is the material specific damping capacity.



## 2.3 Layered composites analysis

In the present paragraph the damping capacity of a composite materials is examined in terms of its constituents. Material sub-elements change according to the dimensional scale considered, in fact in the case of a transversely isotropic lamina the constituents are fibres and hosting matrix, while a laminate could be separated in layers which could be described by their homogenised stiffness matrix in the global laminate reference system.

At each level the material behaviour could be described by the stress-strain relationship, the stiffness matrix, or by its inverse, the compliance matrix. In particular the material behaviour determines the independent elements.

$$\begin{array}{c}
 \left. \begin{array}{l} \epsilon_1 \\ \epsilon_2 \\ \epsilon_3 \\ \gamma_{23} \\ \gamma_{31} \\ \gamma_{12} \end{array} \right\} = \begin{bmatrix} S_{11} & S_{12} & S_{13} & S_{14} & S_{15} & S_{16} \\ S_{12} & S_{22} & S_{23} & S_{24} & S_{25} & S_{26} \\ S_{13} & S_{23} & S_{33} & S_{34} & S_{35} & S_{36} \\ S_{14} & S_{24} & S_{34} & S_{44} & S_{45} & S_{46} \\ S_{15} & S_{25} & S_{35} & S_{45} & S_{55} & S_{56} \\ S_{16} & S_{26} & S_{36} & S_{46} & S_{56} & S_{66} \end{bmatrix} \begin{array}{l} \sigma_1 \\ \sigma_2 \\ \sigma_3 \\ \tau_{23} \\ \tau_{31} \\ \tau_{12} \end{array}
 \end{array}$$

EXTENSION →      EXTENSION-EXTENSION COUPLING      SHEAR-EXTENSION COUPLING  
 ← EXTENSION      ← EXTENSION-EXTENSION COUPLING      ← SHEAR-EXTENSION COUPLING  
 ← SHEAR      ← SHEAR-SHEAR COUPLING

Figure 2- 1: Compliance matrix elements dependences. From [3]

In the global reference system the elements of compliance (stiffness) matrices could be associated to the effects of stress-strain field imposed to the material. In the Figure 2- 1 the coupling deformation associated to the elongational-shear stress are highlighted, in addition the diagonal terms represent the strain induced by pure elongational and shear stress.

### 2.3.1 Micro scale - Unified approach for unidirectional fiber reinforced composites <sup>[6]</sup>

Fiber composites are non homogeneous materials, therefore, candidate sources of composite damping would be: (1) Hysteretic damping in the polymer matrix, (2) hysteretic damping in the fibres and (3) friction damping at the fiber-matrix interface as a result of bonding imperfections, broken fibres, or debonding.

Saravanos and Chamis developed an integrated micromechanics methodology for the prediction of damping capacity for unidirectional fiber-reinforced composites. In the

proposed unified approach they considered all six damping coefficient related to each stress component.

Important assumptions made in their work are *the isotropic* dissipative behaviour for the matrix and *the transversely isotropic* behaviour for the fibers. As a result explicit micromechanics equations based on strain energy approach relating on-axis damping capacity to fiber, matrix and fiber volume fraction are obtained.

The elastic behaviour of a transversely isotropic material is characterized by 5 independent engineering constants  $E_1, E_2, G_{12}, \nu_{12}, \nu_{23}$ , other engineering parameter are related them by the following equations:

$$\begin{aligned} E_3 &= E_2 \\ G_{13} &= G_{12} \\ G_{23} &= \frac{E_2}{2(1 + \nu_{23})} \\ \nu_{13} &= \nu_{12} \end{aligned}$$

the stress strain relationship is expressed as

$$\begin{Bmatrix} \sigma_{11} \\ \sigma_{22} \\ \sigma_{33} \\ \tau_{23} \\ \tau_{13} \\ \tau_{12} \end{Bmatrix} = \begin{bmatrix} C_{11} & C_{12} & C_{13} & 0 & 0 & 0 \\ C_{12} & C_{22} & C_{23} & 0 & 0 & 0 \\ C_{13} & C_{23} & C_{33} & 0 & 0 & 0 \\ 0 & 0 & 0 & C_{44} & 0 & 0 \\ 0 & 0 & 0 & 0 & C_{55} & 0 \\ 0 & 0 & 0 & 0 & 0 & C_{66} \end{bmatrix} \begin{Bmatrix} \epsilon_{11} \\ \epsilon_{22} \\ \epsilon_{33} \\ \gamma_{23} \\ \gamma_{13} \\ \gamma_{12} \end{Bmatrix}$$

where the elements of stiffness matrix could be expressed as function of the engineering constants [3].

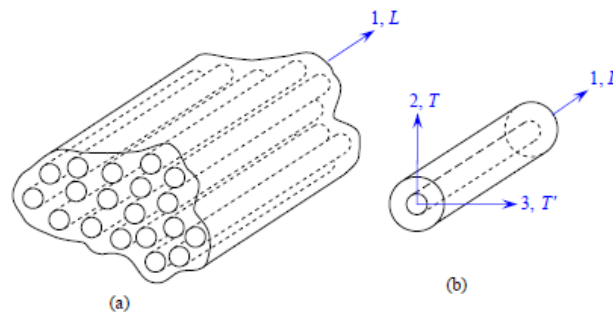


**Figure 2- 2: Unidirectional composite material**

A square packaging array of fibres is assumed representing the average value of randomly distributed fibres, nevertheless similar analysis could be developed for other packaging

patterns. The square array of a ply consists of one fiber and the surrounding matrix [6], assuming that an uniform cyclic longitudinal normal stress of amplitude  $\sigma_{11}$  is applied to the ply, then the strain energy within the representative fiber/matrix would be:

$$U = \frac{1}{2} \int_V \boldsymbol{\sigma} \boldsymbol{\varepsilon} dV = \frac{1}{2} \int_V (\sigma_{11} \varepsilon_{11} + \tau_{12} \gamma_{12} + \dots + \tau_{23} \gamma_{23}) dV$$

a coefficient accounting the energy dissipated in the longitudinal mode is defined regarding the dissipated energy, isolating contribution of fibres and matrices:

$$U_{11} = \frac{1}{2} \int_V \sigma_{11} \varepsilon_{11} dV$$

$$\delta U_{11} = \frac{1}{2} \int_V \psi_{11} \sigma_{11} \varepsilon_{11} dV$$

$$\delta U_{11} = \frac{1}{2} \int_{V_f} \psi_{f11} \sigma_{f11} \varepsilon_{f11} dV + \frac{1}{2} \int_{V_m} \psi_{m11} \sigma_{m11} \varepsilon_{m11} dV$$

Considering the iso-stress load condition for material's constituents and assuming constituent's SDC (Specific Damping Capacity) independent from stress and strains levels:

$$\varepsilon_{11} = \varepsilon_{f11} = \varepsilon_{m11}$$

$$\psi_{11} \int_V E_1 \varepsilon_{11}^2 dV = \psi_{f11} \int_{V_f} E_{f1} \varepsilon_{11}^2 dV + \psi_{m11} \int_{V_m} E_m \varepsilon_{11}^2 dV$$

the SDC associate to the longitudinal modulus could be evaluated by comparison

$$U_{11} = \frac{1}{2} \int_V \sigma_{11} \varepsilon_{11} dV = \frac{1}{2} \int_V E_{11} \varepsilon_{11}^2 dV$$

Further, considering the stored strain energy during one vibration cycle leads to the broadly accepted rule of mixtures for the longitudinal modulus

$$U_{11} = \frac{1}{2} \int_{V_f} \sigma_{f11} \varepsilon_{f11} dV + \frac{1}{2} \int_{V_m} \sigma_{m11} \varepsilon_{m11} dV$$

$$\psi_{11} = \frac{\delta U_{11}}{U_{11}} = \psi_{f11} V_f \frac{E_{f1}}{E_1} + \psi_{m11} (1 - V_f) \frac{E_m}{E_1}$$

In order to evaluate the transverse normal damping a cyclic transverse normal stress of amplitude  $\sigma_{22}$  is applied to the representative, similarly to the normal longitudinal the total stored energy is considered and then the damping factor is calculated:

$$U_{22} = \frac{1}{2} \int_V \sigma_{22} \varepsilon_{22} dV$$

Introducing the SDC, representing the energy fraction dissipated in the transverse normal mode the dissipated energy could be defined as:

$$\delta U_{22} = \frac{1}{2} \int_V \psi_{22} \sigma_{22} \varepsilon_{22} dV$$

Separating energy dissipated in both components (fiber and matrix)

$$\delta U_{22} = \frac{1}{2} \int_{V_f} \psi_{f22} \sigma_{f22} \varepsilon_{f22} dV + \frac{1}{2} \int_{V_m} \psi_{m22} \sigma_{m22} \varepsilon_{m22} dV$$

The stress distribution in the matrix and the fibres is not uniform mainly due to the curvature of fibres, however after Chamis who used successfully this assumption in the development of a simple micromechanics model for lamina properties in the case of transverse and shear modulus.

$$\sigma_{22} = \sigma_{f22} = \sigma_{m22}$$

$$\psi_{22} \int_{V_f} \frac{\sigma_{22}^2}{E_{22}} dV = \psi_{f22} \int_{V_f} dV + \psi_{m22} \int_{V_m} \frac{\sigma_{22}^2}{E_{m22}} dV$$

The final value of the SDC in transverse normal direction is function of the micromechanics model followed

$$\psi_{22} = \psi_{f22} V_f \left( \frac{E_{f22}}{E_{22}} \right)^{-1} + \psi_{m22} (1 - V_f) \left( \frac{E_m}{E_{22}} \right)^{-1}$$

Based on the same assumptions and following a similar procedure as in the case of transverse damping, the in plane shear damping capacity is given by a analogous rule

$$\psi_{12} = \psi_{f12} V_f \left( \frac{G_{f12}}{G_{12}} \right)^{-1} + \psi_{m12} (1 - V_f) \left( \frac{G_m}{G_{12}} \right)^{-1}$$

In the case of the trough the thickness shear damping for a transversely isotropic lamina

$$\psi_{13} = \psi_{12}$$

$$\psi_{23} = \psi_{f23} V_f \left( \frac{G_{f23}}{G_{123}} \right)^{-1} + \psi_{m23} (1 - V_f) \left( \frac{G_m}{G_{23}} \right)^{-1}$$

The final complete lamina dissipative matrix (in terms of loss factors) could be built accounting the dissipative properties relates to each stress component

$$\Psi = \begin{bmatrix} \psi_{11} & 0 & 0 & 0 & 0 & 0 \\ 0 & \psi_{22} & 0 & 0 & 0 & 0 \\ 0 & 0 & \psi_{33} & 0 & 0 & 0 \\ 0 & 0 & 0 & \psi_{23} & 0 & 0 \\ 0 & 0 & 0 & 0 & \psi_{13} & 0 \\ 0 & 0 & 0 & 0 & 0 & \psi_{12} \end{bmatrix}$$

During off-axis cyclic loading, more than one of the non-axis SDC could contribute to the overall ply damping, therefore the off-axis damping is related to both on-axis damping properties and the orientation of fibres. A transformation law could be derived taking in account the invariant property of strain energy to the stress strain transformations.

$$[\Psi_c] = [\mathbf{R}_\sigma]^T [\Psi_c] [\mathbf{R}_\sigma^{-1}]^T$$

The non diagonal terms are indicated as coupling between axial and shear stresses, the off-axis loading will affect the overall damping capacity of a ply altering the diagonal terms of the loss matrix which is equivalent to altering the dissipative capability of the ply and changing the non-diagonal terms which control the amount of energy dissipated by coupled deformation modes.

### 2.3.2 Macro scale - Damping of angled plies composites

By the strain energy method the estimation of dissipated energy is reached through the evaluation of energy allocation in terms of stress contribution within the system. A suitable approach, as obtained at the micro-scale, may include the effect of all the stress component.

The study of dissipative property requires also the study of the elastic behaviour, therefore the homogenization problem for a layered composite is examined both for the elastic and dissipative material feature.

#### 2.3.2.1 Elastic behaviour of laminates

In the field of composite structures, the layerwise laminate theories developed aim to the efficient prediction of the through the thickness composite laminate response.

The three dimensional stress analysis could be performed using mainly two possible approach: 1) *displacement assumed* based on approximation of displacements through the thickness, 2) *equilibrium* where the in plane stresses are computed from the displacement approximation and out of plane stresses from the equilibrium equations [9].

A fundamental concept is that in a perfect theory of laminates the condition of continuity for both the displacement and transverse stresses must be satisfied through the whole thickness of the part. The continuity of transverse stresses at the interface can be satisfied only if transverse strains are discontinuous, there as follows from HOOKE's law, this in turn leads to the discontinuity of the first derivative of displacement at the material interface

The displacement assumed approach assumes that the displacement field can be described by some predetermined set of functions  $u_i(x,y,z) = \Phi_i(x,y,z)$  belonging to some family of polynomial functions. The solution of the problem is formulated in terms of the unknown coefficients in the approximation functions, while in the equilibrium approach the in-plane strains ( $\epsilon_x, \epsilon_y, \gamma_{xy}$ ) and the in-plane stresses ( $\sigma_x, \sigma_y, \tau_{xy}$ ) are calculated following a displacement assumed approach in a first step and then out-of plane stresses ( $\sigma_z, \tau_{xz}, \tau_{yz}$ ) are evaluated by the equilibrium equations using the in-plane stresses previously calculated. The equilibrium approach appears to be the more suitable approach, in fact for calculation of the in-plane stress and strain tensor the well known zero-order lamination theory could be used and then transverse shear stress are evaluated by equilibrium.

#### *In-Plane Stress and Strain tensor evaluation: The Classical Lamination Theory*

The broadly used homogenization approach applied for laminated composites is the zero-order lamination theory by Kirchoff and Love. The basic assumption of the Classical Lamination Theory (CLT) are summarized as follow:

- Each layer of the laminate is quasi-homogeneous and orthotropic
- The laminate is thin compared to the lateral dimensions and is loaded in its plane
- State of stress is plane stress
- All displacements are small compared to the laminate thickness
- Displacements are continuous throughout the laminate
- Straight lines normal to the middle surface remain straight and normal to that surface after deformation.
  - In-plane displacements vary linearly through the thickness,
  - Transverse shear strains ( $\gamma_{xz}$  e  $\gamma_{yz}$ ) are negligible.
- Transverse normal strain  $\epsilon_z$  is negligible compared to the in-plane strains  $\epsilon_x$  and  $\epsilon_y$
- Strain-displacement and stress-strain relations are linear

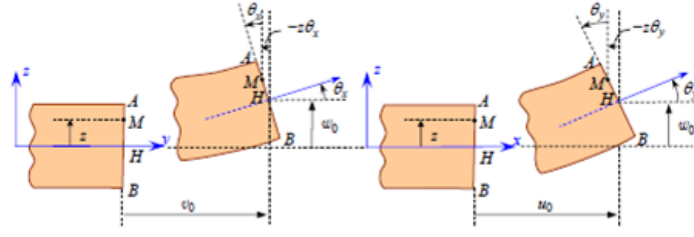


Figure 2- 3: Plate deformation according to Kirchoff-Love assumptions

For an orthotropic lamina the assumption of plane stress and negligibility of the through the thickness effects leads to a simplified expression of the constitutive matrix for each lamina.

$$\begin{cases} \sigma_3 = 0 \\ \tau_{23} = 0 \\ \tau_{13} = 0 \end{cases} \quad \begin{cases} \epsilon_3 = 0 \\ \gamma_{23} = 0 \\ \gamma_{13} = 0 \end{cases}$$

$$\begin{Bmatrix} \sigma_1 \\ \sigma_1 \\ 0 \\ 0 \\ 0 \\ \tau_{12} \end{Bmatrix} = \begin{bmatrix} C_{11} & C_{12} & C_{13} & 0 & 0 & 0 \\ C_{12} & C_{22} & C_{23} & 0 & 0 & 0 \\ C_{13} & C_{23} & C_{33} & 0 & 0 & 0 \\ 0 & 0 & 0 & C_{44} & 0 & 0 \\ 0 & 0 & 0 & 0 & C_{55} & 0 \\ 0 & 0 & 0 & 0 & 0 & C_{66} \end{bmatrix} \begin{Bmatrix} \epsilon_1 \\ \epsilon_1 \\ 0 \\ 0 \\ 0 \\ \gamma_{12} \end{Bmatrix}$$

The displacement field under the cited assumptions is

$$\begin{aligned} u(x, y, z) &= u_0(x, y) - z \frac{\partial w_0}{\partial x}(x, y) \\ v(x, y, z) &= v_0(x, y) - z \frac{\partial w_0}{\partial y}(x, y) \\ w(x, y, z) &= w_0(x, y) \end{aligned}$$

The strain field is the superposition of the in-plane strains (mid-plane strains) and the flexural strains (bending and twisting)

$$\begin{aligned} \epsilon_x &= \frac{\partial u}{\partial x} = \frac{\partial u_0}{\partial x} - z \frac{\partial^2 w_0}{\partial x^2} \\ \epsilon_y &= \frac{\partial v}{\partial y} = \frac{\partial v_0}{\partial y} - z \frac{\partial^2 w_0}{\partial y^2} \\ \gamma_{xy} &= \frac{\partial v}{\partial x} + \frac{\partial u}{\partial y} = \frac{\partial v_0}{\partial x} + \frac{\partial u_0}{\partial y} - 2z \frac{\partial^2 w_0}{\partial x \partial y} \end{aligned}$$

The global laminate behaviour could be expressed in terms of the resultant loads applied by the integration of stress in the volume [3].

The constitutive equation of a laminated plate expresses the resultants and the moments as functions of the in-plane strains and of the curvatures

$$\begin{Bmatrix} \mathbf{N} \\ \mathbf{M} \end{Bmatrix} = \begin{bmatrix} [A] & [B] \\ [B] & [D] \end{bmatrix} \begin{Bmatrix} \boldsymbol{\varepsilon}^0 \\ \mathbf{k} \end{Bmatrix}$$

Where  $\mathbf{N}$  is the resultant in-plane forces vector,  $\mathbf{M}$  is the resultant flexural moments vector,  $\boldsymbol{\varepsilon}^0$  is the in-plane strain vector and  $\mathbf{k}$  represents the mid-plane curvatures.

Inverting the equation in plane strains of reference surface and its curvature are evaluate from applied loads.

Matrices  $A$ ,  $B$  and  $D$  defined as follow are 3x3 material stiffness respectively extensional, coupling and flexural.

$$[A] = \sum_{k=1}^N [Q](z_k - z_{k-1})$$

$$[B] = \sum_{k=1}^N [Q](z_k^2 - z_{k-1}^2)$$

$$[D] = \sum_{k=1}^N [Q](z_k^3 - z_{k-1}^3)$$

The Kirchoff-Love approach (*CLT*) describes accurately the behaviour of laminates in the case of thin beams and plates with layers having comparable stiffness, conditions where the assumption of plane stress represent properly the material status. Moreover, *CLT* based approach does not allow an accurate calculation near boundaries and constraints.

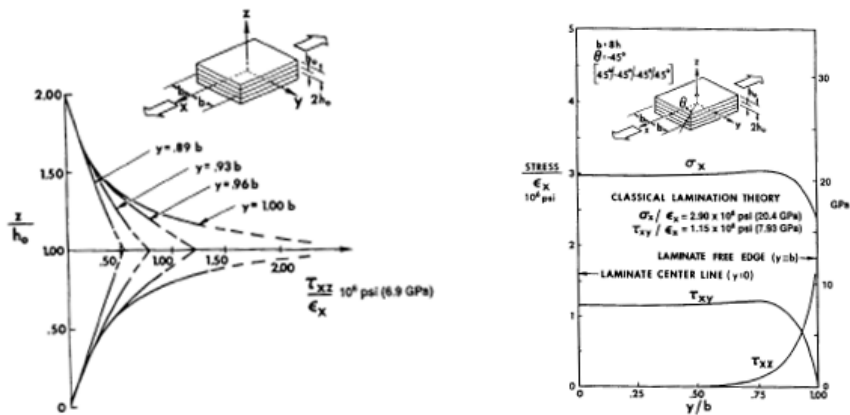


Figure 2- 4: Thickness and boundary affecting solution



*Out of plane Stress and Strain evaluation*

Integrating over the thickness the transverse shear part of the material law  $\tau_z^k = G^k \gamma$  gives the resultant transverse shear forces  $R = H\gamma$ , where  $G^k$  represents shear moduli matrix of the  $k^{\text{th}}$  lamina.

Transverse shear stress could be evaluated by the integration of equilibrium equations:

$$\begin{aligned}\tau_{xz}^k &= - \int_{\zeta=0}^{\zeta=z} \left( \frac{\partial \sigma_x^k}{\partial x} + \frac{\partial \tau_{xy}^k}{\partial y} \right) d\zeta \\ \tau_{yz}^k &= - \int_{\zeta=0}^{\zeta=z} \left( \frac{\partial \tau_{xy}^k}{\partial x} + \frac{\partial \sigma_y^k}{\partial y} \right) d\zeta\end{aligned}$$

Following Rolfes and Rohwer [10] in the case of cylindrical bending transverse stresses are related directly to resultant matrices defined in the previous step.

Using in-plane material law for the  $k^{\text{th}}$  lamina :

$$\boldsymbol{\sigma} = \begin{Bmatrix} \sigma_x \\ \sigma_y \\ \tau_{xy} \end{Bmatrix} = \mathbf{Q}^k (\boldsymbol{\varepsilon}^0 + z \mathbf{k})$$

Where  $\mathbf{Q}^k$  is the reduced stiffness matrix the vector of transverse shear stresses could be expressed as

$$\boldsymbol{\tau}_z = - \int_{\zeta=0}^{\zeta=z} \left[ \mathbf{B}_1 \mathbf{Q}^k \left( \frac{\partial \boldsymbol{\varepsilon}^0}{\partial x} + z \frac{\partial \mathbf{k}}{\partial x} \right) + \mathbf{B}_2 \mathbf{Q}^k \left( \frac{\partial \boldsymbol{\varepsilon}^0}{\partial y} + z \frac{\partial \mathbf{k}}{\partial y} \right) \right] d\zeta$$

$\mathbf{B}_1$  and  $\mathbf{B}_2$  are Boolean matrices

$$\mathbf{B}_1 = \begin{bmatrix} 1 & 0 & 0 \\ 0 & 0 & 1 \end{bmatrix} \quad \mathbf{B}_2 = \begin{bmatrix} 0 & 0 & 1 \\ 0 & 1 & 0 \end{bmatrix}$$

Since strain and curvature of laminate reference surfaces could be related to the resultant applied load  $\boldsymbol{\tau}_z$  could be expressed in terms of the load derivatives:

$$\boldsymbol{\tau}_z = -\mathbf{B}_1 \mathbf{F}(z) \frac{\partial \mathbf{M}}{\partial x} - \mathbf{B}_2 \mathbf{F}(z) \frac{\partial \mathbf{M}}{\partial y}$$

The matrix  $\mathbf{F}(z)$  is defined as

$$\mathbf{F}(z) = \left( \mathbf{a}(z) \mathbf{A}^{-1} \mathbf{B} - \mathbf{b}(z) \right) \mathbf{D}^{*-1}$$

Where  $\mathbf{a}(z)$  and  $\mathbf{b}(z)$  are the partial membrane and coupling stiffnesses of the laminate

$$\mathbf{a}(z) = \int_{\zeta=0}^{\zeta=z} \mathbf{Q} d\zeta \quad \mathbf{b}(z) = \int_{\zeta=0}^{\zeta=z} \mathbf{Q} \zeta d\zeta$$

In the case of cylindrical bending the derivatives of moments are related to shear forces by

$$R_{xz} = -\frac{\partial M_x}{\partial x} \quad R_{yz} = -\frac{\partial M_y}{\partial y}$$

Which finally results in

$$\boldsymbol{\tau}_z = \begin{bmatrix} F_{11} & F_{32} \\ F_{31} & F_{22} \end{bmatrix} \begin{Bmatrix} R_{xz} \\ R_{yz} \end{Bmatrix} = \mathbf{f}(z) \mathbf{R}$$

The contribution to total strain energy of transverse shear forces could be easily evaluated

$$I_c = \frac{1}{2} \int \boldsymbol{\tau}^T \mathbf{G}^{-1} \boldsymbol{\tau} dz = \frac{1}{2} \mathbf{R}^T \check{\mathbf{H}}^{-1} \mathbf{R}$$

An improved transverse shear matrix based on equilibrium is then provided

$$\check{\mathbf{H}} = \left[ \int \mathbf{f}^T \mathbf{G}^{-1} \mathbf{f} dz \right]^{-1}$$

After the calculation of transverse shear stress the transverse normal stress could be evaluated by integrating the third out of plane equilibrium equation [11]:

$$\sigma_z^k = - \int_{\zeta=0}^{\zeta=z} \left( \frac{\partial \tau_{xz}^k}{\partial x} + \frac{\partial \tau_{yz}^k}{\partial y} \right) d\zeta$$

### 2.3.2.2 Laminate loss matrix definition

Laminate overall damping capacity depends on both the material stacking and the resultant loads applied. In fact the load pattern could induce some coupling effects due to the particular material structure, for example in a layered material, which stacking sequence has a strong gradient in mechanical properties, loaded in pure bending presents not only dissipation effect due to the bending moment applied (longitudinal stress) but also transverse shear stresses affect the system dissipated energy.

The trough the scales homogenization approach followed aims to the definition of a constitutive formulation of material damping that describes the dissipative potential for each stored energy component.

The total stored energy in the laminate is given as sum of each stress-strain component contribution, similarly the overall dissipated energy is the sum of energy dissipated in each mode. The energy stored for each component of stress-strain tensor is defined as

$$U_{ij} = \frac{1}{2} \int_V \sigma_i \varepsilon_j dV \quad i, j = 1, 2, 3$$

$$\Delta U_{ij} = \frac{1}{2} \int_V \psi_{ij} \sigma_i \varepsilon_j dV \quad i, j = 1, 2, 3$$

Final laminate damping is the ratio of total dissipated and the total stored energy

$$\psi = \frac{\sum_k U^k}{\sum_k \Delta U^k}$$

where energy stored and dissipated in the  $k^{\text{th}}$  lamina is defined as follows:

$$U^k = U_{11}^k + U_{22}^k + U_{33}^k + U_{12}^k + U_{13}^k + U_{23}^k$$

$$\Delta U^k = \psi_{11}^k U_{11}^k + \psi_{22}^k U_{22}^k + \psi_{33}^k U_{33}^k + \psi_{12}^k U_{12}^k + \psi_{13}^k U_{13}^k + \psi_{23}^k U_{23}^k$$

The energy distribution is evaluated by the elastic characterization previously examined, as in the elastic analysis dissipation, is studied separating in-plane and out-of-the plane effects. Laminate loss matrix is separated in two sub-matrices one accounting in plane loss elements and another accounting transverse elements.

$$\Psi_1 = \begin{bmatrix} \psi_{11} & 0 & 0 \\ 0 & \psi_{22} & 0 \\ 0 & 0 & \psi_{12} \end{bmatrix} \quad \Psi_s = \begin{bmatrix} \psi_{13} & 0 \\ 0 & \psi_{23} \end{bmatrix}$$

Off-axis analysis accounting the effective laminate stacking respect the same transformation rule as the stiffness matrices examined in previous paragraph.

In plane contribution to total stored and dissipated energy is evaluated as follow

$$U = \frac{1}{2} \int_{-\frac{h}{2}}^{\frac{h}{2}} \{\sigma\} \cdot \{\varepsilon\} dz = \frac{1}{2} \int_{-\frac{h}{2}}^{\frac{h}{2}} \{\varepsilon\}^T \cdot [Q] \cdot \{\varepsilon\} dz$$

$$\Delta U = \frac{1}{2} \int_{-\frac{h}{2}}^{\frac{h}{2}} \{\varepsilon\}^T \cdot [Q][\Psi] \cdot \{\varepsilon\} dz$$

Integration leads to the definition of equivalent dissipative matrices for in plane effects to the homologues for elastic behaviour

$$[A_d] = \sum_{k=1}^N [Q][\Psi](z_k - z_{k-1})$$

$$[B_d] = \sum_{k=1}^N [Q][\Psi](z_k^2 - z_{k-1}^2)$$

$$[D_d] = \sum_{k=1}^N [Q][\Psi](z_k^3 - z_{k-1}^3)$$

The in plane total dissipated energy reads as

$$\Delta U = \frac{1}{2} \begin{Bmatrix} \boldsymbol{\varepsilon}_0 & \mathbf{k} \end{Bmatrix} \begin{bmatrix} [A_d] & [B_d] \\ [B_d] & [D_d] \end{bmatrix} \begin{Bmatrix} \boldsymbol{\varepsilon}_0 \\ \mathbf{k} \end{Bmatrix}$$

Transverse shear contribution to total strain energy is the integration of shear stress strain relationship,

$$U_s = \frac{1}{2} \int_{-\frac{h}{2}}^{\frac{h}{2}} \{\boldsymbol{\tau}\} \cdot \{\boldsymbol{\gamma}\} dz$$

$$\Delta U_s = \frac{1}{2} \int_{-\frac{h}{2}}^{\frac{h}{2}} [\Psi_s] \boldsymbol{\tau}^T \mathbf{G}^{-1} \boldsymbol{\tau} dz$$

The corresponding dissipative transverse shear matrix could be defined as

$$[H_d] = \sum_{k=1}^N [\Psi_s] (\mathbf{f}^T \mathbf{G}^{-1} \mathbf{f}) (z_k - z_{k-1})$$

Out of plane dissipate energy could be then evaluated from the resultants shear forces as

$$\Delta U_s = \frac{1}{2} \mathbf{R}^T \widetilde{\mathbf{H}}_d^{-1} \mathbf{R}$$

## 2.4 Nano scale – Damping of nanocomposites

Micromechanical improvements in composite material damping results from changes in damping properties and geometries at or below the lamina constituents material level. Some of the micromechanical level geometric and material parameters that affect the damping of the composite system are fiber aspect ratio, fiber orientation, fiber spacing, fiber and matrix properties.

In this paragraph the problem of damping evaluation for nano-loaded composites is presented. The simplest approach to describe nanocomposite behaviour is to adapt theoretical models for short fiber reinforced composites.

As previously showed, following Saravanos approach, it is possible describe the dissipative behaviour for an anisotropic material by the energetic analysis starting from its elastic properties. In the simplest possible case the composite could be modelled as an isotropic, elastic matrix filled with aligned elastic fibres. Assuming that fibres and matrix are well bonded, the application of a load in fiber direction produce the same strain field in the

fiber and in the matrix, under this circumstances the composite tensile modulus in the aligned direction is given by

$$E_C = (E_f - E_m)V_f + E_m$$

where  $E_f$  is the filler modulus,  $E_m$  is the matrix modulus and  $V_f$  is the fiber volume fraction. This represent the well known rule of mixtures. When is applied a load the stress is transferred to the fiber by the interfacial stress, the entity of stress transferred scales with fiber length. This means that short fibres would carry loads less efficiently than long fibres, this results in a lower effective modulus for the matrix reinforcement. Cox showed in the case of aligned fiber that composite modulus depends on a factor accounting the length efficiency of the filler.

$$E_C = (\eta_l E_f - E_m)V_f + E_m$$

where  $\eta_l$  represents the length efficiency factor and it can be described by the following expression [15]

$$\eta_l = 1 - \frac{\tanh(a l/D)}{a l/D} \quad a = \sqrt{\frac{-3 E_m}{2 E_f \ln V_f}}$$

The length efficiency factor approaches 1 for  $l/D > 10$ , underlining the fact that high aspect ratio fillers are preferred for reinforcing material.

The case of misaligned fibres could be included in the model by the introduction of an efficiency factor accounting the fibres orientation

$$E_C = (\eta_0 \eta_l E_f - E_m)V_f + E_m$$

$\eta_0$  values 1 in the case of aligned fibres, 3/8 for fibres oriented in a plane and 1/5 for fibres randomly oriented in space. The description of mechanical behaviour of nanoloaded material is quite difficult since its response is strictly dependent on how good is the filler dispersion. In addition carbon nanotubes tend to re-aggregate and clustering creating a material including more than one dimensional filler which implies an anisotropic behaviour. Assuming a good level of dispersion within the hosting matrix and a randomly dispersion of the filler, condition achievable in the case of low filler content, it is an acceptable approximation to assume the composite behave isotropically.

An isotropic material is described by two elastic constants, the elastic modulus evaluable by the proposed model and another parameters such as the Poisson ratio, moreover in the case of low filler content the Poisson could be assumed as invariable from matrices value.

In the case of isotropic material the shear modulus is related by other two independent parameters by the following simple rule

$$G = \frac{E}{2(1 + \nu)}$$

Finally the specific damping capacity of the nanocomposite could be evaluated by applying the energetic analysis as showed in paragraph 2.3

To account the possible load condition according to the previously consideration a generalised expression for the SDC of a two phase material is proposed as follows.

$$\psi = \psi_i V_i \left( \frac{P_i}{P_c} \right)^{\cos 2\alpha} + \psi_j (1 - V_i) \left( \frac{P_j}{P_c} \right)^{\cos 2\alpha}$$

## 2.5 References

- [1] Ungar EE, Kerwin EM 1962. Loss factors of viscoelastic systems in terms of energy concepts. *Journal of Acoustical Society of America* 34.
- [2] Hashin Z 1970. Complex moduli of viscoelastic composites: I General theories and application to particulate composites. *International Journal of Solids and Structures* 6.
- [3] Jones R 1998. Mechanics of composite materials. *Taylor & Francis*
- [4] Ni RG, Adams RD 1984. A rational method for obtaining the dynamic mechanical properties of laminate for predicting the stiffness and damping of laminated plates and beams. *Composites* 1.
- [5] Chandra R, Singh SP, Gupta K 1999. Damping studies in fiber-reinforced composites a review. *Composite Structures* 46
- [6] Finegan I, Gibson RF 1999. Recent enhancement of damping in polymer composites. *Composite Structures* 44
- [7] Saravanos DA, Chamis CC 1989. Unified micromechanics of dampin for unidirectional fiber reinforced composites. *NASA Technical Memorandum 102107*
- [8] Chamis CC, 1984. Simplified composite micromechanics equations for hygral, thermal and mechanical properties. *SAMPE Quaterly Vol 15-3*
- [9] Bogdanovic AE, Pastore CM, Deepak BP, 1994. A comparison of various 3-D approach for the analysis of laminated composite structures. *Composites Engineering Vol. 5-9*
- [10] Rolfes R, Rohwer K, 1997. Improved transverse shear stresses in composite finite elements based on first order shear deformation theory. *International Journal for Numerical Methods in Engineering Vol 40*
- [11] Rolfes R, Rohwer K, Ballerstaedt M, 1998. Efficient linear transverse normal stress analysis of layered composite plates. *Computers and Structures* 68
- [12] Saravanos DA, Chamis CC, 1989 Mechanics of damping for fiber composite laminates including hygro-thermal effects. *NASA Technical Memorandum 102329*
- [13] Berthelot JM, Assarar M, Sefrany Y, El Mahi A 2007. Damping analysis of composite materials and structures. *Composite Structures* 72
- [14] Finegan IC, Tibbetts GG, Gibson RF, 2003. Modelling and characterization of damping in carbon nanofiber/polypropylene composites. *Composites Science and Technology* 63.
- [15] Carman GP, Reifsnider KL, 1992. Micromechanics of short fiber composites. *Composites Science and Technology* 43.

# Measuring composite damping

## 3.1 Summary

The objective of this chapter is to introduce the fundamentals of damping by means of viscoelastic material and measuring the relevant parameters for any specific polymer.

Damping is an important parameters related to the study of dynamic behaviour of fiber-reinforced composite structures, the successful characterization of dynamic response of viscoelastically damped composite materials is essential for verify the effectiveness of analytical methods based upon its constituents.

In the first paragraph the main damping mechanisms are described, the attentions is focused then on the viscoelastic materials which are characterized by high ratio between the dissipative and elastic features, therefore suitable for improve damping feature of a structure.

Finally measuring techniques are described, structural damping is based on the analysis of a vibrating structure and damping characteristic is measured at system's resonance, this is usually indicated as modal damping. Furthermore, the dynamical mechanical approach is described, in that case the material damping is expressed in terms of the phase shift form exiting sinusoidal applied force and the material response.



## 3.2 Damping mechanisms

Damping is an invisible requirement for good mechanical design. The reason for this is that most structures, machines and vehicles are designed and built to meet many often conflicting requirements.

The dynamic response and sound transmission characteristics of structures are determined by essentially three parameters: mass, stiffness and damping. Mass and stiffness are associated with storage of kinetic and strain energy, respectively, whereas damping relates to the dissipation of energy, i.e. to the conversion of mechanical energy associated with a vibration to a form (usually heat) that is unavailable to the vibration.

Damping in essence affects only those vibrational motions that are controlled by a balance of energy, vibrational motion that depends on a balance of forces are virtually unaffected by damping. For example, consider the response of a classical mass-spring-dashpot system subject to a steady sinusoidal force, if the applied force acts at frequencies much lower than system's natural frequency the response is controlled by a balance between the applied force and the spring force, instead if the applied force acts at frequencies considerably higher than system's natural the response is controlled by a balance between the applied force and the mass's inertia. However, at resonance, where the force frequency match the natural frequency of the system, spring and inertia effects cancel each other and the applied force supplies some energy to the system.

The simplest approach to introduce damping mechanism is to consider the viscous damping, where energy dissipation results from a force that is proportional to the velocity of a vibrating system and act opposite to the velocity. Viscous damping is linear, so that the observed response does not change qualitatively as the amplitude increases. This is usually not the case of internal damping mechanism which come into play when metals, alloy and many other structural materials are deformed during vibration. The amount of energy dissipated for each cycle is extremely small for many metals unless the material is deformed near the yield point, some other metal exhibit a much greater degree of damping.

One way of viewing the internal damping behaviour of materials is to examine the plot stress versus strain under steady harmonic excitation, the area of the hysteresis loop is a direct measure of the damping.

Some other damping mechanism rely on the presence of air, or any other fluid, to dissipate energy in a structure. For example when a thin panel vibrates at a specific frequency, it disturbs the surrounding medium and causes sound waves to radiate away from the panel taking energy with them and thereby providing a mechanism of dissipation.

When structural panels are constructed from multiple sheets, the joints require overlap of surfaces, and rivets or bolts are used to hold together the sheets, in that case as the panel vibrates laterally the overlapping zones can be cyclically displaced in such way that air is pumped into and out to the gap between the surfaces. Material that have both damping (energy dissipation) and structural (strain energy storage) capability are called *viscoelastic*. Although, virtually all materials falls in this category, the terms is generally applied only to materials, such as plastics and elastomers, that have relatively high ratios of energy dissipation to energy storage capability.

### 3.2.1 Viscoelastic materials

Viscoelastic materials have a relationship between stress and strain which depends on time and frequency. The loss angle  $\delta$  is the phase angle between stress and strain during sinusoidal deformation in time. The loss angle or the loss tangent  $\tan\delta$  is a measure of damping or internal friction in a linear material. It is advantageous as is clearly defined in terms of observable quantities.

Viscoelastic material properties are generally modelled in the complex domain because of the nature of viscoelasticity. As previously discussed, viscoelastic materials possess both elastic and viscous properties. The moduli of a typical viscoelastic material are given in equation set

$$E^* = E' + jE''$$

$$G^* = G' + jG''$$

where the ‘\*’ denotes a complex quantity. In the equation set, as in the rest of this report, E and G are equivalent to the elastic modulus and shear modulus, respectively. Thus, the moduli of a viscoelastic material have an imaginary part, called the loss modulus, associated with the material’s viscous behavior, and a real part, called the storage modulus, associated with the elastic behavior of the material. This imaginary part of the modulus is also sometimes called the loss factor of the material, and is equal to the ratio of the loss modulus to the storage modulus. The real part of the modulus also helps define the stiffness of the material. Furthermore, both the real and imaginary parts of the modulus are temperature, frequency (strain rate), cyclic strain amplitude, and environmentally dependent.

### *Temperature Effects on the Complex Modulus*

The properties of polymeric materials which are used as damping treatments are generally much more sensitive to temperature than metals or composites. Thus, their properties, namely the complex moduli represented by  $E'$ ,  $G'$ , and the loss factor  $\tan \delta$ , can change fairly significantly over a relatively small temperature range. There are three main temperature regions in which a viscoelastic material can effectively operate, namely the glassy region, transition region, and rubbery region [2]-[3].

Figure 3- 1 shows how the loss factor can vary with temperature. The glassy region is representative of low temperatures where the storage moduli are generally much higher than for the transition or rubbery regions. This region is typical for polymers operating below their brittle transition temperature. However, the range of temperatures which define the glassy region of a polymeric material is highly dependent on the composition and type of viscoelastic material. Thus, different materials can have much different temperature values defining their glassy region. Because the values of the storage moduli are high, this inherently correlates to very low loss factors. The low loss factors, in this region, are mainly due to the viscoelastic material being unable to deform (having high stiffness) to the same magnitude per load as if it were operating in the transition or rubbery regions where the material would be softer. On the other material temperature extreme, the rubbery region is representative of high material temperatures and lower storage moduli. However, though typical values of storage moduli are smaller, like the glassy region the material loss factors are also typically very small. This is due to the increasing breakdown of material structure as the temperature is increased. In this region, the viscoelastic material is easily deformable, but has lower interaction between the polymer chains in the structure of the material.

Cross-linking between polymer chains also becomes a less significant property as temperature is increased. A lower interaction between the chains results in the material taking longer to reach equilibrium after a load is removed. Eventually, as the temperature hits an upper bound critical value (also known as the flow region temperature), the material will begin to disintegrate and have zero effective loss factor and zero storage modulus.

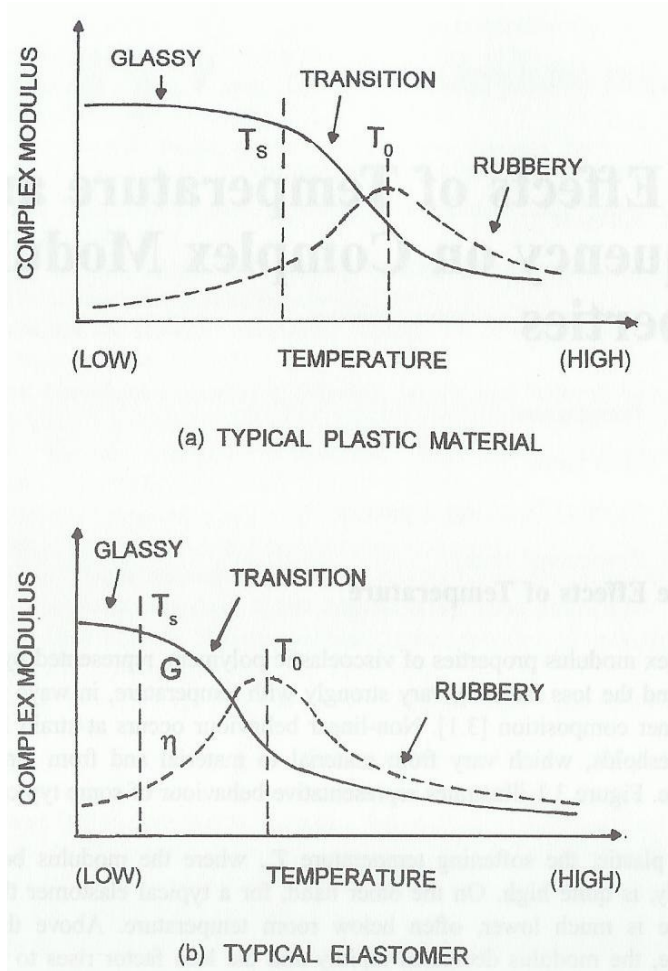


**Figure 3- 1: Temperature effects on complex modulus and loss factor material properties.**

**From Jones, Handbook of Viscoelastic Damping, 2001.**

The region falling between the glassy and rubbery regions is known as the transition region. Materials which are used for practical damping purposes generally should be used within this region because loss factors rise to a maximum. In more detail, if a material is within the glassy region and the temperature of the material is increased, the loss factor will rise to a maximum and the storage modulus will fall to an intermediate value within the transition region. As the material temperature is further increased into the rubbery region, the loss factor will begin to fall with the storage modulus.

Therefore, it is extremely important to know the operating temperature range during the design phase of a host structure to which a viscoelastic damping treatment will be applied so that the viscoelastic treatment will be maximally effective.

### *Frequency Effects on the Complex Modulus*

Like temperature, frequency also has a profound effect on the complex modulus properties of a viscoelastic polymer, though to a much higher degree with an inverse relationship. The three regions of temperature dependence (glassy, transition, rubbery) can sometimes be a few hundred degrees, more than covering a typical operational temperature range of an engineered structure. But the range of frequency within a structure can often be several orders of magnitude. The frequency dependence on complex moduli can be significant from as low as  $8 \cdot 10^{-4}$  Hz to  $8 \cdot 10^4$  Hz, a range much too wide to be measured by any single method [2]. Furthermore, relaxation times after deformation of a viscoelastic material can be anywhere from nanoseconds to years and will greatly affect one's measurement methods, especially at low temperatures.

Frequency has an inverse relationship to complex moduli with respect to temperature. At low frequency, the storage moduli are low and the loss factors are low. This region is synonymous with the rubbery region (high temperatures). This is due to the low cyclic strain rates within the viscoelastic layer. As the frequency is increased, the material hits the transition region where the loss factor hits a maximum value. As the frequency is increased further, the storage moduli increase as the loss factor decreases. Thus, the transition region is again the range of frequency for which a material should be chosen to correspond to a host structure's typical operating range. Figure 3- 2 illustrates this behavior.

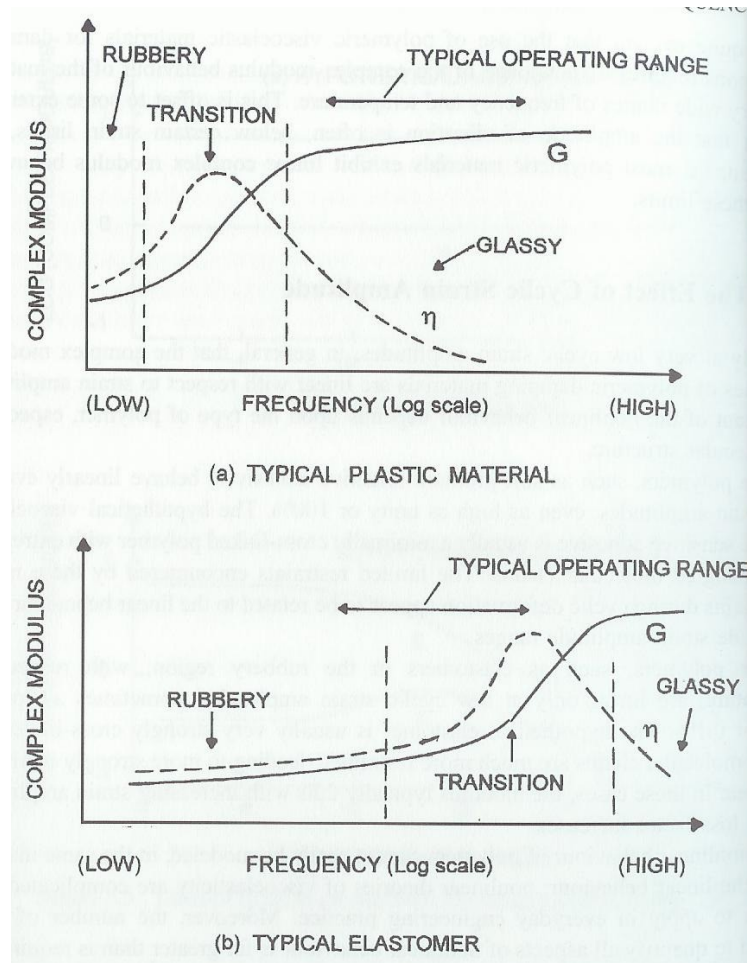


**Figure 3- 2: Frequency effects on complex modulus and loss factor material properties.**  
**From Jones, Handbook of Viscoelastic Damping, 2001.**

The effect of cyclic strain amplitude on polymeric complex moduli is highly dependent on the composition and type of the polymer, particularly the molecular structure. Experiments have shown that the complex moduli of polymers generally behave linearly only at low cyclic strain amplitudes.

There are, however, polymers such as pressure sensitive adhesives, which exhibit linearity even at high cyclic strain amplitudes. These polymers usually have very few cross links between long, entangled polymer chains. Therefore, the low interaction between these chains seems to have an effect on the linear behavior over wide strain amplitude ranges. However, most viscoelastic polymers used in typical damping applications behave nonlinearly at high strain amplitudes. This nonlinearity is very difficult to model accurately and involves very complicated theories and a significant number of tests, many more than for linear complex modulus behaviour, to gather data sufficient to establish trends for a specific material [2].

### 3.3 Measuring damping of materials

Most approach of measurement of damping of structure are based on the response of simply systems, in fact many of the approaches applicable to simply system can be applied only to structural modes whose response could be separated from all others because of differences in natural frequencies or in mode shapes. The mainly used method for measuring the viscoelastic response of material are briefly described in the following subparagraph, moreover the dynamical mechanical approach is explained as allows the characterization of material behaviour independently from the structure.

#### 3.3.1 Vibration damping

A vibrating structure, such as a panel, has a carries kinetic energy related to its mass and potential energy related to its stiffness. The dissipated energy, i.e. by heating the structure, during vibration is defined as structural damping.

The mostly used approach for measure the structural damping is to excite the structure in frequency domain, methods based on this approach evaluate damping by isolating each mode in system's transfer function.

However, for structures characterised by an high modal density this methods hardly accurately measure system's damping coefficients. A more accurate approach is to consider the Hilbert envelope, which does not use the temporal signals but their envelope.

Figure 3- 3 shows the test set-up, specimen is hung to an heavy holder by two spring with the aim to replicate boundary condition of free sample in the space. Two springs are needed to avoid rotation of specimen during the test, moreover spring stiffness have to be accurately studied, in fact the holder system may have a resonant frequency much lower than the predicted first specimen's natural mode.

All the test fixture is placed in a climatic chamber able to keep the specimen at temperature range from  $-60^{\circ}\text{C}$  to  $20^{\circ}\text{C}$ .

Specimen would be excited by a shaker in frequency range from 0 to 10000 Hz, the dynamic response is acquired by a number of accelerometers bonded to the vibrating sample

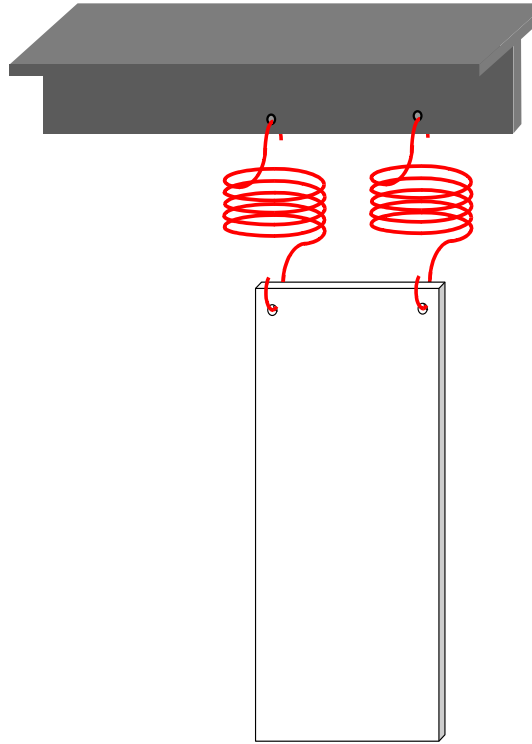


Figure 3- 3: Damping test set-up.

Damping is calculated from acquired data in the range of frequencies below 2000 Hz by the half-power bandwidth method, in fact in this range usually modal shapes and modal frequency could be individually observed and isolated for damping calculation. Above 2000 Hz the Hilbert approach is considered as more accurately due to the superposition of specimen's modal shapes.

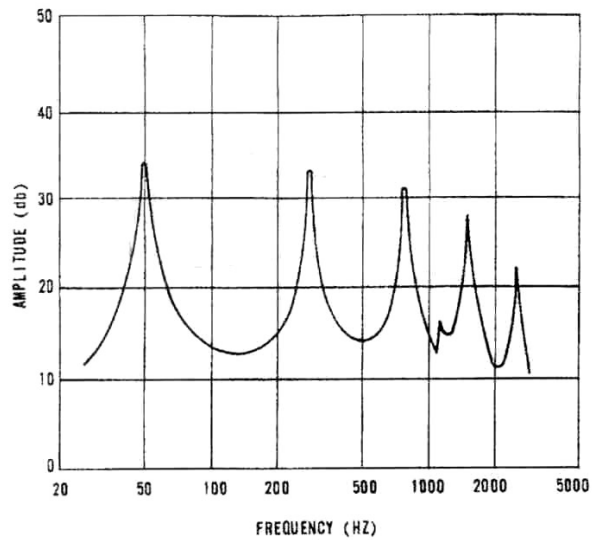


Figure 3- 4: Typical frequency response of a vibrating cantilever beam.



The half bandwidth method could be synthesized as follow: using the response curve from each mode, measure the resonant frequency and the frequencies above and below the resonant frequency where the value of the response curve is 3 dB less (the 3 dB down points) than the value at resonance. The frequency difference between the upper 3 dB down point and the lower 3 dB down point is the half-power bandwidth of the mode. The modal loss factor ( $\eta$ ) is the ratio of the half-power bandwidth to the resonant frequency.

$$\eta = \frac{\Delta f}{f_n}$$

The higher the frequency the higher is the modes having close frequencies then the Hilbert method may be applied analysing data in terms of octave of the bandwidth.

*Decay of unforced vibration*<sup>[1]</sup>

Many aspects of the behaviour of vibrating system can be understood in terms of the simple ideal linear mass system, if the system is displaced by an amount  $x$  from its equilibrium position, the mass less spring produce a force of magnitude  $kx$  tending to restore the mass toward its equilibrium position, while the mass less dashpot produces a retarding force of magnitude  $c\dot{x}$ ;  $k$  is known as spring constant and  $c$  as viscous damping coefficient.

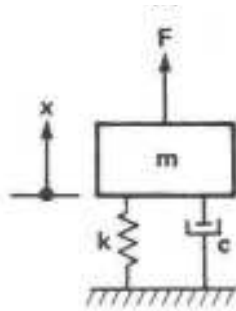


**Figure 3- 5: System with one degree of freedom. From Beranek, Noise and Vibration Control [1].**

If the system is displaced from its equilibrium position by an amount  $X_0$  and then released, the resulting displacement varies with the time as:

$$x = X_0 e^{-j \omega_n t} \cos(\omega_d t + \phi)$$

where  $\omega_n$  and  $\omega_d$  represent the undamped and damped natural frequencies of the system.

These obey

$$\omega_n = \sqrt{\frac{k}{m}} = 2\pi f_n$$

$$\omega_d = \omega_n \sqrt{(1 - \zeta^2)}$$

With  $f_n$  representing the cyclic natural frequency, the constant  $\zeta$  is called damping ratio or fraction of critical damping.

$$\zeta = \frac{c}{c_c}; \quad c_c = 2\sqrt{km} = 2m\omega_n$$

Where  $c_c$  is known as critical damping coefficient.

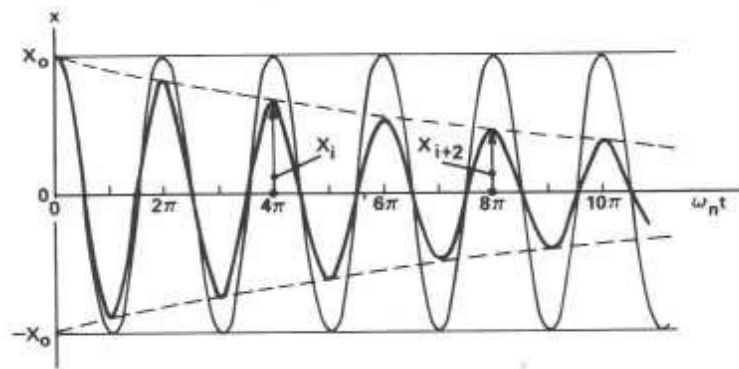


Figure 3- 6: Time variation of displacement of mass-spring-dashpot system released by initial position  $X_0$ .

The logarithmic decrement  $\delta$  is a convenient representation of how rapidly a free oscillation decays

$$\delta = \frac{1}{N} \ln \left( \frac{X_i}{X_{i+N}} \right)$$

Where  $X_i$  represent the value of  $x$  at any selected peak,  $X_{i+N}$  represent the value at the peak at  $N$  cycles from the mentioned one. For a viscously damped system  $\delta = 2\pi \zeta$ .

The total energy  $W$  of the considered simple system consists of the kinetic energy  $W_k$  of the mass and the potential energy of stored in the spring  $W_p$ . The dissipated energy correspond to the work that is done from the dashpot  $W_d$ .

The ratio of the energy dissipated per cycle to the energy present in the system is called damping capacity  $\psi$ . The ratio of the average energy dissipated per radian to the energy in the system is called the loss factor. The loss factor then is equal to  $1/2\pi$  times the damping capacity and for a viscous damped system is related to  $\zeta$  as

$$\eta = \frac{W_d}{2\pi W_{tot}} = 2\zeta$$

### 3.3.2 Dynamical mechanical analysis

Dynamic mechanical properties refer to the response of a material as it is subjected to a periodic force. These properties may be expressed in terms of a dynamic modulus, a dynamic loss modulus, and a mechanical damping term.

For an applied stress varying sinusoidally with time, a viscoelastic material will also respond with a sinusoidal strain for low amplitudes of stress. The sinusoidal variation in time is usually described as a rate specified by the frequency ( $f = \text{Hz}$ ;  $\omega = \text{rad/sec}$ ). The strain of a viscoelastic body is out of phase with the stress applied, by the phase angle,  $\delta$ . This phase lag is due to the excess time necessary for molecular motions and relaxations to occur. Dynamic stress,  $\sigma$ , and strain,  $\epsilon$ , given as

$$\sigma = \sigma_0 \sin(\omega t)$$

$$\epsilon = \epsilon_0 \sin(\omega t + \delta)$$

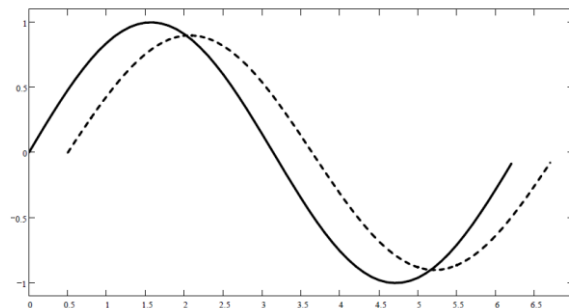


Figure 3- 7: Stress-strain phase shift for a sinusoidally excited material.

The storage modulus is often times associated with “stiffness” of a material and is related to the Young’s modulus,  $E$ . The dynamic loss modulus is often associated with “internal friction” and is sensitive to different kinds of molecular motions, relaxation processes, transitions, morphology and other structural heterogeneities. Thus, the dynamic properties provide information at the molecular level to understanding the polymer mechanical behaviour.

Axial analyzers allow a great deal of flexibility in the choice of fixtures, which allows for the testing of a wide range of materials. Three-point bending depends on the specimen being a freely moving beam, and the sample should be about 10% longer on each end than the

span. The four sides of the span should be true, i.e., parallel to the opposite side and perpendicular to the neighbouring sides. There should be no nicks or narrow parts. Rods should be of uniform diameter. Throughout the experiment the beam should be freely pivoting: this is checked after the run by examining the sample to see if there are any indentations in the specimen. If there are, this suggests that a restrained beam has been tested, which gives a higher apparent modulus. The sample is loaded so the three edges of the bending fixture are perpendicular to the long axis of the sample.

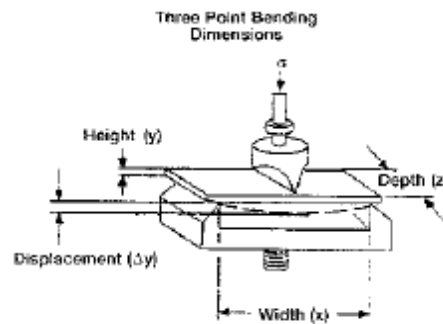


Figure 3- 8: Three point bending testing set-up

#### *Time-Temperature Superposition*

Due to the viscoelastic nature of polymeric materials, the analysis of their long term behaviour is essential. For a viscoelastic polymer, the modulus is known to be a function of time at a constant temperature. The modulus is also a function of temperature at a constant time. According to this time-temperature correspondence, long term behaviour of a polymer may be measured by two different means. First, experiments for extended periods of time can be carried out at a given temperature, and the response measured directly. This technique becomes increasingly time consuming due to the long response times of many polymers. The second method takes advantage of the principles of time-temperature correspondence wherein experiments are performed over a short time frame at a given temperature, and then repeated over the same time frame at another temperature. The two methods are equivalent according to the principles of time-temperature super-positioning. These principles for studying long-term behaviour of polymers have been well established by Williams, Landel, and Ferry [3]. The methods of time-temperature super-positioning (i.e. reduced variables) are used to accelerate the mechanism of a relaxation or molecular event by either increasing the temperature or increasing the stress, in the experiment. A classic example of such a procedure is given below where the stress relaxation modulus from a tensile test is plotted as a function of time, over an accessible time scale, for various

temperatures. A reference temperature of  $T_0=25^\circ\text{C}$  was selected and the modulus-versus-time curves for the remaining isotherms were horizontally shifted towards this reference until an exact superposition is accomplished.

Shifting of each isothermal curve results in a much larger, smooth continuous curve known as a *master curve*. It can be seen that this procedure results in a dramatic increase in the range of the time scale. The inset below is known as the shift factor plot. The shift factor,  $a_T$ , represents the magnitude of shifting along the x-axis, necessary for a specific isotherm to superimpose on its neighbour in the final master curve with respect to a given reference temperature. The  $\log a_T$  versus temperature plot should be a smooth monotonic curve, provided the mechanism of relaxation remains the same during the process. An inflection in the shift factor plot would be indicative of a change in the mechanism of the process, thus invalidating the procedure.

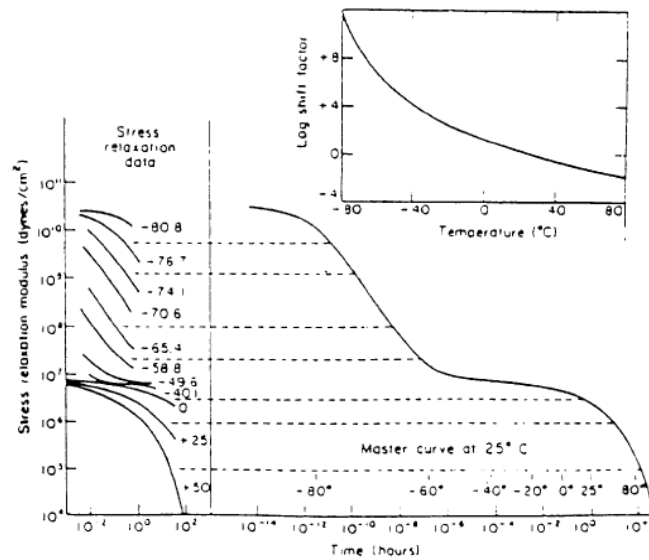


Figure 3- 9: Typical master curve for a viscoelastic material

The actual graphical procedure can be mathematically described for a shifted isotherm  $T_1$  as

$$E(T_0, t) = E(T_1, t/a_T)$$

This implies that the effect of changing temperature is the same as multiplying the time scale by a factor  $a_T$ , i.e., an additive factor to the log time-scale.

The criteria for the application of time-temperature super-positioning have been described in detail in Ferry's text. The first criterion is that all adjacent curves should overlap over a

reasonable number of data points. The second criterion is that the same values of the shift factor must translate all of the viscoelastic functions. Finally, the shift factor must follow one of the well-established relationships. The shift factor is usually described either by the WLF equation or the Arrhenius relationship. The WLF equation, named after its founders Williams, Landel, and Ferry, is described as

$$\log a_T = \frac{-C_1(T - T_g)}{C_2 + (T - T_g)}$$

and is associated with the transition, plateau, and terminal regions of the time scale. The constants  $C_1$  and  $C_2$  are material dependent parameters that have been associated with fractional free volume. The values of  $C_1=17.4$  and  $C_2=51.6^\circ\text{K}$  were originally thought to be “universal” and are still widely used. The glassy region of a polymer is accurately described by the second form of the shift factor, namely the Arrhenius form

$$\log a_T = \frac{-\Delta E}{2.303 R} \left( \frac{1}{T} - \frac{1}{T_{\text{ref}}} \right)$$

Where  $\Delta E$  is the activation energy (kJ/mole),  $R$  is the universal gas constant,  $T$  is temperature ( $^\circ\text{K}$ ) and  $T_{\text{ref}}$  the reference temperature ( $^\circ\text{K}$ ). The material response is shifted by a phase angle  $\delta$  ( $<0$ ) representing the damping character of the material under testing. The total stored energy for a system sinusoidally stressed could be easily evaluated as the integral over a cycle of vibration:

$$W_{\text{tot}} = \int_0^{\frac{2\pi}{\omega}} \sigma \varepsilon dt$$

Recalling the stress-strain relation

$$\sigma = \sigma_0 \sin(\omega t)$$

$$\varepsilon = \varepsilon_0 \sin(\omega t + \delta) = \varepsilon_0 [\sin \omega t \cos \delta + \cos \omega t \sin \delta]$$

the total stored energy is

$$W_{\text{tot}} = \frac{1}{2} \sigma_0 \varepsilon_0 \cos \delta = \frac{1}{2} E' \varepsilon_0^2$$

Instead the dissipated energy during a cycle of vibration is

$$W_d = \int_0^{\frac{2\pi}{\omega}} \sigma \frac{d\varepsilon}{dt} dt$$

$$W_d = \pi \sigma_0 \epsilon_0 \sin \delta = \pi E'' \epsilon_0^2$$

The loss factor is evaluated as

$$\eta = \frac{W_d}{2\pi W_{\text{tot}}} = \frac{E'}{E''} = \tan \delta$$

Because of this equivalence between loss factor and  $\tan \delta$ , in the rest of the work the two terms would indifferently used.

### 3.4 References

- [1] Beranek LL, Vèr IL, 1992. Noise and Vibration Control Engineering: Principles and Applications. *John Wiley & Sons*.
- [2] Jones DG, 2001. Handbook of viscoelastic vibration damping. *John Wiley & Sons*.
- [3] Menard KP, 1999. Dynamic Mechanical Analysis, A practical introduction. *CRC press*.
- [4] ASTM E-756, 2004. Standard test method for measuring vibration-damping properties of materials. *ASTM International*.
- [5] Lakes RS, 2004. Viscoelastic measurement techniques. *Review of Scientific Instruments* 75.
- [6] Ungar EE, Kerwin EM 1962. Loss factors of viscoelastic systems in terms of energy concepts. *Journal of Acoustical Society of America* 34



# Hybrid composites embedding damping features

## 4.1 Summary

In this chapter, hybrid laminate architecture enhancing damping features are presented and described. The passive damping of a composite material could be improved by modifying the laminate structure at each of its characteristic level.

The well known interleaved solution is examined considering the experimental works published by Berthelot et al., the insertion of a viscoelastic sheet within laminate contribute to enhance damping of the laminate. This architecture induce greater interlaminar stresses within the soft viscoelastic layer due to the stiffness gradient, then dissipation gain due to capability of the viscoelastic material.

The passive damping of a composite lamina could be enhanced by imagining an hybrid fiber preform which includes viscoelastic material or by means of a lamina consisting in an high damping matrix. In the fourth paragraph. based on the concept of directional damping a novel hybrid architecture is presented, viscoelastic material is embedded in the lamina as long fibres arranged along carbon tow into the preform. Passive damping of the hosting matrix could be improved by dispersing carbon nanotubes within the resin before the lamina infusion.

## 4.2 Enhancement of damping in polymer composites

Polymer composites have generated increasing interest, in the development of damped structural materials, because of their low density and excellent stiffness and damping characteristics, it appears that design changes enhancing in damping will also cause a corresponding reduction in stiffness and strength. The improvement of damping can be achieved by active and/or passive means. Active damping control requires sensors and actuators, a source of power, etc... Passive damping control consists of the use of structural modifications, damping materials and/or isolation techniques. Passive damping typically requires high loss viscoelastic materials or fluid material and thermal control. Material damping can contribute to the passive control system by using the inherent capacity of the material to dissipate vibrational energy. Due to reduced system complexity, passive damping contributes more effectively to the improvement of machine and structures reliability than active solutions. In addition, some passive damping may be required in order to have a stable active control system.

At the macro-mechanical level, research has emphasized the study of constituent layer properties and orientations, interlaminar effects, vibration coupling, surface attachments and damping treatments, co-cured damping layers and hybridization of laminae, all of this parameters may have a significant influence on the attainment of improved damping characteristics. At micromechanical level, damping increment could be achieved by optimizing the fiber orientation, fiber aspect ratio, fiber spacing, fiber/matrix interphase effects, fiber coating, fiber and matrix properties, and by using constituent material hybridization.

The objective of designing composite structures with improved or optimized damping characteristics has led to the development of mechanical theories for the modelling of composite damping at the micromechanical and macromechanical levels. Improved damping of composite materials combined with high stiffness and strength can be realized by control of the geometrical and mechanical properties at several levels.

One passive method for increasing the damping capacity of composite structures involve the use of surface damping treatments, this can be achieved by the application of damping tapes to the structure after manufacturing. The damping tape is typically a viscoelastic material sandwiched between the base structure and a thin constraining layer;; damping will be improved by the fact that the vibration energy will be dissipated by shearing motion of the viscoelastic layer as the base structure vibrates in flexure. Damping due to constrained layer could also be optimized by selecting the proper length of the constraining layer.

Interlaminar stresses generally arise at lamina interfaces near free edges in composite laminates, the existence of this interlaminar stresses means that part of the total energy dissipation in a laminate will be due to inter laminar damping. Hwang and Gibson [2] by using a three dimensional finite element/ strain energy techniques showed that there exist an optimal fibres orientation and an optimal laminate width to thickness ratio ( $w/t$ ) for maximizing the contribution of interlaminar damping, it was also shown that the interlaminar damping is important only when the laminate is thick.

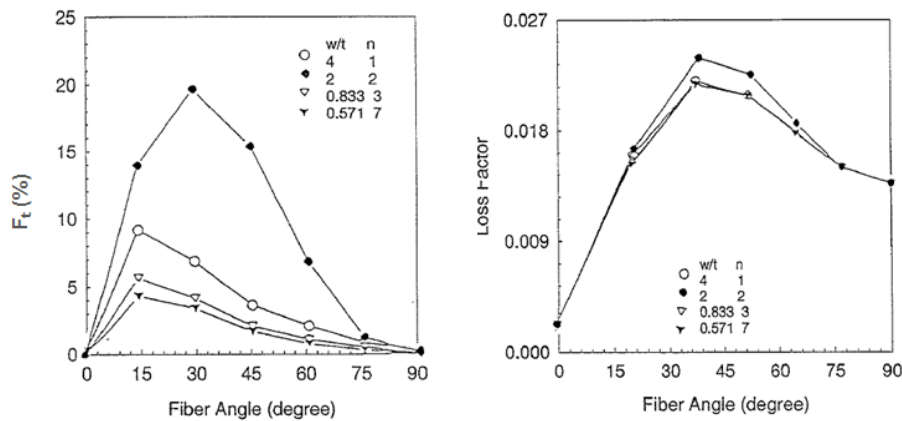


Figure 4- 1- A) Contribution of interlaminar damping as function of fibres orientation. B) Variation of total loss factor with fibres orientation under uniaxial extension. From Hwang and Gibson [2]

Coupling effects could also be used for damping enhancement, in fact, additional dissipation mechanism could be induced in the laminate by change the structure deformation mode (e.g. properly defining the stacking sequence). The damping of fiber-reinforced composite materials is often too low for many applications and appropriate form modifications are usually required. Starting from basic dissipation mechanism within composite materials (Chapter II) it is possible to design hybrid composites integrating damping features based on the use of a appropriately chosen filler, capable to improve the passive dissipation performance of the material. Hybrid solutions could be proposed by modifying the material architecture over different dimensional scales. At macro level the interlaminar damping dissipative mechanism could be triggered by inserting a viscoelastic layer in stacking sequence, whereas at micro level hybrid solution could be implemented making hybrid the dry preform or toughening the resin. The main focus of this chapter is to examine suitable architectures paying attention on the dimensional scale. The hybrid architecture examined consist of a carbon-fiber based laminate with damping material embedded. Hybrid architectures at lamina level (micro scale) could be proposed or integrating viscoelastic material within the dry preform, or functionalizing the resin system.

### 4.3 Macro scale: Interleaved visco-elastic layer

Although surface damping treatments can increase damping significantly, the constrained layer adds undesirable weight to the structure. The advantage of the using composites with embedded co-cured viscoelastic layer is that no extra constraining layer is needed and the weight add to the system is less than the weight added by the constrained layer in surface treatment. In the Figure 4- 2 the concept of interleaved layer architecture is shown, a layer of damping material is embedded within the laminate building a sandwich-like structure with a dissipative core and two orthotropic faces.

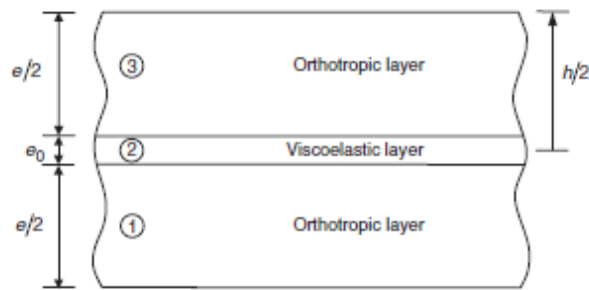


Figure 4- 2: Hybrid laminate, Interleaved viscoelastic layer architecture

At the laminate level, damping is strongly dependent on the layer constituent properties as well as layer orientations, interlaminar effects and stacking sequence.

The concept behind this solution is the interlaminar damping effect highlighted in the previous paragraph, as first choice the viscoelastic layer is positioned at laminate center as the interlaminar stress reach its maximum value. Architectures with more than one viscoelastic layer could be valuable after a study of the interlaminar stress distribution based on mechanical stiffness of each layer and on stacking sequence.

#### 4.3.1 Experimental proof of concept

In this paragraph, experimental data from literature are reviewed as proof of the capability of enhance the damping by increasing the ratio of total energy stored in transverse shear mode. The effectiveness of this architecture for damping enhancement has been proven by Kishi et al. [4], in their study unidirectional prepreg tapes has been considered (supplied by Toray Industries Inc.).

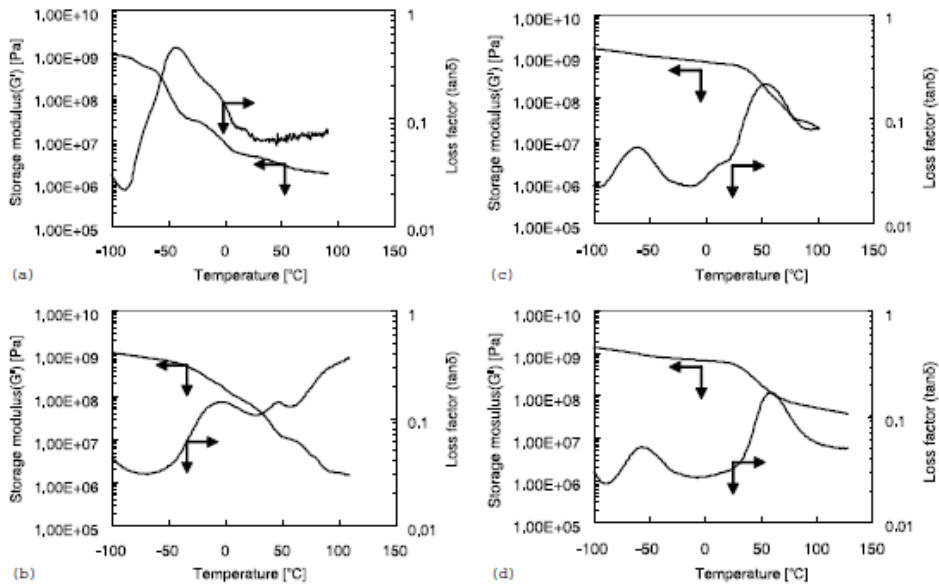


Figure 4- 3: Dynamic visco-elastic properties of thermoplastic elastomers considered as interleaf films, measured at the frequency of 10 Hz. From Kishi et al. [4]

Thermoplastic materials have a storage modulus significantly less than the carbon reinforced ply (order of 100 GPa along and 10 GPa orthogonal fibres), moreover they exhibit a strong damping capacity.

Hence in the lower stiffness interleaf films higher strain would be easily achieved and it would absorb more energy, apart from the gradient in stiffness within the material the energy stored (and then the dissipated energy) could be increased by tailoring the arrangements of the ply in the laminate.

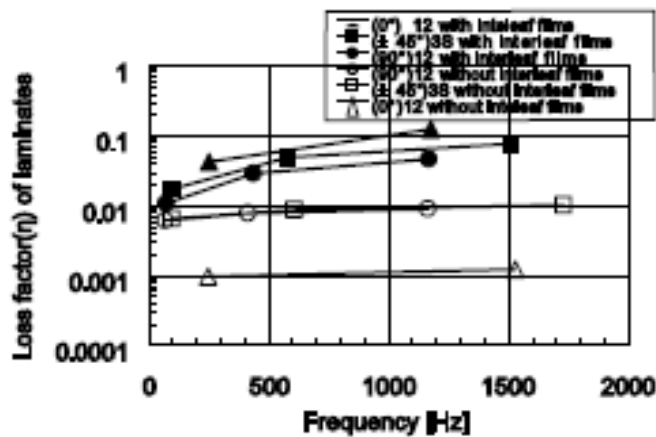


Figure 4- 4: Damping properties of thermoplastic polyurethane interleaved laminates and non interleaved laminate, depending on the lay-up sequences. From Kishi et al. [4]

For simple laminate sequences without interleaf films, the loss factor of  $(\pm 45^\circ)_{3S}$  laminates was higher than that of  $(0^\circ)_{12}$ , but the loss factor of the  $(0^\circ)_{12}$  with an interleaved layer is greater than the  $(\pm 45^\circ)_{3S}$  using the same film disposition (Figure 4- 4). The arrangement of

the reinforcing fibres control the stiffness of the interlaminar zone and it would have considerable influence on the amount of local strain of the interlaminar film.

Another decisive effect may be considered in this architecture configuration, is represented by the resultant reduction in modulus of the composite laminate whilst obtaining better damping properties, which is a disadvantage for structural applications.

Berthelot and Sefrani published in 2006 ([10], [6]) the experimental data on unidirectional tapes of glass fiber composites, they systematically proven the effectiveness of this architecture for damping improvement, they proposed also a theoretical model based on the Ritz method for the modal solution of equation of motion. Three types of laminates have been investigated by Berthelot and Sefrani: a) a laminate with a single viscoelastic layer interleaved at the mid-plane with nominal thickness of 200  $\mu\text{m}$ , b) ) a laminate with a single viscoelastic layer interleaved at the mid-plane with nominal thickness of 400  $\mu\text{m}$  and c) a laminate with two viscoelastic layers of 200  $\mu\text{m}$  symmetrically disposed from the middle plane.

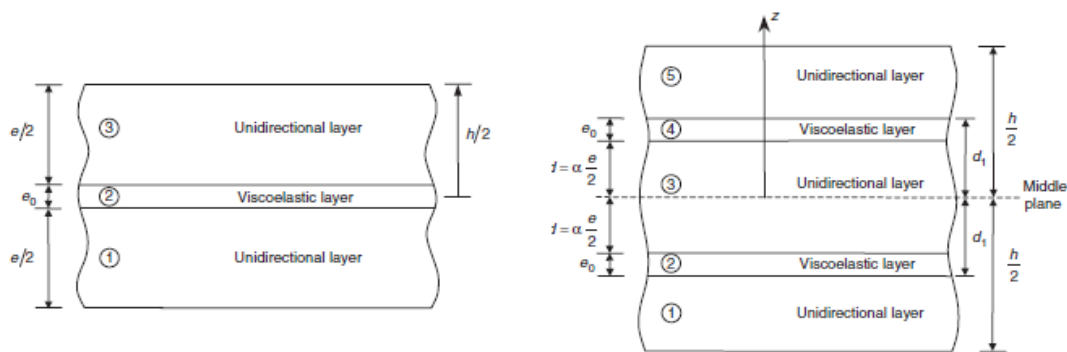


**Figure 4- 5: Two different laminates with interleaved visco elastic layers. a) a layer interleaved in the mid-plane and b) two layers interleaved away from the mid-plane**

The test specimens have been tested by the impulse test, an instrumented hammer is used to induce the excitation of flexural vibrations of the beam and the beam response is detected by using a laser vibrometer [7]. Data shows a strong improvement in damping capacity of the specimen (Figure 4- 6, Figure 4- 7) in each case the insertion of a damping layer inside the material lead to a better damping behaviour of the material.

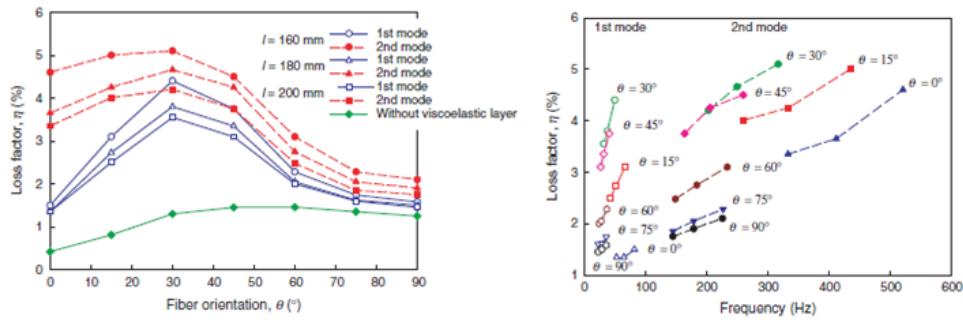


Figure 4- 6: Experimental results in the case of glass fiber composites with a single viscoelastic layer of thickness of 200  $\mu\text{m}$  interleaved in the middle plane and for three lengths of the test specimens. a) laminate damping as function of the fiber orientation and b) laminate damping as function of the modal frequency. From Berthelot and Sefrani [10].

In Figure 4- 7 the behaviour of laminates with the same volume content of damping for the first two modes have been reported, in fact in both laminates an overall thickness of 400  $\mu\text{m}$  are embedded but in the second laminate the damping material is split in two layer of 200  $\mu\text{m}$  positioned away from the middle plane. Both cases exhibit an increment in damping but the best solution is the middle plane positioning of the damping material.

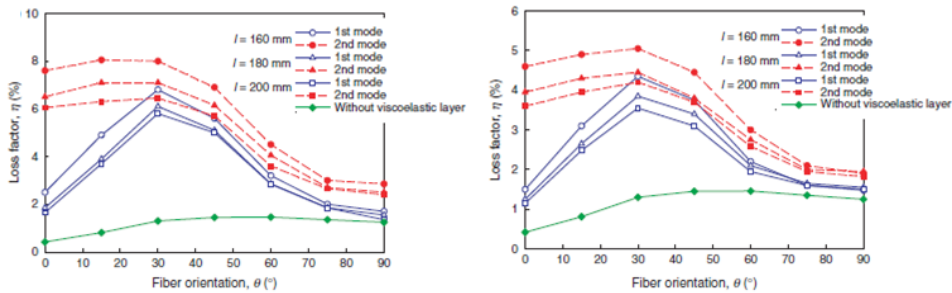


Figure 4- 7: Experimental laminate damping as function of the fiber orientation for three lengths of the test specimens. a) laminate with a single viscoelastic layer of thickness 400  $\mu\text{m}$  interleaved at middle plane, b) laminate with two viscoelastic layers of 200  $\mu\text{m}$  interleaved away from the middle plane. From Berthelot and Sefrani [10].

Berthelot and Sefrani experimental analysis allows to remark regarding, the effect of interlaminar damping, they considered in experimental work unidirectional tape, where the shear stress are distributed as a parabola which reaches its maximum value at the beam neutral axis (in this case it coincides with the middle plane) therefore to maximize the strain energy stored in the viscoelastic material is opportune to stack the damping layer in its correspondence. This general concept could be applied to an angle ply laminates, where the shear stress are distributed as arc of parabola within the single ply continuous at the boundary but with discontinuous tangent value related to the stiffness of each lamina.

As evidence for an angle ply laminated composite the enhancement in passive damping could be tailored by the analysis of shear stresses distribution, in fact the presence of  $\pm 45^\circ$  layers could create a central region in the laminate where the shear stresses are quite constants, in that way not only the shear strain energy of the viscoelastic material could contribute to dissipating phenomenon. In fact, if the viscoelastic layer is away from neutral axis normal strains are non zero and the elongational components of the stress / strain tensor could contribute.

### 4.3.2 Macro-mechanics for hybrid laminates

Under the hypotheses of perfect bonding, interleaved layer could be analysed by the theoretical approach proposed in the chapter II, where the proposed 3-D laminates analysis allows the evaluation of energy stored in both in-plane and out-of-plane mode.

The visco-elastic layer is accounted in the stacking sequence as a ply with isotropic elastic behaviour. For an isotropic material, certain relations between the engineering constants must be satisfied, the shear modulus is defined in terms of the Young modulus E and Poisson's ratio  $\nu$ , as

$$G = \frac{E}{2(1 + \nu)}$$

therefore the elastic behaviour of an isotropic material could be described by only two independent parameters. The stiffness matrix is then represented as follows

$$\begin{Bmatrix} \sigma_1 \\ \sigma_2 \\ \sigma_3 \\ \tau_{23} \\ \tau_{13} \\ \tau_{12} \end{Bmatrix} = \begin{bmatrix} C_{11} & C_{12} & C_{12} & 0 & 0 & 0 \\ C_{12} & C_{11} & C_{12} & 0 & 0 & 0 \\ C_{12} & C_{12} & C_{11} & 0 & 0 & 0 \\ 0 & 0 & 0 & \frac{(C_{11}-C_{12})}{2} & 0 & 0 \\ 0 & 0 & 0 & 0 & \frac{(C_{11}-C_{12})}{2} & 0 \\ 0 & 0 & 0 & 0 & 0 & \frac{(C_{11}-C_{12})}{2} \end{bmatrix} \begin{Bmatrix} \varepsilon_1 \\ \varepsilon_2 \\ \varepsilon_3 \\ \gamma_{23} \\ \gamma_{13} \\ \gamma_{12} \end{Bmatrix}$$

Similarly the loss matrix could be arranged, as well as for the elastic characterization two independent parameters describes the loss behaviour of an isotropic material [8], the elongational loss factor  $\eta_{11}$  and the shear loss factor  $\eta_{12}$  then the on-axis loss matrix is formulated in terms of SDC (specific damping capacity  $2\pi \eta$ , as demonstrated in the chapter III)



$$[\Psi] = \begin{bmatrix} \Psi_{11} & 0 & 0 & 0 & 0 & 0 \\ 0 & \Psi_{11} & 0 & 0 & 0 & 0 \\ 0 & 0 & \Psi_{11} & 0 & 0 & 0 \\ 0 & 0 & 0 & \Psi_{12} & 0 & 0 \\ 0 & 0 & 0 & 0 & \Psi_{12} & 0 \\ 0 & 0 & 0 & 0 & 0 & \Psi_{12} \end{bmatrix}$$

A transformation law could be derived taking in account the invariant property of strain energy to the stress-strain transformation,

$$[\psi_c] = [R_\sigma]^T [\psi] [R_\sigma^{-1}]^T$$

The off-axis loads could induce coupling effects contributing at the global dissipation.

Below the hypothesis of perfect bonding with adjacent orthotropic layers the approach presented in the chapter II allows the evaluation of damping performances of an hybrid laminate embedding viscoelastic layers, in order to utilize the numerical model the complete elastic and loss matrices have to be split in their sub-matrices including in plane and out of plane components.

The in-plane elastic and dissipative matrices in the material principal reference system (on-axis) are formulated as [8],[9]:

$$[Q] = \frac{E}{1-\nu^2} \begin{bmatrix} 1 & \nu & 0 \\ \nu & 1 & 0 \\ 0 & 0 & \frac{1-\nu}{2} \end{bmatrix}$$

$$[\Psi] = \begin{bmatrix} \Psi_{11} & 0 & 0 \\ 0 & \Psi_{11} & 0 \\ 0 & 0 & \Psi_{11} \end{bmatrix}$$

The out of plane sub-matrices representing transverse shear elements in the material principal reference system (on-axis)

$$[Q_s] = \frac{E}{2(1+\nu)} \begin{bmatrix} 1 & 0 \\ 0 & 1 \end{bmatrix}$$

$$[\Psi_s] = \begin{bmatrix} \Psi_{12} & 0 \\ 0 & \Psi_{12} \end{bmatrix}$$

The approximation of the model suggested ensures the transverse stress continuity at the layer interfaces, then the strains within materials are calculated by the constitutive laws assuming the perfect bonding from layers.

The strain in the viscoelastic sheet is a critical parameter because as results of the external loads excessive deformation could incur.

#### 4.4 Micro scale: hybrid layers

As matter of fact, the overall composite stiffness is an averaged properties based on their constituents and their configuration within the material, since the increment of interlaminar shear energy enables to a stronger dissipation, then a soft material is required for properly assemble the hybrid laminate. Two effects may be accounted for hybrid laminates with interleaved “soft” layer: a) a softer material implies a loss in the material stiffness, and b) the increment of transverse shear effects implies greater interlaminar stresses. Both these effects can be very dangerous due to reduction of laminate delamination strength and potential failure which can occur in the soft material to the stress level reached.

Many studies have been conducted to decrement the hazard of an excessive loss in mechanical performance of the final composite, in particular modifications based on the interleaved configuration have been proposed, bearing in mind, the concept of the stiffening up of the viscoelastic layer [11]. However, the simple stiffening of viscoelastic layer leads to the decrement in elastic modulus gradient in thickness direction and then the possibility of decrease the interlaminar damping worsening overall performance of the material.

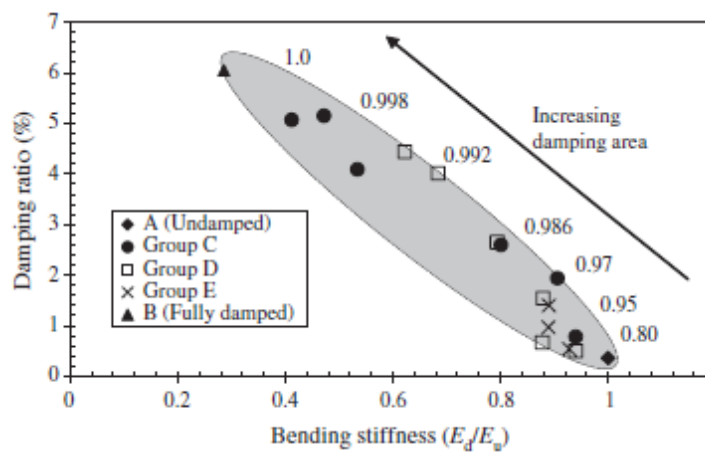


Figure 4- 8: Damping ratio vs normalised bending stiffness, from [10]

In the previous figure, the relationship between the bending stiffness and measured damping is presented for an interleaved layer hybrid laminate. It is observed that as the damping area increases the bending stiffness decreases and damping increases, thus the bending stiffness is sacrificed to achieve higher damping [10].

A suitable strategy for improving material damping capacity is to use the distinguishing anisotropy behaviour of composites to define an hybrid architecture able to dissipate

energy not mainly in interlaminar damping but thought up that it is capable to store energy also in elongational mode.

In their pioneering works on the damping behaviour of composite materials Adams et al. [12], [13] assumed that the damping mechanism for a orthotropic composite material consists of only three components: longitudinal damping, transverse damping and longitudinal shear damping, afterwards following Saravanos and Chamis [14] the damping behaviour of the lamina has been characterised by six damping component each associate with the corresponding element in the stress tensor. Hence the damping mechanism depends on the load pattern and the capability of the material to allocate energy in the six available modes.

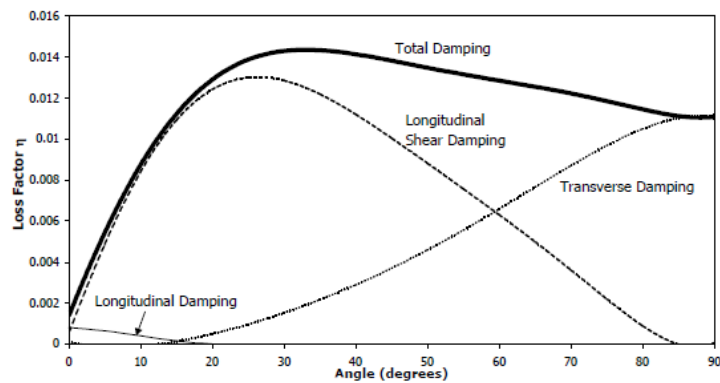


Figure 4- 9: Allocation of dissipation components vs fiber orientation in a composite beam [11].

The hybrid architecture proposed has the damping material embedded at lamina level as long fibres in carbon tows.

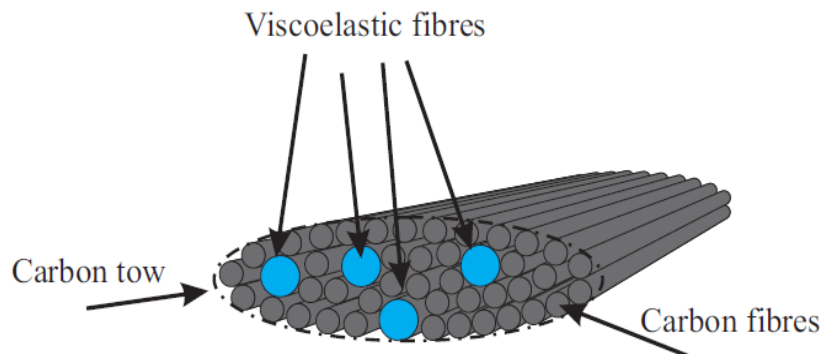


Figure 4- 10: Proposed hybrid lamina architecture

The conceptual idea behind this architecture is based on the concept of energy allocation within the lamina, the insertion of a viscoelastic material in the carbon tow direction allows a less decrease of mechanical modulus of the final composite, moreover the geometry itself of the added damping material generate a dominant deformation in elongational mode, rising up the corresponding stored energy and consequently the energy dissipated by this component. In addition, the novel architecture proposed implies lower interlaminar stress and then a better failure strength for the final composite.

#### 4.4.1 Visco-elastic modelling for hybrid fiber layers

Hybrid composites have higher degree of freedom than single fiber reinforced composites as well as more advanced comprehensive qualities. By impregnating two or more kinds of fiber in one matrix, hybrid composites can provide a large range of properties. The establishment of hybrid model not only aids to the survey of the hybrid mechanism, but also provides a theoretical foundation for the design of mechanical properties in materials. Evaluation of viscoelastic properties of the hybrid composite require an estimation of fiber content for each type of filler.

$$V_{\text{fibres}} = \frac{S_F + S_f}{S}$$

If fibres have comparable diameters their content in the final composite is represented by volume fraction of perform within the composite, then in reason of the dry perform composition the volume fraction in each case could be calculated.

More considerations need the case of hybrid lamina with different diameter fibres, a simple mechanical model was proposed in the case of hybrid systems constituted of BF-CFRP or SiCF-CFRP [15]. Fibres are assumed to be arranged tightly, closely and regularly; large diameter fibres are tangent to each other and small diameter fibres are nested into the interval space formed. Regular triangle and quadrilateral hybrid formation are two kinds of the most popular model. If smaller diameter fibres are arranged as in the regular triangular model, Figure 4- 11a, indicating as  $v_f$  the fiber volume fraction of the single small diameter, fiber composite, the number of fibres nested is equal to:

$$n_f = \frac{(\sqrt{3}-\pi/2) R^2 v_f}{\pi r^2}$$

Whereas if fibres are arranged as the regular quadrilateral model the number of small fibres included in the representing area is:

$$n_f = \frac{(4-\pi) R^2 v_f}{\pi r^2}$$

where R and r are respectively the diameters of large and small fibres.

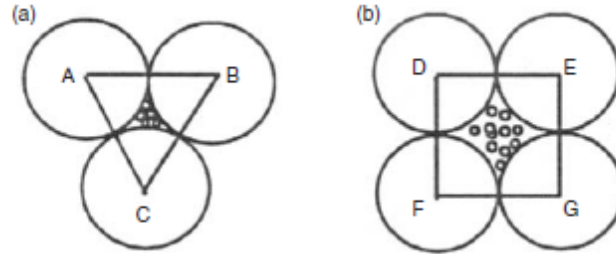


Figure 4- 11: Two ideal hybrid models: a) regular triangle model b) regular quadrilateral model.

Assuming a region with area, S including  $n_f$  large diameter fibres, whose filled area is

$$S_F = n_F (\pi R^2)$$

while the area occupied by the small fiber

$$S_f = \left( \frac{S_F}{V_F} - S_F \right) v_f = n_F (\pi R^2) \left( \frac{1}{V_F} - 1 \right) v_f$$

Then the fiber volume content in hybrid composites is

$$v_f = \frac{S_F + S_f}{S} = \frac{S_F + S_f}{S_F/V_F} = V_F + (1 - V_F) v_f$$

Starting from the fiber volume content in each case the mechanical and dissipative properties could be calculated by a simple application of the rules of mixtures for composites and averaging the mechanical and dissipative properties.

In the proposed approach, the hybrid fibres lamina is divided in two composites, which mechanical and dissipative properties are function of their fiber content and by the unified micromechanical approach explained in the chapter II completely determined by the constituents properties. The final hybrid lamina properties would be evaluated by considering how the amount of fiber in the composite is arranged in terms of percentage content for each fiber type. The final stiffness matrix and the final loss matrix are evaluated by averaging the stiffness and loss matrices of each sub-composite in reason of their content.

## 4.5 Increment of dissipation energy by nano-fillers

An alternative to the examined architectures for increment the material damping is to engineering the damping properties into the structure by introducing nanoscale fillers (such as carbon nanotubes) into the hosting matrix . There are numerous reports in literature on the use of carbon nanotubes to augment mechanical properties of composite materials, these reports have focused primarily on static strength and stiffness [17-19]. For such nanocomposites, the combination of extremely large interfacial contact area and low mass density of the filler materials implies that frictional sliding of nanoscale fibres within the matrix has the potential to cause significant dissipation of energy with minimal weight penalty. Figure 4- 12 shows the stick-slip mechanism, when a normal tensile stress is applied to a composite, it starts elongating, as a results of the applied stress the matrix starts to applying a shear stress on the nanutube, thus causing the load to be transferred to nanotubes. When the applied stress is small, the nanotubes remain bonded to the epoxy (sticking phase), as the applied stress increases the shear stress on nanotubes increases too. If the shear stress the critical value for the debonding the matrix start flowing over the surface of nanotube, and no more load is transferred, there occurs energy dissipation due to the slippage between the matrix and the filler.

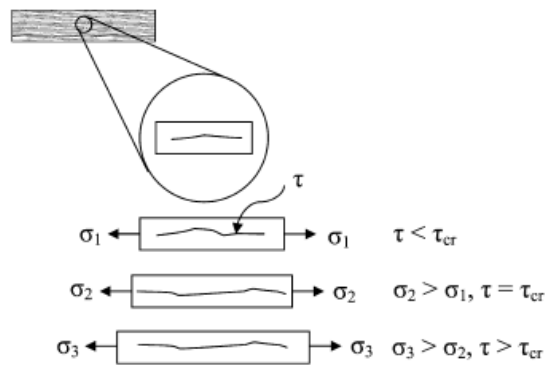


Figure 4- 12: Stick-slip mechanism.

If the adhesion between nanotubes and epoxy is good, less slippage will occur. The stiffness of the composite increases as a result of good adhesion and better load transfer. Higher stiffness leads to an increase in the natural frequency of the composite. On the other hand, if the adhesion between nanotubes and epoxy is poor, there would not be any significant load transfer. Instead, there will be more slippage at the interface which will result in more dissipation of energy.

Several papers have reported significant increases in internal damping of polymer nanocomposites when CNTs are used as reinforcement. Koratkar et al. [20] reported that densely packed MWNT nanofilms have been embedded as inter-layers within laminates sandwich to enhance both stiffness and damping of the laminates.

Rajora and Jalili [21] examined the stiffness and the damping properties of carbon nanotube-epoxy system, an increment of material damping up to 700% had observed.

In their study a comparison of damping feature for epoxy nano-composites filled by both single walled and multi-walled carbon nanotubes has conducted. The multi-walled nanotubes exhibit a damping enhancement extremely stronger than single walled.

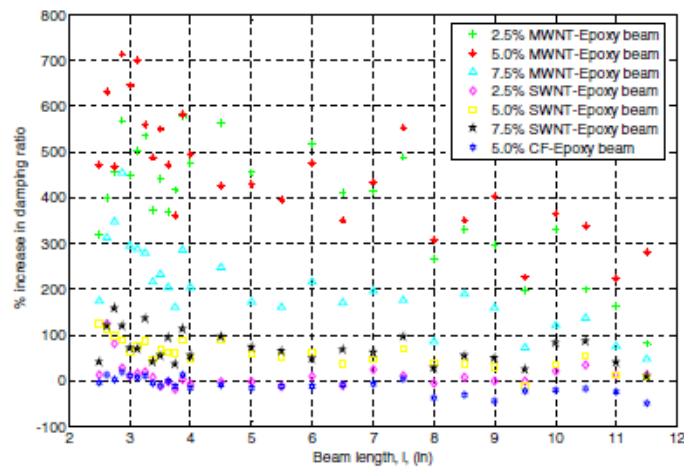


Figure 4- 13: percent increment of passive damping changing dimension. From Rajora [20].

Moreover they experimentally observed the existence of an optimum content of carbon nanotubes within the matrix, phenomenon that could be related to the state of dispersion of filler.

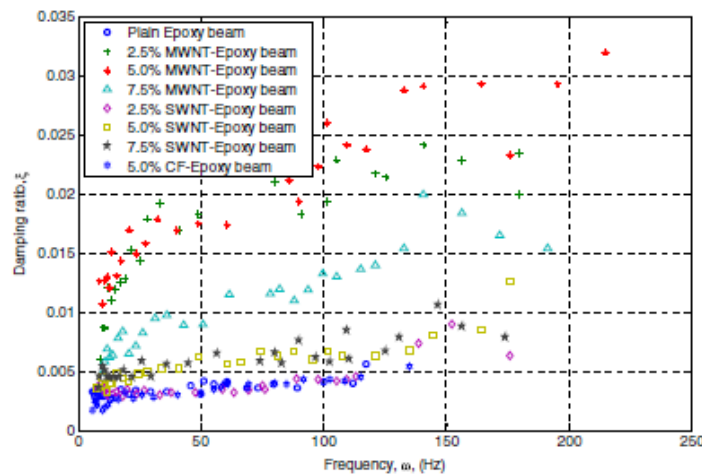


Figure 4- 14: Effect of filler content in damping ratio. From Rajora [20].

## 4.6 References

- [1] Finegan IC, Gibson RF, 1999. Recent enhancement of damping in polymer composites. *Composite Structures Vol. 44*.
- [2] Hwang SJ, Gibson RF, 1992. The use of strain energy-based finite element techniques in the analysis of various aspects of damping of composite materials and structures. *Journal of Composite Materials Vol. 26*.
- [3] Biggerstaff JM, Kosmatka JB, 1999. Damping performance of co-cured graphite/epoxy composite laminates with embedded damping materials. *Journal of Composite Materials 33*.
- [4] Kishi H, Kuwata M, Matsuda S, Asami T, Murakami A, 2004. Damping properties of thermo-plastic interleaved carbon fiber-reinforced epoxy composites. *Composites Science and Technology Vol. 64*.
- [5] Berthelot JM, Sefrani Y, 2006. Damping analysis of unidirectional glass fiber composites with interleaved viscoelastic layers: Experimental investigation and discussion. *Journal of Composite Materials Vol. 40*.
- [6] Berthelot JM, Sefrani Y, 2006. Damping analysis of unidirectional glass fiber composites with interleaved viscoelastic layers: Modelling. *Journal of Composite Materials Vol. 40*.
- [7] Berthelot JM, Sefrani Y, 2004. Damping analysis of unidirectional glass and Kevlar fibre composites. *Composite Science and Technology Vol. 64*.
- [8] Saravanos DA, Chamis CC, 1991. The effects of interplay damping layers on the dynamic response of composite structures. *NASA Technical Memorandum 104497*
- [9] Jones R 1998. Mechanics of composite materials. *Taylor & Francis*.
- [10] Robinson MJ, Kosmatka JB, 2006. Improved damping in VARTM composite structures using perforated viscoelastic layers. *Journal of Composite Materials Vol. 40*.
- [11] Biggerstaff JM and Kosmatka JB, 1999. Directional damping materials for integrally damped composite plates. *SPIE Proceeding of "Passive damping and isolation"*
- [12] Adams RD, Bacon DGC, 1973. Effect of fibre orientation and laminate geometry on the dynamic properties of CFRP. *Journal of Composite Materials Vol. 7*
- [13] Ni RG, Adams RD, 1984. The damping and dynamic moduli of symmetric laminated composite beams-Theoretical and experimental results. *Journal of Composite Materials Vol. 18*
- [14] Saravanos DA and Chamis CC, 1989. Unified micromechanics of damping for unidirectional fiber reinforced composites. *NASA Technical memorandum 102107*.



- [15]Mingchao W, Zuoguguang Z and Zhijie S, 2009. The hybrid model and mechanical properties of hybrid composites reinforced with different diameter fibers. *Journal of Reinforced Plastics and Composites Vol.28*.
- [16]Tsai JL, Chi YK, 2008. Effect of fiber array on damping behaviours of fiber composites. *Composites: Part B Vol. 39*.
- [17]Gojny FH, Wichmann MHG, Kopke U, Fielder B, Sculte K, 2004. Carbon nanotube reinforced epoxy composites: enhanced stiffness and fracture toughness at low nanotube content. *Composites Science and Technology 64*.
- [18]Coleman JN, Khan U, Blau W, Gun'ko Y, 2006. Small but strong: A review of the mechanical properties of carbon nanotube-polymer composites. *Carbon 44*.
- [19]Formicola C, Martone A, Zarrelli M, Giordano M, 2009. Reinforcing efficiency of different aspect ratio carbon nanotube/epoxy composites. *Proceeding of CNTComp, 4<sup>th</sup> International Conference on carbon based nanocomposites*.
- [20]Suhr J, Koraktar N, 2008. Energy dissipation in carbon nanotube composites: a review. *Journal of Material Science 43*.
- [21]Rajora H, Jalili N, 2005. Passive vibration enhancement using carbon nanotube epoxy reinforced composites. *Composites Science and Technology 65*.
- [22]Sun L, Gibson RF, Gordaninejad F, Suhr J, 2009. Energy absorption of nanocomposites: a review. *Composites Science and Technology 69*.
- [23]Martone A, Formicola C, Zarrelli M, Giordano M, 2008. Structural damping efficiency in carbon nanotubes/monocomponent epoxy nanocomposites. *Proceeding of AIDC2008, Workshop on nanomaterials production characterization and their industrial applications*.

# 5

## Multi-scale modelling of hybrid composites

### 5.1 Summary

The analytical model describing the damping behaviour of hybrid composite material proposed in the previous chapters allows the design of hybrid multifunctional material accounting not only the mechanical performances but also its dissipative features.

The numerical tool, based on the presented model, has embedded in the multi-objective platform modeFRONTIER, which integrate optimization and statistical procedure which are used for the individuation of the optimal hybrid architecture related to the specific boundary conditions.

In this chapter, first the numerical analysis on the mechanical and dissipative behaviour of hybrid unidirectional laminae are presented; in particular the hierarchical procedure for the evaluation of mechanical properties of multiscale unidirectional composites is discussed.

The integrated multi-level procedure for the analysis of hybrid composites is described and later applied to analyse two possible hybrid laminate characterised by 3% in volume of damping material. The final engineering constants and the final dissipative constants for the two systems are evaluated and discussed.

## 5.2 Nano scale: hybrid matrices integrating carbon nanotubes

Much of the attention in nanocomposites research has been directed toward the use of carbon nanotubes as reinforcement, for modelling purpose nanocomposites consistent of an hosting matrix filled by carbon nanotubes could be analysed following the theoretical approaches proposed for both particulate composites and short fiber composites.

Good agreement with experimental data were found by the application of the simple model based on the mixture rule for the analysis of mechanical properties of nano-composites below its statistical percolation threshold content [1].

The reinforcement effects due to a short fiber within an hosting matrix is explained by the shear stresses transferred between the two phases, which is inversely proportional to the filler length, this lead to an effective reinforcement modulus expressed lower from short fiber filler. As examined in the chapter II, the effect of the length and fiber orientation could be accounted in the elastic modulus predictions by the introduction of two separated efficiency factor  $\eta_l$  and  $\eta_0$  respectively.

$$E_c = (\eta_0 \eta_l E_f - E_m) V_f + E_m$$

This expression could be easily rewritten in the rule of mixture form, introducing a term representing the equivalent modulus carried by the filler phase in the system.

$$E_c = E_\eta V_f + (1 - V_f) E_m$$

$$E_\eta = \eta_0 \eta_l E_f$$

The percolation threshold represents the limiting concentration from which nanotubes could not be consider individually dispersed, that is the maximum volume content of the filler before the creation of a connected paths within the system. In the case of non interacting rods this statistical limit depends on the filler aspect ratio as follows

$$\phi_{St} = 0.5 AR^{-1}$$

Figure 5- 1 reports the effective reinforcement modulus simulation for a nanocomposite in function of the filler's aspect ratio. The matrix is assumed to have elastic modulus of 2.8 GPa, this values is assumed as typical for an epoxy system at room temperature, whereas nanotubes modulus is assumed of 2000 GPa value reported from literature data. Fillers with higher aspect ratios are the more suitable reinforcement when the mechanical properties is the primary material performance to improve [2-3].

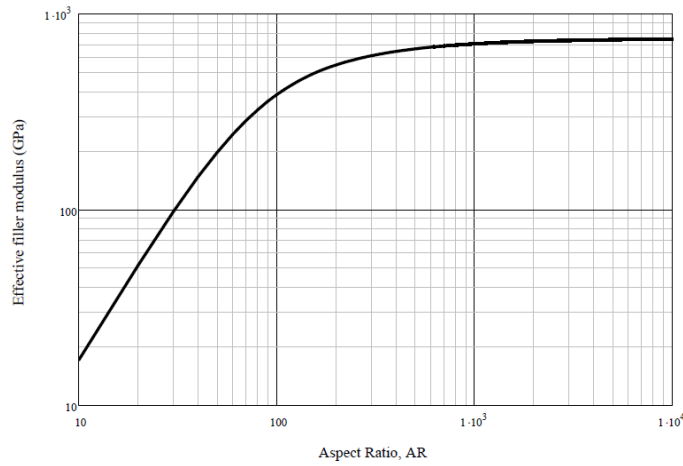


**Figure 5- 1: Effective reinforcement modulus vs filler aspect ratio**

Assuming the filler well dispersed within the hosting matrix the nanoloaded composite could be considered an isotropic material, hence only two independent parameters will describe its mechanical behaviour the elastic modulus as previously evaluated, moreover as the amount of CNT is typically small, considering percolation threshold, the Poisson's ratio could be assumed to be the same of the hosting system, hence the shear modulus for a nanocomposite matrix could be evaluated as follows:

$$G_{NT} = \frac{E_{NT}}{2(1 + \nu)}$$

Below the hypotheses of isotropic behaviour two independent loss factors describe its dissipative behaviour.

The specific damping capacity of the system could be then evaluated by energetic analysis following Saravanos unified approach as previously explained. In calculations the filler mechanical properties used was the effective reinforcement modulus for filler phase in the system. A comprehensive form for the evaluation of composite dissipative loss factor could be written with the following formalism

$$\Psi = \Psi_{CNT} V_{CNT} \left( \frac{E_{\eta}}{E_c} \right)^{\cos 2\alpha} + \Psi_m (1 - V_{CNT}) \left( \frac{E_m}{E_c} \right)^{\cos 2\alpha}$$

The Figure 5- 2 reports the loss factor component evaluated as linear combination ( $\alpha=0$ ) of nanotubes and matrix loss factors, in the micromechanics analogy this represent an isostrain deformation field between matrix and filler, also in this case the fiber content is

assumed as the maximum possible for individually dispersed fillers. Short fibres does not contribute to increment the dissipation mechanism if they operate in this condition.

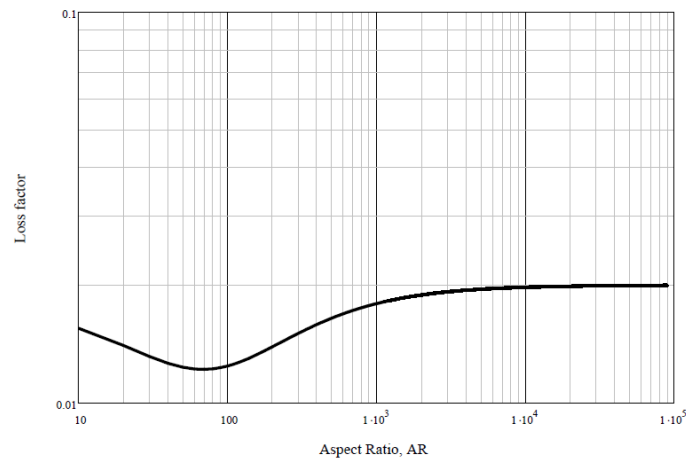


**Figure 5- 2: Longitudinal loss factor vs filler aspect ratio**

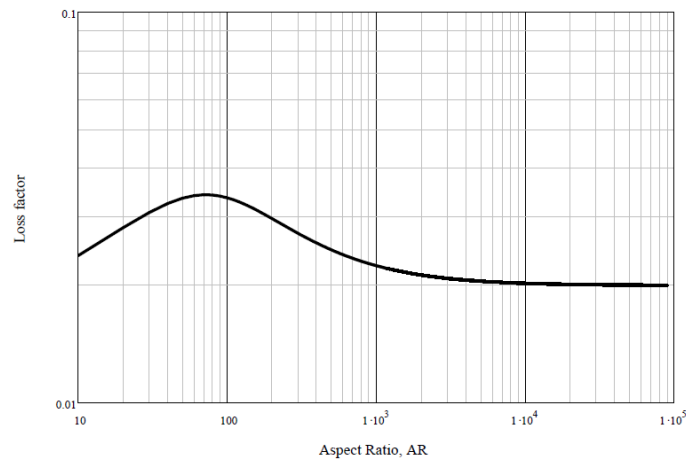


**Figure 5- 3: Transverse loss factor vs filler aspect ratio**

Figure 5- 3, reports the loss factor evaluated assuming iso-stress field between matrix and filler; under these conditions, the lower aspect ratio filler contribute to an enhancement in dissipation mechanism, moreover as known transverse and in plane shear could be analysed in analogy with the iso-stress condition, therefore considering the overall nanocomposite behaviour the use of low aspect ratio filler definitely contributes to the improvement of the material loss factor.

### 5.2.1 Transversely isotropic lamina

To predict material properties of multiscale composites, the previous proposed model and the boundary micromechanics would be used in hierarchy. First, for mechanical properties of carbon nanotube composites the independent viscoelastic parameters were evaluated.

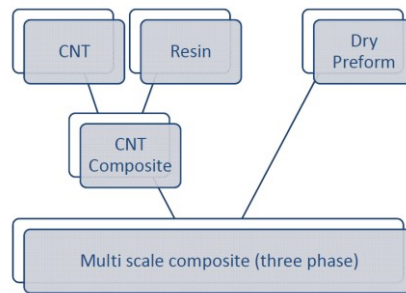


Figure 5- 4: Schematic of composite hierarchy for computation of viscoelastic properties of hybrid composites

The carbon nanotube composite properties were then utilized to compute the viscoelastic properties of the multiscale composite using the Saravanos unified micromechanics.

### 5.3 Micro scale: Hybrid dry preform

In the previous paragraph, the modelling problem of an hybrid matrix has been discussed. The final considered hybrid lamina is composed by structural fibres embedded in an hybrid matrix. In the present paragraph, the hybrid lamina consists of an hybrid dry preform which contains a viscoelastic material arranged as fibres contiguous to structural reinforcement within the material.

The analytical approach followed to model the viscoelastic behaviour of this hybrid system is schematically represented in the Figure 5- 5. The system is considered as two transversely isotropic laminae which mechanical and dissipative behaviour would be examined by the unified micromechanics approach (chapter II) then stiffness and dissipative matrices for the hybrid lamina were formulated by weighted average.

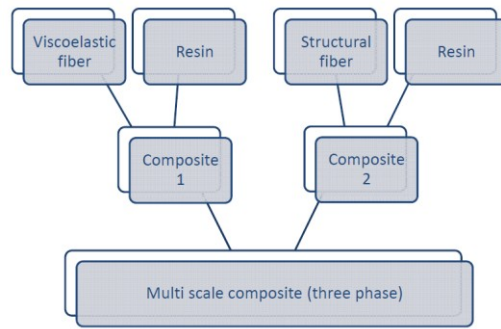


**Figure 5- 5: Schematic of composite hierarchy for computation of viscoelastic properties of hybrid dry preform composites**

Key parameter in this analysis is represented by the accurate evaluation of the fiber content for each reinforcement embedded in the hosting matrix, in the case of fibres having similar diameters it could be assumed each composite constituent the lamina containing the same volume fraction of fibres equal to the overall dry preform volume fraction of the final lamina, in fact it is easily understood that the influence region for the stress transfer is similar. More attention requires the case of different diameter fibres, in this case the volume fraction of each fiber system could be evaluated following the approach explained in the fourth chapter.

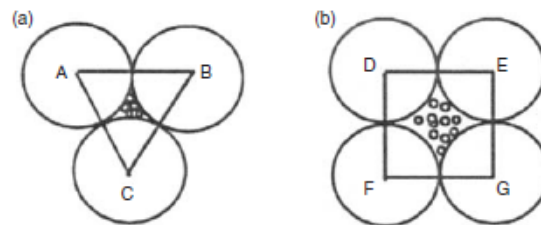


**Figure 5- 6: Different diameter fibres arrangement**

The volume fraction of the smaller fibres is evaluated as function of the volume fraction of the larger diameters ones. The following formula indicates the overall volume fiber content of the material, the small fiber content could be straightforwardly by inversion.

$$V_f^* = V_F + (1 - V_F) v_f$$

The total hybrid lamina mechanical properties could be evaluated by superposition of the two stiffness matrices. In the hierarchy introduced in the Figure 5-5, an additional step could be considered when the matrix is itself a composite, i.e. a nanoloaded resin, in that case the resin is modelled as a matrix filled by carbon nanotubes, and in next step the homogenised stiffness matrix is accounted.

### 5.3.1 Viscoelastic definition set for hybrid dry preform composites

In this paragraph an application of the suggested modelling procedure is proposed. In particular, an hybrid configuration is examined where one of the reinforcement fixed in the hosting matrix has not structural features, but only the capability of dissipate energy, in fact viscoelastic material have usually elastic modulus quite smaller than epoxy resin and reinforcement fibres, but respect the latter an damping ratio considerably higher.

The three phases composite examined has two different fiber with comparable diameters, that is the same volume fraction it is assumed for the two constituents composites. The following table 5-1 reports typical properties for each phase. These materials are isotropic, stiffness and dissipative matrices would be described by only two independent parameters. The elastic parameters considered are Young modulus and Shear modulus, while the dissipative behaviour is represented by the longitudinal and shear specific damping capacity.

**Table 5- 1: Properties of the three different phases constituent the hybrid laminate**

	Carbon fiber	Viscoelastic fiber	Epoxy resin
<b>E (MPa)</b>	260000	20	3500
<b>G (MPa)</b>	104000	7.7	1300
$\Psi_{11}$	0.0055	0.167	0.029
$\Psi_{12}$	0.0055	0.167	0.029

Following the proposed homogenization technique, the lamina is divided in two composites. The two constituents are both transversely isotropic materials and their mechanical properties are described by five independent parameters,  $E_1$ ,  $E_2$ ,  $\nu_{12}$ ,  $G_{12}$ ,  $G_{23}$  whereas their dissipative properties are described by four independent parameters  $\psi_{11}$ ,  $\psi_{22}$ ,  $\psi_{12}$ ,  $\psi_{23}$ . The engineering constants representing the constituent composites are evaluated by applying the generalization of the unified micromechanics, and completely described by the constituents properties.

$$P = [V_i P_i^{\cos\alpha} + (1 - V_i)P_j^{\cos\alpha}]^{\frac{1}{\cos\alpha}}$$

$$\psi = V_i\psi_i \left(\frac{P_i}{P}\right)^{\cos\alpha} + (1 - V_i)\psi_j \left(\frac{P_j}{P}\right)^{\cos\alpha}$$

where  $P$  is the generic composite elastic property,  $V_i$  is the volume fraction of the  $i^{\text{th}}$  constituent,  $\psi_i$  the damping capacity for the  $i^{\text{th}}$  constituent,  $\alpha$  a fitting parameters which



allows to modulate the combination law from the simple rule of mixtures (iso-strain field) to the iso-stress condition.

The final hybrid lamina mechanical and dissipative properties are evaluated by the weighted average.

$$P_c = \chi_1 P_1 + (1 - \chi_1) P_2$$

$$\Psi_c = \chi_1 \Psi_1 + (1 - \chi_1) \Psi_2$$

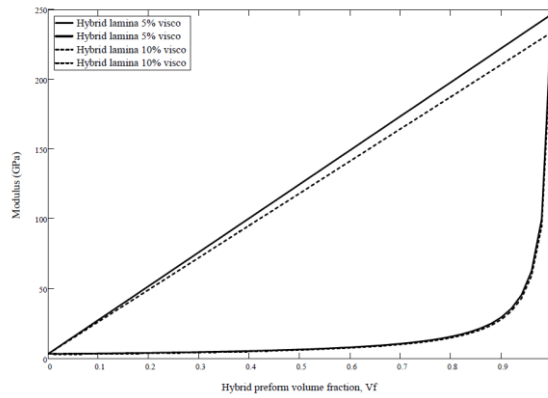


**Figure 5- 7: Hybrid composite elastic domain**

Figure 5- 7 shows the set for the mechanical properties of an hybrid composites constituted by three phase as function of the volume fraction content of the dry preform. The two curves corresponds to an hybrid preform which contain 5% vol. of viscoelastic fibres and the case of 10% vol. of dry preform. The linear upper curves represent the longitudinal modulus which significantly change by increasing the viscoelastic material content, less marked is the change in the transverse modulus. In terms of elastic properties, the main effect associated with the introduction of viscoelastic fibres within the laminate is represented by a decrement in the longitudinal modulus, in fact the structural fiber content decrease in reason of the viscoelastic fibre. Transverse modulus, instead, depends on the matrix properties which is comparable with elastic modulus of elastic fibres, this property is less affected by the detrimental effects due to the introduction of a softer phase in the lamina.

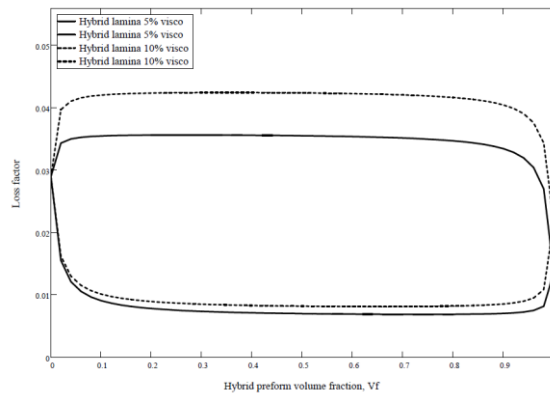


**Figure 5- 8: Hybrid composite dissipative domain**

In Figure 5- 8, the definition set for the loss factor of hybrid laminae containing 5 %vol. and 10 %vol. of viscoelastic fibre respectively are reported. The lower curves represents the elongational damping capacity of material. The effect in the transverse damping coefficient is need to be highlighted because does not correspond to a strong variation in the transverse mechanical property.

An increasing of the viscoelastic material content lead to a shift of the curve rising up both the longitudinal and the transverse damping parameter; however, the augmentation of damping material content is significant only at volume content above the 10%, content which implies a strong decrease in the structural performance of the material. In addition increasing the viscoelastic fiber content the manufacturing of the dry preform would be difficult implemented since the viscoelastic fibres could hardly arranged without induced deformation due to the strong gradient of stiffness.

## 5.4 Macro scale: Damping of hybrid laminates

In this paragraph, the specific damping capacity for laminates is proposed. A matlab software based on the theory background examined in the Chapter 2 is developed with the aim of analyse the behaviour of laminated composites. In this paragraph first the analysis of a conventional laminate is proposed, data available in literature were used to potentially validate the numerical procedure.

An additional sub-paragraph analyse hybrid laminates based on the hybrid architectures previously proposed and analytically modelled.

### 5.4.1 Damping of angle-ply laminates

In this paragraph the matlab tool developed upon the laminate numerical analysis previously proposed is applied to describe viscoelastic behaviour of laminated composites.

Literature experimental data have been used to verify model efficiency. Radford and Mèlo, have investigated experimentally viscoelastic behaviour of transversely isotropic laminae for unidirectional bend-beam specimen for a complete material characterization through dynamical mechanical analysis. In table 5-2 three point bending PEEK/IM7 data have been reported [13], the clamp span was 50 mm for the equipment used.

As preliminary validation of the numerical tool a bending beam reproducing the three point bending experiment set-up reported by Radford and Mèlo, has executed, span was set equal to 50 mm and stacking sequence of  $[(0/90)_2]_{sym}$ . Simulation reproduced for the cross ply laminate the loss factor  $4.82 \cdot 10^{-3}$  within the 5% error respect to the measured data. In this system 99.3% of energy is stored in extensional mode.

The numerical tool was integrate in the multi-objective platform modeFRONTIER<sup>®</sup>. The modeFRONTIER software allows to statistically discussing the behaviour of the laminate, in fact a design of experiment, DOE, is required to start each analysis.

The increment of damping performance of the material could induce a decrease in mechanical properties, therefore according to the application, the geometry of the structure and its boundary condition the Pareto analysis could individuate the optimum configuration which allows an increment in damping response of the system without sacrificing the mechanical performance.

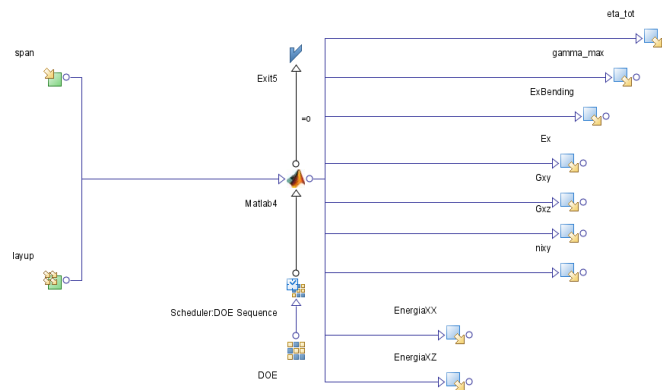


**Figure 5- 9: The matlab tool developed was integrate in the multi-objeive platform, modeFRONTIER.**

A symmetric and balanced layered composite constituted of eight layer is numerically analysed, this laminate will be considered in the further analysis as base for the hybrid architecture modelling.

The laminate stacking sequence is assumed to be  $[0/45/-45/90]_{sym}$ , each lamina is constituted of the PEEK-IM7 prepreg unidirectional tape, which nominal thickness is 0.125 millimeters.

**Table 5- 2: Mechanical and dissipative properties of PEKK-IM7 unidirectional prepreg at -20°C**

$E_1$ (GPa)	$E_2$ (GPa)	$G_{12}$ (GPa)	$\nu_{12}$	$\nu_{23}$	$\eta_{11}$ ( $10^{-3}$ )	$\eta_{12}$ ( $10^{-3}$ )	$\eta_{23}$ ( $10^{-3}$ )
155.4	10.2	7.4	0.34	0.48	4.7	7.8	8.8

A composite beam subject to a transverse force of 1N in three point bending mode is considered. The laminate thickness is of 1 millimeter, the span distance is assume to be 60 millimeters. The following figure represent the scheme for a three point bending test.

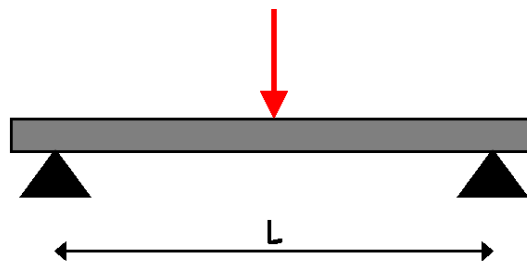


**Figure 5- 10: Beam subjected to three point bending load scheme**

Firstly the mechanical analysis of the beam is led to understand the forces acting in each section. In the three point loading scheme the momentum is maximum at the section where load is applied and there is a shear force in each section with half intensity respect to the applied load.

The Figure 5- 11 reports the stress distribution within the laminate at the section  $x = L/4$ , the only non zero stresses in the material are the longitudinal stress, and the transverse shear stress due the bending.

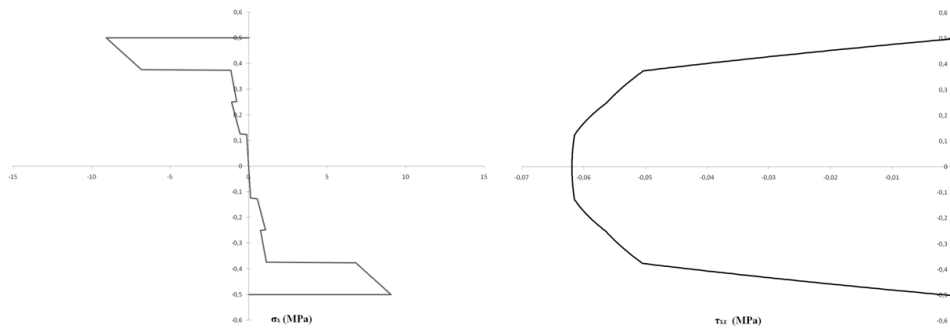


**Figure 5- 11: Static stress distribution within the laminate thickness at the section  $x=L/4$  .  
A)Longitudinal normal stress, B)Transverse shear stress.**

The following table reports the numerical results for the composite beam analysed. It is important to notice that the energy stored in this simple structure is principally in longitudinal normal mode, in fact calculation reports that 99.4% of the total energy is due to normal stress associated to the cylindrical bending of the structure.

**Table 5- 3: Predicted laminate properties**

$E_x$ (GPa)	$E_{xB}$ (GPa)	$G_{xy}$ (GPa)	$G_{xz}$ (GPa)	$\eta_{tot}$ ( $10^{-3}$ )
61.3	101	23.7	9.14	5.045

Figure 5- 12 shows the effect of distance between the beam supports. It is verified according to usual bending test procedure that load scheme with span to thickness ratio above 50 the loss factor approach to an asymptotic value, whereas for lower span to thick ratio there is an increase in the system loss factor.

Considering the energy distribution, it could be observed that higher the span to ratio the higher is the energy stored in normal stress mode, at the asymptotic value the energy stored in normal mode become 99.9% of the total with loss of  $5.022 \cdot 10^{-3}$ , this value represents the elongational dissipative character of the material.

When span decreases a similar behaviour is noticed, at the span distance of 2 millimetres the loss factor predicted is  $8.222 \cdot 10^{-3}$  corresponding to 82% of energy stored in transverse shear energy mode.

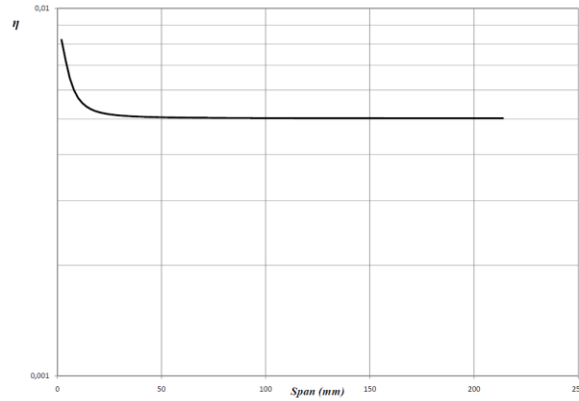


**Figure 5- 12: Laminate loss factor in function of the distance between supports**

The latter remark suggest the possibility of identify the homogenised dissipative constants for a material trough the simulation of condition exciting each of the energy components.

## 5.5 Multi-scale analysis of hybrid laminates

In this paragraph is presented the integrate procedure for the analysis of an hybrid laminate composite. The Figure 5- 13 hierarchically describes the proposed approach; the inputs are split in two separate action, the first belongs to material mechanics, whilst the second action describe the structure which material is computed in the upper part of the scheme.

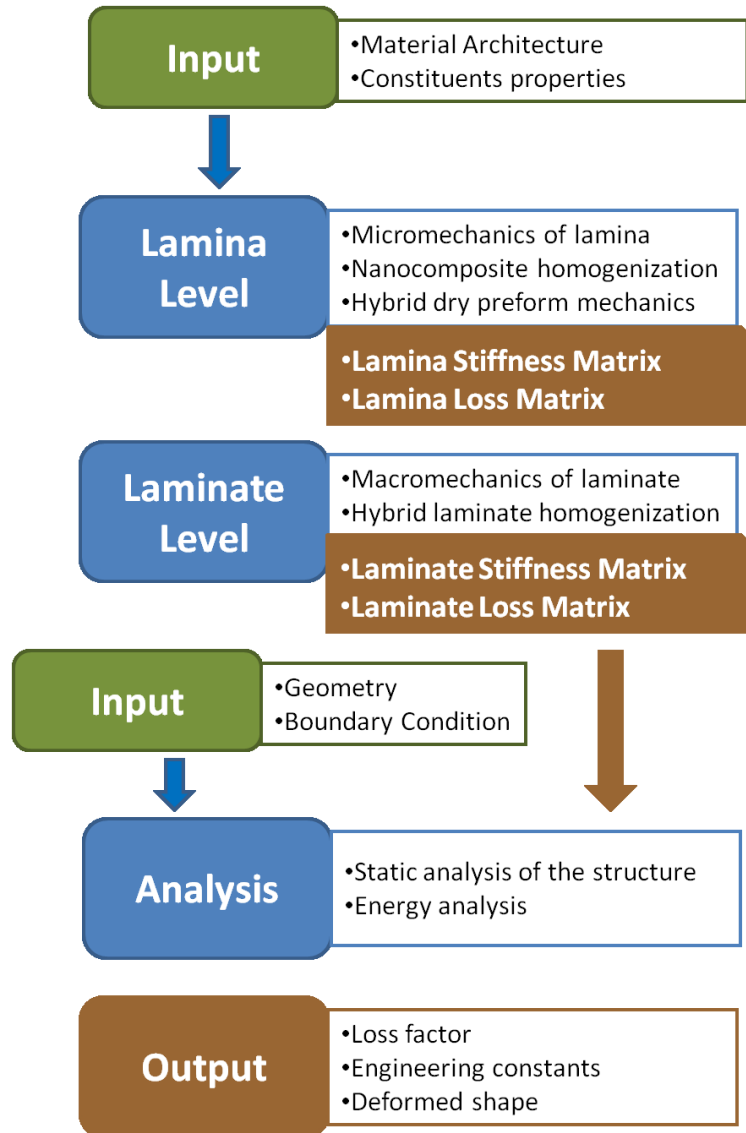


Figure 5- 13: Schematic representation for the integrated analysis of hybrid laminates

The lamina level include computational analysis of the material at micro and nano scale, in fact in this calculation box (blu-shadowed) the lamina material is assembled starting from its constituents, in the case of long fiber composites or short fiber composites the usual micromechanics rules would be applied, while if an hybrid architecture is selected the computational procedure for hybrid dry preform lamina or for hybrid matrix are exited.

At lamina level, instead, the laminate is assembled starting from its stacking sequence, which corresponds to stiffness and loss matrices for each lamina and the orientation in material reference system. Both computational levels give as output homogenised stiffness and loss matrices, which describe all the material behaviour. Afterwards, the energetic analysis is led over the structure calculating the overall loss factor and the stress distribution.

As an application of the shown procedure the analysis on two hybrid composites embedding 3 % in volume of viscoelastic material was conducted and hereafter presented. The two examined architectures are respectively the interleaved and the hybrid preform.

For the simulation the basic laminate, examined in the previous paragraph, is assumed as neat material for further hybridization. The viscoelastic material considered has Young modulus of 20 MPa, Shear modulus of 8 MPa and loss factor of 0.167 in both direction.

In order to compare the damping features of the described composites a simple structural scheme of a three points bending was considered.

The table 5-4 reports the obtained simulation results. The best solution in terms of damping behaviour has resulted for the interleaved configuration, however this architecture reduces the mechanical performances of the material. The strong difference in mechanical modulus for the composite laminae and the viscoelastic sheet lead to a very low transverse shear stiffness due to more pronounced effect determined by the viscoelastic material.

**Table 5- 4: Comparison for architecture**

	$E_x$ (GPa)	$E_{xB}$ (GPa)	$G_{xy}$ (GPa)	$G_{xz}$ (GPa)	$\eta_{tot}$ ( $10^{-3}$ )
Reference	61.3	101	23.7	9.14	5.045
Interleaved	59.5	99.8	22.97	0.20	34.57
Hybrid preform	61.3	101	23.7	9.14	5.949

The hybrid preform architecture, instead, allows the increment in loss factor withstanding mechanical performances, even if the increment is smaller respect to the interleaved configuration, an 18% increment is reached.

It is worth to highlight the asymptotic results for each configuration, the analysis at different span in the two hybrid cases allows the individuation of the material characteristic constant. The asymptotic values reached for interleaved and hybrid preform are respectively  $5.608 \cdot 10^{-3}$  and  $5.840 \cdot 10^{-3}$ ; a span tending to infinite means that the only significant energetic component becomes the elongational damping related to the bending, these values represent then the elongational damping capacity of the two architectures.



In the case of span approaching to zero, the only significant component is represented by the transverse shear. Moreover due to the architecture, the rate of zeroing the elongational contribution and the final values are different, in fact the shear damping factors are 0.162 and 0.0151 respectively for interleaved and hybrid preform. As expected the interleaved configuration contribute by transverse shear mode to the dissipating energy mechanism.

It is worth noting that performed analyses have been conducted beyond the hypothesis of linear elastic behaviour, and the simulations do not account for material failures. In fact the insertion of a softer material at laminate middle plane induce high interlaminar shear stresses which could lead material to failure.

## 5.6 The HYLAN.m code

```

% MULTISCALE MODELLING OF HYBRID STRUCTURAL COMPOSITES WITH INTEGRATED
% DAMPING FEATURES

% Hybrid Laminates ANalyzer
%-----
%                               MAIN PROGRAM
%-----

function [eta,Ratio] = damping
global MAT MATDISS NMAT LAYUP ID SP NPLY T NZ NX SPAN FX FY %A B D Q z
geometryinput
[N,M,R,x]=BC('SS',SPAN,FX,FY);
%type 'SS' Simply Supported Beam
%   'CC' Double Cantilever Beam
materialinput
laminatinput
%-----
% Laminate Properties: IN-PLANE Calculation
[A,B,D,Q,z,D1]=CLT(MAT,NMAT,LAYUP,ID,SP);
[Ad,Bd,DD]=CLTDiss(NMAT,MATDISS,LAYUP,ID,SP,NPLY,Q,z);
% Laminate Properties: OUT-OF-PLANE Calculation
[H,Hd]=FSDT(NMAT,MAT,MATDISS,NPLY,LAYUP,ID,SP,T,NZ,Q,z,A,B,D1);
%-----
% Laminate Beam: Deformation of the neutral axis
[rot,eps]=neutralaxis(N,M,A,B,D1);
% rot(x) eps(x)
%-----
% Energy Analysis : IN-PLANE Calculations
[EiP,EiPd]=Einplane(eps,rot,A,B,D,Ad,Bd,DD);
% Energy Analysis : OUT-OF-PLANE Calculations
[EoP,EoPd]=Eoutplane(H,Hd,R,NX);
% EiP(x) EiPd(x) EoP(x) EoPd(x)
%-----
% INTEGRATION: IN-PLANE
[OEiP,OEiPd]=integration(x,EiP,EiPd);
% INTEGRATION: OUT-OF-PLANE
[OEoP,OEoPd]=integration(x,EoP,EoPd);
%-----
EnergyTot=sum(OEiP)+sum(OEoP);
DissEnergyTot=sum(OEiPd)+sum(OEoPd);
Ratio=[OEiP; OEoP]./EnergyTot;
Lossfactor=DissEnergyTot/EnergyTot;
eta=Lossfactor/(2*pi);
end
%%
%-----
% SUBROUTINES
%-----
%%
% GEOMETRIC PARAMETERS
%-----
function geometryinput
% GLOBAL VARIABLES: geometrical definition of the problem
global SPAN FX FY NX NZ
SPAN=40;
FX=1;
FY=0;
NX=100;
NZ=500;
end
%%
% LOADS AND CONSTRAINTS
%-----
% Two possible load/BC:
% "Simply Supported Beam" "Double Cantilever Beam"

function [N,M,R,x]=BC(type,SPAN,FX,FY)

global NX x
d=SPAN/(2*NX);
x1=linspace(0,SPAN/2-d,NX);
x2=SPAN/2;
x3=linspace(SPAN/2+d,SPAN,NX);
x=[x1 x2 x3];
switch type
case {'SS'}
disp('Simply Supported Beam')
Mx1=0.5*FX*x1;
Mx2=0.250*FX*SPAN;
Mx3=0.5*FX*(SPAN-x3);
Mx=[Mx1 Mx2 Mx3]; My=zeros(1,length(x)); Mxy=zeros(1,length(x));
M=[Mx;My;Mxy]; % 3 rows x NX columns

Nx=zeros(1,length(x)); Ny=zeros(1,length(x)); Nxy=zeros(1,length(x));
N=[Nx;Ny;Nxy];

Rxz1=0.5*FX*ones(1,length(x1));
Rxz2=FX;
Rxz3=-0.5*FX*ones(1,length(x1));
Rxz=[Rxz1 Rxz2 Rxz3];
Ryz=zeros(1,length(x));
R=[Rxz;Ryz];

```

```

case {'CC'}
disp('Double Cantilever Beam')
Mx1=-0.125*FX*(SPAN-4*x1);
Mx2=0.125*FX*SPAN;
Mx3=-0.125*FX*(4*x3-3*SPAN);
Mx=[Mx1 Mx2 Mx3]; My=zeros(1,length(x)); Mxy=zeros(1,length(x));
M=[Mx;My;Mxy];

Nx=zeros(1,length(x)); Ny=zeros(1,length(x)); Nxy=zeros(1,length(x));
N=[Nx;Ny;Nxy];

Rxz1=0.5*FX*ones(1,length(x1));
Rxz2=FX;
Rxz3=-0.5*FX*ones(1,length(x1));
Rxz=[Rxz1 Rxz2 Rxz3];
Ryz=zeros(1,length(x));
R=[Rxz;Ryz];
end
end
%%
% LAMINATE DEFINITION
%-----
function laminateinput
% GLOBAL VARIABLES: Laminate definition
global LAYUP ID NPLY SP T SMAT
% Stacking sequence
LAYUP=[0 45 0 -45 90 90 -45 0 45 0];
NPLY=length(LAYUP);
% Materials
ID=[1 1 1 1 1 1 1 1 1 1];

% Thickness assignation
for i=1:NPLY
    SP(i)=SMAT(ID(i));
end

%Laminata thickness
T=sum(SP);

end
% Elastic formulation of classical lamination theory
% cfr. Mechanics of Composite materials, Jones...
%-----
function [A,B,D,Q,z,D1]=CLT(MAT,NMAT,LAYUP,ID,SP)

format short;
%GLOBAL VARIABLES:
global T NPLY %A B D Q z
% In-plane compliance matrix definition

for k=1:NMAT
    Slam(:,k)=[1/MAT(k,1),-MAT(k,3)/MAT(k,1),0;...
              -MAT(k,3)/MAT(k,1),1/MAT(k,2),0;0,0,1/MAT(k,4)];
end

% Conversion matrix for Teps Tsig
% Berthelot.....
RR=[1,0,0;0,1,0;0,0,2];
% Vector of plies
z(1)=-T/2;

%Inizializzazione delle matrici A,B,D
A=zeros(3,3); %Matrice A
B=zeros(3,3); %Matrice B
D=zeros(3,3); %Matrice D

% Calculation of elongational A, coupling B, bending D stiffness matrices
for id=1:NPLY
    S=Slam(:, :, ID(id)); %Matrice S di ogni layer
    phi=(pi/180)*LAYUP(id); %Conversione in radianti degli angoli
    m=cos(phi);
    n=sin(phi);

    %Matrice di rotazione e sua inversa
    TT=[m*m,n*n,2*m*n;n*n,m*m,-2*m*n;-m*n,m*m,m*m-n*n];
    TTinv=[m*m,n*n,-2*m*n;n*n,m*m,2*m*n;m*n,-m*n,m*m-n*n];

    Q(:, :, id)=TTinv*inv(S)*(RR*TT*inv(RR));%Rotazione della matrice Q
    z(id+1)=z(id)+SP(id);%Vettore z delle posizioni attraverso lo spessore

    A=A+Q(:, :, id)*(z(id+1)-z(id)); %Calcolo della matrice A
    B=B+Q(:, :, id)*(z(id+1)^2-z(id)^2); %Calcolo della matrice B
    D=D+Q(:, :, id)*(z(id+1)^3-z(id)^3); %Calcolo della matrice D
end

B=(1/2)*B;
D=(1/3)*D;
D1=D-B*inv(A)*B;
%d=inv(D1);
%a=inv(A)+inv(A)*B*d*B*inv(A);

end

%%
% CLASSICAL LAMINATION THEORY
% Dissipative formulation of CLT
% cfr. Saravanos NASA Technical Memorandum.....

function [Ad,Bd, Dd]=CLTDiss(NMAT,MATDISS,LAYUP,ID,SP,NPLY,Q,z)

format short;
global T

```

```

%Calcolo della matrice di perdita dei tipi di lamine utilizzati nel
%laminato
for k=1:NMAT
    psiqlam(:, :, k)=2*pi*[MATDISS(k,1),0,0;...
        0,MATDISS(k,2),0;0,0,MATDISS(k,3)];
end

RR=[1,0,0;0,1,0;0,0,2];

%Inizializzazione delle matrici Ad,Bd,Dd
Ad=zeros(3,3); %Matrice Ad
Bd=zeros(3,3); %Matrice Bd
Dd=zeros(3,3); %Matrice Dd

%Calcolo delle matrici Ad,Bd,Dd
for id=1:NPLY;
    psiq=psiqlam(:, :, ID(id)); %Matrice psi di ogni layer
    phi=(pi/180)*LAYUP(id); %Conversione in radianti degli angoli
    m=cos(phi);
    n=sin(phi);

    %Matrice di rotazione e sua inversa
    TT=[m*m,n*n,2*m*n;n*n,m*m,-2*m*n;-m*n,m*m,n*n-m*n];
    TTinv=[m*m,n*n,-2*m*n;n*n,m*m,2*m*n;m*n,-m*n,m*m-n*n];

    psi(:, :, id)=(RR*T*inv(RR))*psiq*T; %Rotazione della matrice psi

    Ad=Ad+psi(:, :, id)*Q(:, :, id)*(z(id+1)-z(id)); %Calcolo di Ad
    Bd=Bd+psi(:, :, id)*Q(:, :, id)*(z(id+1)^2-z(id)^2); %Calcolo di Bd
    Dd=Dd+psi(:, :, id)*Q(:, :, id)*(z(id+1)^3-z(id)^3); %Calcolo di Dd
end

Bd=(1/2)*Bd;
Dd=(1/3)*Dd;

end
function [H,Hd]=FSDT(NMAT,MAT,MATDISS,NPLY,LAYUP,ID,SP,T,NZ,Q,z,A,B,D1)

[G,Ginv]=SHEARSTIFF(NMAT,MAT,LAYUP,NPLY,ID);
GG=SHEARDISS(NMAT,NPLY,MATDISS,LAYUP,ID,G);
[zit,ir]=zita(SP,T,NPLY,NZ);
[a,b]=ab(Q,z,NPLY);
[az,bz]=azbz(NZ,Q,ir,zit);
f=effe(NPLY,A,B,D1,a,b);
fz=effe(NZ-1,A,B,D1,az,bz);
H=acca(Ginv,f,z,NPLY);
Hd=acca(GG,f,z,NPLY);

end
function [G,Ginv]=SHEARSTIFF(NMAT,MAT,LAYUP,NPLY,ID)

%Matrice G di ogni tipo di lamina costituente il laminato
for i=1:NMAT
    Glam(:, :, i)=[MAT(i,5),0;0,MAT(i,4)];
end
for id=1:NPLY;
    Gl=Glam(:, :, ID(id));%Matrice G del layer considerato
    phi=(pi/180)*LAYUP(id); %Conversione in radianti degli angoli
    m=cos(phi);
    n=sin(phi);
    R=[m,-n;n,m];
    G(:, :, id)=inv(R)*Gl*R;
    Ginv(:, :, id)=inv(G(:, :, id));
end
end
function GG=SHEARDISS(NMAT,NPLY,MATDISS,LAYUP,ID,G)
for i=1:NMAT
    PSItagliolam(:, :, i)=2*pi*[MATDISS(i,4),0;0,MATDISS(i,3)];
end
for id=1:NPLY;
    PSItagliol=PSItagliolam(:, :, ID(id));%Matrice PSI del layer considerato
    phi=(pi/180)*LAYUP(id); %Conversione in radianti degli angoli
    m=cos(phi);
    n=sin(phi);
    R=[m,-n;n,m];
    PSItaglio=inv(R)*PSItagliol*R;
    GG(:, :, id)=PSItaglio*inv(G(:, :, id));
end
end
function [zit,ir]=zita(SP,T,NPLY,NZ)
spessum(1)=-T/2+SP(1);
for id=2:NPLY
    spessum(id)=spessum(id-1)+SP(id);
end
zit=linspace(-T/2,T/2,NZ);
k=1;
ir(1)=1;
for i=2:NZ-1
    if zit(i)<=spessum(k)
        ir(i)=ir(i-1);
    else
        ir(i)=ir(i-1)+1;
        k=k+1;
    end
end
end
function [a,b]=ab(Q,z,NPLY)
a(:, :, 1)=Q(:, :, 1)*(z(2)-z(1));
b(:, :, 1)=Q(:, :, 1)*((z(2))^2-(z(1))^2));

for i=2:NPLY
    a(:, :, i)=a(:, :, i-1)+Q(:, :, i)*(z(i+1)-z(i));

```

```

    b(:, :, i) = b(:, :, i-1) + Q(:, :, i) * (z(i+1)^2 - z(i)^2);
end

b = (1/2) * b;
end

function [az, bz] = azbz(NZ, Q, ir, zit)
az(:, :, 1) = Q(:, :, ir(1)) * (zit(2) - zit(1));
bz(:, :, 1) = Q(:, :, ir(1)) * ((zit(2))^2 - (zit(1))^2);

for i = 2:NZ-1
    az(:, :, i) = az(:, :, i-1) + Q(:, :, ir(i)) * (zit(i+1) - zit(i));
    bz(:, :, i) = bz(:, :, i-1) + Q(:, :, ir(i)) * (zit(i+1)^2 - zit(i)^2);
end

bz = (1/2) * bz;

end

function f = effe(Nlayer, A, B, D1, a, b);

for i = 1:Nlayer
    F(:, :, i) = (a(:, :, i) * inv(A) * B - b(:, :, i)) * inv(D1);
    f(:, :, i) = [F(1, 1, i), F(3, 2, i); F(3, 1, i), F(2, 2, i)];
end

end

function [rot, eps] = neutralaxis(N, M, A, B, D1)
%rot(x) function
rot = inv(D1) * (M - B * inv(A) * N);
%eps0(x)
eps = inv(A) * N - inv(A) * B * rot;

end

function [EiF, EiPd] = Einplane(eps, rot, A, B, D, Ad, Bd, Dd)

AAe = (A * eps + B * rot);
BBe = (B * eps + D * rot);
AAAd = (Ad * eps + Bd * rot);
BBd = (Bd * eps + Dd * rot);

EiF = 0.5 * (eps * AAe + rot * BBe);
EiPd = 0.5 * (eps * AAAd + rot * BBd);
End

function [EoP, EoPd] = Eoutplane(H, Hd, R, NX)

for i = 1:NX
    FF(:, i) = H * R(:, i);
    EoP(:, i) = (R(:, i) .* FF(:, i)) / 2;
end

for i = 1:NX
    FF(:, i) = Hd * R(:, i);
    EoPd(:, i) = (R(:, i) .* FF(:, i)) / 2;
end

end

end

function [En, Endiss] = integration(x, Energy, DissEnergy)
dx = x(2) - x(1);
n = size(x, 2); %
numcomp = size(Energy, 1)
En = zeros(numcomp, 1); %
dimEnElem = size(Energy, 2)
if dimEnElem == n
    for i = 1:numcomp
        for k = 1:n-1
            En(i) = En(i) + ((Energy(i, k) + Energy(i, k+1)) / 2) * dx;
        end
    end
else
    for i = 1:numcomp
        for k = 1:dimEnElem
            En(i) = En(i) + Energy(i, k) * dx;
        end
    end
end

end

```

## 5.7 References

- [1] Martone A, Formicola C, Zarrelli M, Giordano M, 2009. The effect of aspect ratio of carbon nanotubes on their effective reinforcement modulus in an epoxy matrix. Submitted to *Applied Physics Letters*.
- [2] Suarez SA, Gibson RF, Sun CT, Chaturvedi SK, 1986. The influence of fiber length and fiber orientation on damping and stiffness of polymer composite materials. *Experimental Mechanics* 26.
- [3] Finegan IC, Tibbetts GG, Gibson RF, 2003. Modelling and characterization of damping in carbon nanofiber/polypropylene composites. *Composite Science and Technology* 63.
- [4] Saravanos DA, Chamis CC 1989. Unified micromechanics of dampin for unidirectional fiber reinforced composites. *NASA Technical Memorandum 102107*.
- [5] Melo JDD, Radford DW, 2004. Time and temperature dependence of the viscoelastic properties of PEEK/IM7. *Journal of Composite Materials Vol. 38*.
- [6] Martone A, Giordano, 2008. Multiscale modelling of hybrid structural composites with integrated damping features. *Proceeding of International Conference on Times of Polymers & Composites (TOP2008)*.

# Manufacturing and testing of hybrid composites

## 6.1 Summary

In this chapter, the experimental analysis of the proposed hybrid architecture will be presented. For each proposed architecture, unidirectional coupons were tested to verify the increment in loss factor.

The hybridization of the laminate is experimentally studied over all dimensional scales. On the macro scale, laminates with macroscopically integrated viscoelastic layer have been fabricated and tested. Moreover, the concept of hybrid lamina is examined in terms of hybrid preforms, where viscoelastic material is integrated as fiber along carbon tow direction, and in terms of laminae infused by a nanoloaded epoxy system,

In each case a valuable increment in passive damping were measured, mainly at the requirement temperature, i.e. the cruise condition in the case of an aeronautical application. Both the interleaved layer and the hybrid dry preform lead to a loss in mechanical performances for the considered material, although the material damping is enhanced at each testing temperature. In the case of nano loaded matrix composites, mechanical performances are kept over all test condition, but the enhancement in material damping is sensible only at temperatures below zero degrees.

## 6.2 Manufacturing of hybrid multi-scale laminates

The main purpose leading this work is the study of laminated architectures which allows an enhancement in the loss property of the final composite. The study is arranged following a through the scale approach by proposing architectures which modify the laminate at its different dimensional scales.

To modify laminate architecture it is possible to operate on the laminate constituents, on the macro-scale the simplest modify proposed is to insert as a ply in the laminate a material with improved passive damping. The ply could be a lamina of damping material, then the hybridization is attended at laminate level (hybrid laminate), however even each lamina could be an orthotropic hybrid layer modified in its constituents for passive damping enhancement. The hybridization could be execute by modifying the weave fiber preform (at micro-scale) or loading resin with a filler (for example carbon nanotubes) able to enhance matrix dissipative character.. Figure 6- 1 describes the dimensional scale path for laminate hybridization.

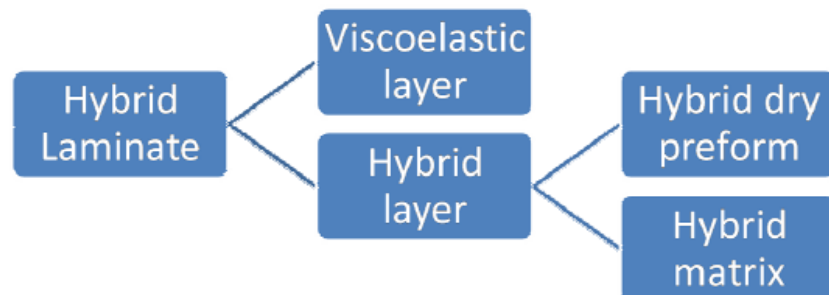


Figure 6- 1: Hybrid laminate hierarchy

A valuable technology for manufacturing composite materials have to be flexible in changing constituents properties as well as to allow an insertion of softer material as lamina; moreover, the manufacturing process should also allow the use of hybrid layer in the material forming and being easily extended on large dimension coupon production.

Among the different process technologies, liquid moulding allows all listed item. Liquid moulding is a composite fabrication process capable to fabricate extremely complex and accurate dimensionally parts. One of the main advantages is part count reductions, in situations where a number of parts would normally made individually, and either fastened or bonded together, these are integrated into a single moulded part. Another advantage is the ability to incorporate molded-in features, such as sandwich core section in the interior



of a liquid moulded part. The resin transfer moulding, RTM, is the most widely used of liquid molding processes it consists of fabricating dry fiber preform which is placed in a closed mold, impregnated with a resin, and then cured. The basic resin transfer moulding process consists of the following steps:

- Fabricate a dry composite preform,
- Place the preform in a closed mold,
- Inject the preform with a low viscosity liquid resin under pressure,
- Cure the part at elevated temperature in the closed mold under pressure,
- Demoulded and clean up the cured parts.

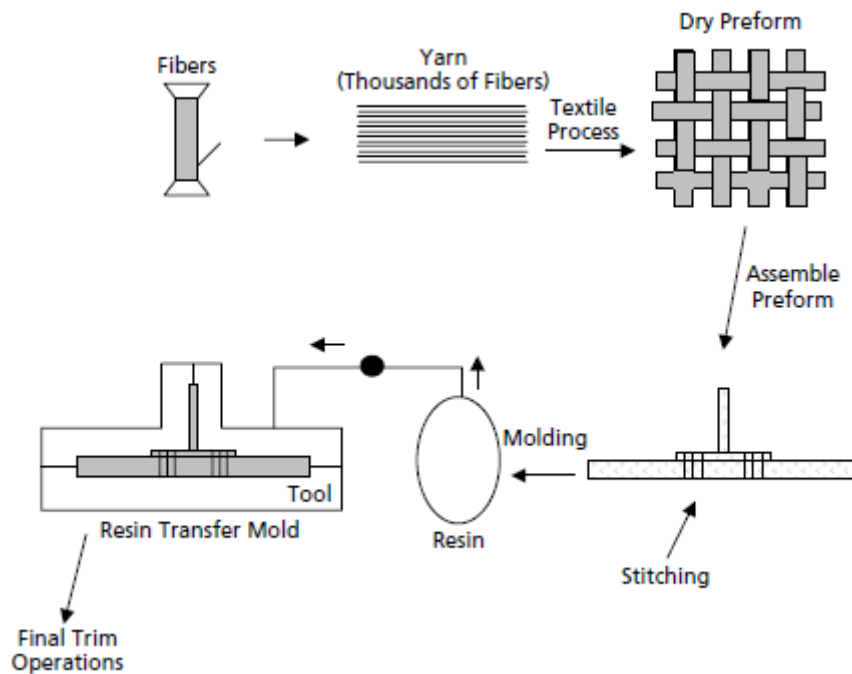


**Figure 6- 2: Process flow for Resin Transfer Molding**

There are many variations developed for this process, including RFI (Resin Film Infusion), VARTM (Vacuum Assisted Resin Transfer Moulding) and SCRIMP (Seeman’s Composite Resin Infusion Molding Process).

By the RTM process it is easily possible fabricate hybrid composites based on the considerations proposed in the previous chapters. An hybrid laminate could be manufactured by placing a layer of viscoelastic material before inserting preform in the mould, as well as hybrid dry preform could be used in the first phase or liquid resin could be injected after it is mixed with a properly chosen filler.

In addition, by using this technology, complex structure, like a stiffened plate, could be manufactured monolithically integrating features previously tested on the coupon scale. In the following sub-paragraph, VARTM process is briefly summarised, the manufacturing process for the fabrication of hybrid dry preform and the dispersion process of nanofillers in the hosting matrix are examined in next paragraphs [1].

### 6.2.1 The VARTM process

Since VARTM processes use only vacuum pressure for both injection and cure, the single biggest advantage of VARTM is that the tooling cost is much less, and simpler to design, than for conventional RTM. In addition, since an autoclave is not required for curing, the potential exists to make very large structures using the VARTM process. Also Since much lower pressures are used in VARTM processes, lightweight foam cores can easily be incorporated into lay-ups. VARTM type processes have been used for many years to build fiber-glass boat hulls, but have only recently attracted the attention of the aerospace industry.

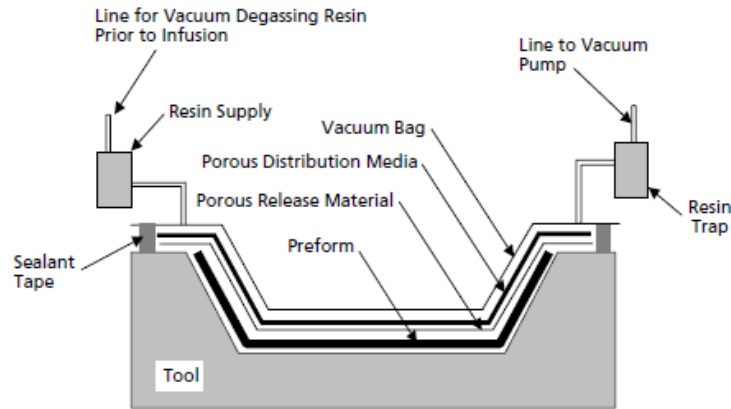


Figure 6- 3: Typical VARTM process set-up

A typical VARTM process, shown in Figure 6- 3, consists of single-sided tooling with a vacuum bag. VARTM processes normally use some type of porous media on top of the preform to facilitate resin distribution. The porous distribution media should be a highly permeable material that allows resin to flow through the material with ease, the resin typically flows through the distribution media and then migrates down into the preform.

Since the VARTM process uses only vacuum pressure for both injection and cure ovens and integrally heated tools are normally used, and since the pressures are low, low-cost lightweight tool can be used.

The resin used for VARTM processing should had even a lower viscosity than those used for traditional RTM to let the flow to impregnate the preform at vacuum pressure. Vacuum degassing prior the infusion is normally used to help to remove entrained air from the mixing operation. For large scale parts sizes, multiple injection and venting ports are utilized.

### 6.2.2 Materials

The matrix used in this research is a commercially available thermosetting resin, denominated RTM6. It is a mono-component premixed epoxy-amine system already degassed, specifically developed to fulfil the requirements of the aeronautical and space industries to manufacture composite parts by Liquid Infusion processes (LI). According to material supplier, this resin is recommended to be infused within the rage 100°C-120°C depending on preheating of the mould. The system was provided by Hexcel Composites (Duxford, UK). Figure 6- 4 reports viscosity of the resin in isothermal scans at different temperature rates.

The RTM6 resin is processed in a two step curing cycle, 1h at 160°C for the cure and a second step of post curing 2h at 180°C . The resin has its glass transition temperature near 190°C, furthermore resin has a secondary transition at -50°C as it is shown by the dynamical mechanical test in Figure 6- 5 .

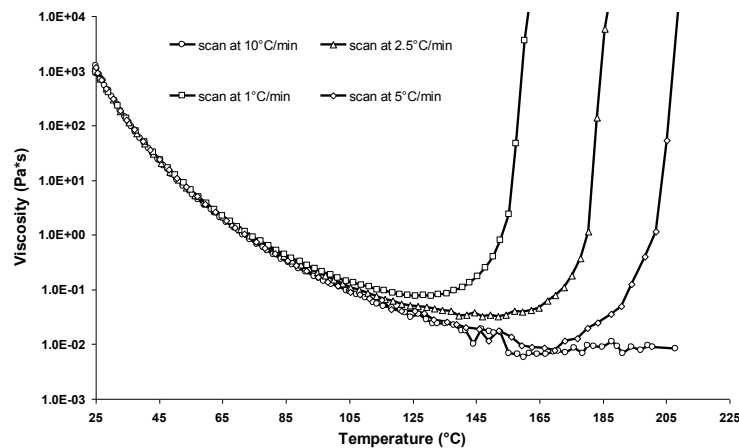


Figure 6- 4: Dynamic viscosity profiles at three different heating rate 1-2.5-10°C/min

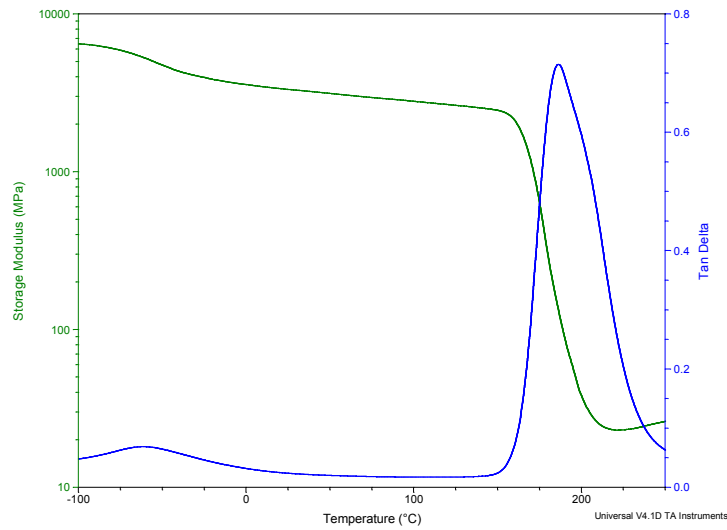


Figure 6- 5: Dynamical mechanical analysis of the Hexcel RTM6

The hybrid architectures, proposed in the chapter IV, required the availability of viscoelastic materials in form of sheet and fiber.

Commercial damping material are commonly available in form of adhesive films, for the manufacturing of hybrid laminates the thermoplastic polyurethane MOBILON<sup>®</sup> supplied from Nisshinbo has used. Viscoelastic sheets have been received as adhesive film of controlled thickness. The Figure 6- 6 reports the Mobilon nomograph.

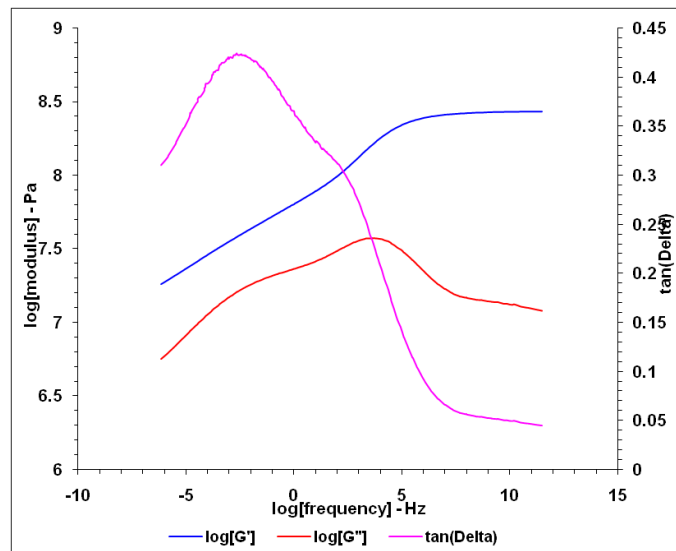
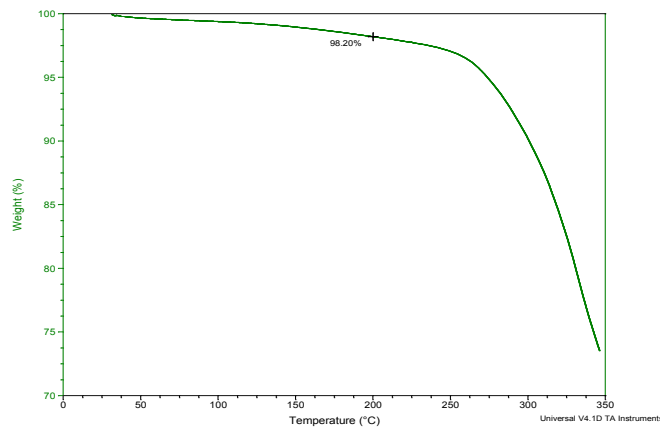


Figure 6- 6: Nomograph Nisshimbo Mobilon<sup>®</sup> Film

Unfortunately, viscoelastic material does not are easily obtainable in form of fiber for damping treatment, although a class of thermoplastic polyurethanes is available for fashion purpose. The commercial product Lycra<sup>®</sup> supplied form INVISTA is used as fiber in the hybrid preform manufacturing as proof of concept, in fact the main issue of this work if verify if the insertion of a softer material along structural reinforcement could lead to increasing the passive damping capacity of material in its elongational component.

The viscoelastic material selected are both thermoplastic polyurethanes, as first proof for feasibility of the VARTM process a test for weight decrease in the curing process has been done. Figure 6- 7 reports the Thermogravimetric analysis for Lycra, test shows that any volatile substances are released in the heating.



**Figure 6- 7: Thermoplastic Polyurethane Thermogravimetric analysis. Lycra<sup>®</sup> does not release flier substances at temperature of curing cycle for the epoxy system used.**

Figure 6- 8 and Figure 6- 9 report results of dynamical mechanical test on the viscoelastic materials. Materials were scanned at the frequency of 1 Hz over temperature range of -100 °C to up 100 °C. Polyurethanes have glass transition temperature well below thus the final composite.

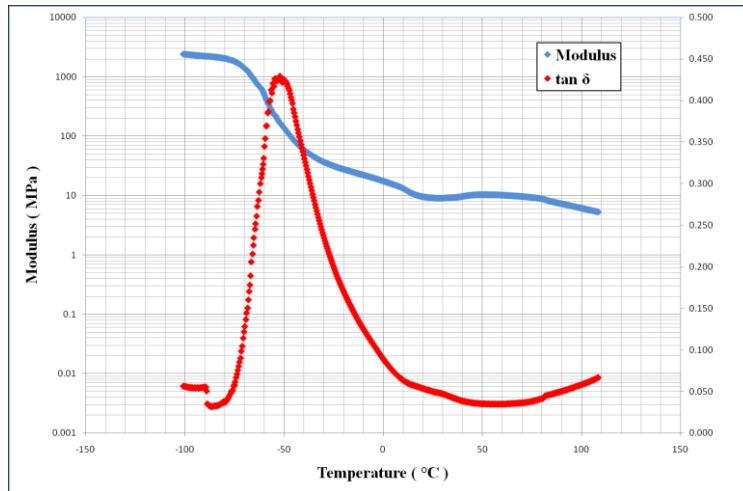


Figure 6- 8: Dynamical mechanical analysis of the MOBILON®

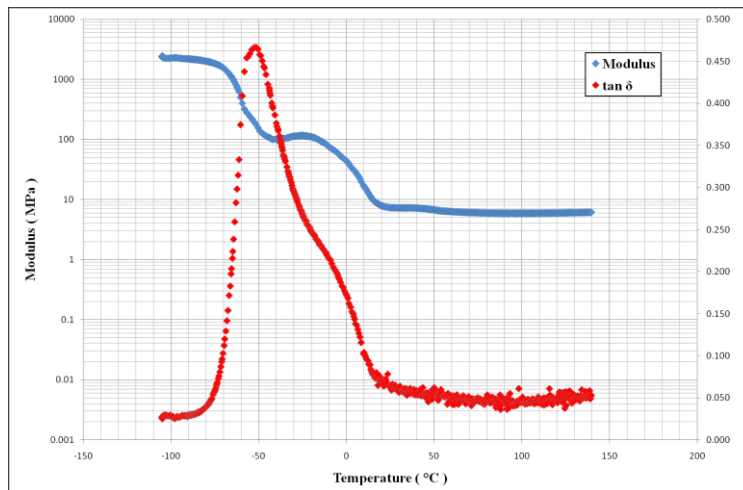


Figure 6- 9: Dynamical mechanical analysis of the Lycra®

The two selected thermoplastic polyurethanes exhibit the peak of  $\tan\delta$  at about  $-50^{\circ}\text{C}$ , since the reference cruise temperature for a commercial liner aircraft corresponds to  $-30^{\circ}\text{C}$  both the material maintain in a much stable region than the peak of transition a good viscoelastic behaviour, therefore both the material are suitable for the requirement of improve passive damping of the hybrid composite.

### **6.3 Set-up hybrid dry preform technology**

The most important types of preforms for liquid moulding processes are, woven, knitted, stitched and braided. In many cases conventional textiles machinery has been modified to handle the high modulus fibres needed in structural applications.

Weaving is essentially the action of producing a fabric by the interlacing of two sets of yarns: warp and weft. The warp yarns run in the machine direction, the  $0^\circ$  direction, and are fed into the weaving loom from a source of yarn. This source can consist of a multitude of individual yarn packages located on a frame (a creel), or as one or more tubular beams onto which the necessary amount of yarn has been pre-wound (warp beams). The warp yarns may then go through a series of bars or rollers to maintain their relative positioning and apply a small amount of tension to the yarns, but are then fed through a lifting mechanism which is the crucial stage in the weaving process. The lifting mechanism may be mechanically or electronically operated and may allow individual yarns to be selectively controlled (jacquard loom) or control a set of yarns simultaneously.

The crucial point is that the lifting mechanism selects and lifts the required yarns and creates a space (the shed) into which the weft yarns are inserted at right angles to the warp (the  $90^\circ$  direction). The sequence in which the warp yarns are lifted controls the interlinking of the warp and weft yarns and thus the pattern that is created in the fabric. It is this pattern that influences many of the fabric properties, such as mechanical performance, drapability, and fibre volume fraction. Therefore to manufacture a suitable 2D or 3D preform an understanding of how the required fibre architecture can be produced through the design of the correct lifting pattern is crucial in the use of this manufacturing process [2].

#### **6.3.1 Textile geometry**

The commonly used hybrid advanced composites are fabricated by weaving different types. Hybrid dry preform are manufactured inserting the distinct fiber yarn in the weft direction, or arranging onto the creel layout the yarn of different material. Textile process subject yarns to bending and abrasion, in general the higher the modulus of the fiber, the harder it will be the process. The definition of geometry have to keep in account that the hybrid system proposed has two critical points, in fact the assignment is to insert as viscoelastic fiber in the dry preform. As previous noticed the high modulus of carbon fiber leads to a massive weaving process, moreover below to equal loads the viscoelastic fiber deformation

is considerably stronger than carbon fibres thus could induce a shrinkage on the final hybrid dry preform.

As discussed in Chapter IV, with the aim of producing a composite able to store and then dissipate a larger part of its total energy in elongational mode, viscoelastic fibres may be arranged along warp direction.

The unidirectional fabric used as reference for further hybridization weaving is a plain weave carbon unidirectional fabric where the carbon yarn (8000 dtex) is sewn with a glass fiber yarn (34 dtex), the final dry perform is large 200 millimetres which weights is distributed in 92% in warp direction. In the following figure the datasheet of pristine dry perform is reported.

<b>G. Angeloni</b> reference		<b>TCU 260</b>		
<b>CHARACTERISTICS</b>		<b>Nominal</b>	<b>Tolerance</b>	<b>Normative</b>
Mass per unit area	gr/sqm.	<b>260</b>	± 5%	ISO 4605
Weave		<b>Plain</b>		ISO 2113
Standard Width	mm.	200 mm.	± 2,5%	
Laminate thickness	mm.	<b>0,26</b>	± 2,5%	(**)
Other informations				
<b>Nominal Construction</b>		<b>WARP</b>		<b>WEFT</b>
Fibre description		HR carbon fiber 12K - 8000 dtex		Glass fiber EC 9 34 tex
Thread Count	ends/cm.	<b>3,0</b>	ISO 4602	<b>3 x 2</b> ISO 4602
Weight distribution	gr/sqm.	12k carbon fibre : <b>240</b>		Glass fibre : <b>20</b>
	%	92%		8%
	gr/sqm.			
	%			

**Figure 6- 10: Pristine dry perform datasheet**

Two possible architectures are drawn in the Figure 6- 11. In the upper picture, the softer viscoelastic fibres are attached to the carbon yarns and then dragged in the weaving, another scenario consists in keeping viscoelastic fibres isolated from carbon tows and weaving them independently in the preform.



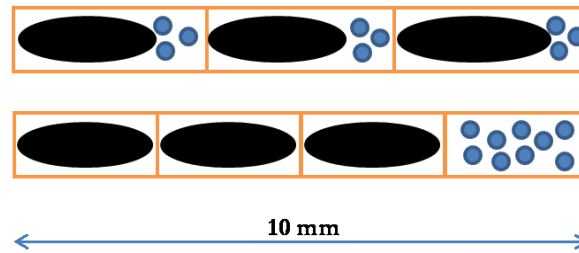


**Figure 6- 11: Suitable preform micro-architectures. a) viscoelastic fibres are arranged alongside of carbon yarn. b) viscoelastic fibres are arranged to form an independent yarn in the preform.**

Since viscoelastic fibres are much deformable respect to the carbon fiber yarns the architecture used in the final weaving process is to use the carbon yarn characterised by a low deformability to drag along the viscoelastic fibres, this solution avoids the shrinkage of the final dry preform.

The final hybrid dry preforms were produced at two viscoelastic material content, a first batch accounting 5 percent in volume of Lycra® fibres (dtex 78) and a second batch containing 10 percent of Lycra® fibres, the preform kept its width of 200 millimetres and the nominal thickness of 260 µm.

### 6.3.2 Manufacturing hybrid dry preform

Weaving the hybrid preform did not required particular precautions respect to the standard procedure. A critical issue would be the problem of carrying viscoelastic fibres into the fabric, but the idea of attach them to carbon yarns allows to proceed in the manufacturing process by applying only a simple adjustment on the yarn positioning into the creel. In the following pictures the main moments in the weaving process have been reported. First operation was to move Lycra form pristine package to many cardboard cylinders each of the required length, Figure 6-7 reports the reel in of viscoelastic fibres.

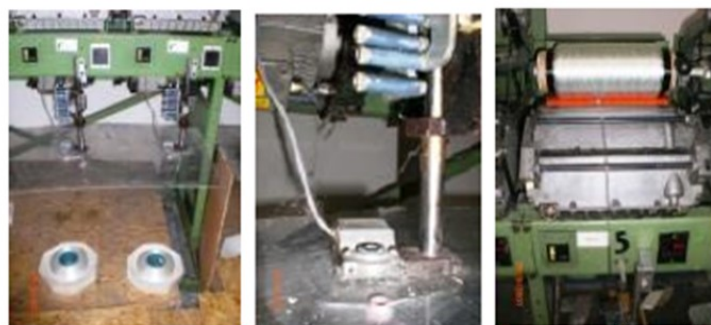


**Figure 6- 12: Phases of reeling in process for Lycra® fibres in roll compatibles with the weaving creel**

Afterwards Lycra reels are disposed on the creel according to the chosen architecture, Figure 6-8 reports the arrangement of yarns on the weaving creel.



**Figure 6- 13: Arrangement of yarns on the weaving creel.**

The following figures (Figure 6-9, 6-10) report the fabric manufacture in the loom. In Figure 6-9 a) the hybrid yarn, i.e. the carbon tow carrying the needed viscoelastic wires, enter the loom, in Figure 6-9 b) the application of weft glass fibres is shown.



**Figure 6- 14: Weaving phases. a) the carbon hybrid yarns input in the loom. b) weft yarn positioning.**

Figure 6-10 shows the final dry preform output from the loom and automatically packaged in reel.



Figure 6- 15: The final hybrid preform is automatically reel in cardboard cylinder by the loom.

## 6.4 Hybrid nano-loaded epoxy system

In the present paragraph the enhancement of material passive damping at lamina level is examined by providing hybridization of the epoxy system before the infusion process.

An high damping nanofiller that could be embedded in resin are carbon nanotubes, Suhr et al. [7] observed approximately 200% increase in damping ratio by addition of multi-walled nanotubes (MWNTs) in a rubbery state polymer matrix. Such good enhancement in damping ratio could be further improved by increasing proportion and improving dispersion and alignment of CNTs, Rajora et al. [8].

### 6.4.1 Dispersion of nanotubes

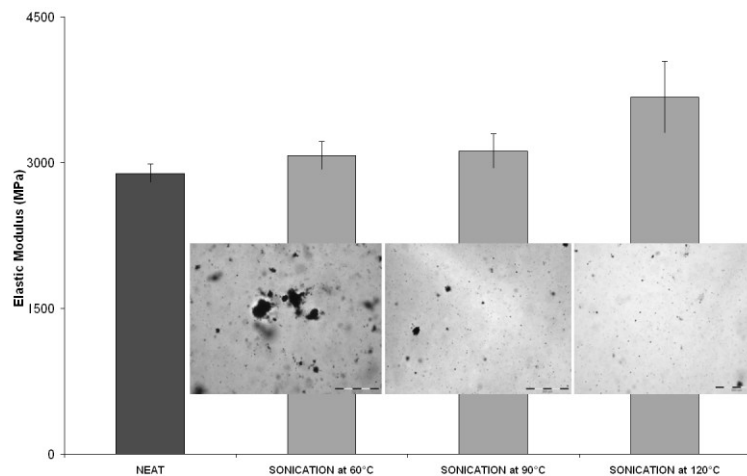
The nano-composites investigated were prepared using 40 mL of resin, sonicated for a constant time (1 hour) at the temperature of 120 °C with a nominal power of 18W.

The high energy sonicator used is a Misonix S3000, characterised by a generator with 600 W output, a 20 kHz convertor and a temperature controller. A titanium tapped horn with a 1/2" (12.7 mm) diameter tip was connected with the convector and directly put into the liquid mixture of resin and MWCNTs to perform dispersion.

All mixtures were degassed in vacuum oven at 90°C for 30 min, and then cast in an aluminium mould and cured; in all cases an identical temperature profile (1 h at 160°C followed by 2 h at 180°C) was adopted. According to the previously found kinetics results, this cure and co-cure temperature profile will lead to complete polymerization with highest obtainable value of glass transition.

It is well known that the effect of ultrasonication is likely associated with cavitation phenomenon in the liquid medium, *i.e.* the formation of bubbles or cavities which form and expand with the impressed pressure field when the wave pressure is lower than the actual liquid pressure. The bubbles originate by two distinct factors: the presence of gas dissolved or entrapped in the liquid (*gaseous cavitation*) or due to the vapours of the hosting medium itself (*vapours cavitation*). The maximum intensity of the cavitation phenomenon is reached just below the horn tip, therefore a *cone-like zone*, where the effect of cavitation is more intensive, is originated. The density gradient produced by the collapsing of the cavitated bubbles gives a rise to convective flows which progressively moves different volumes of the mixture under the *cone-like zone*. Viscosity, along with other factors such as sizes of nuclei, amount of dissolved gasses, vapour pressure and time of sonication represent the most influencing parameter of the sonication on-set, affecting the rate of growth and the collapsing of the cavitation bubbles, therefore very high viscosity may preclude the generation of cavitation reducing the cone-like extension and effectiveness and also, weakening the convective flows.

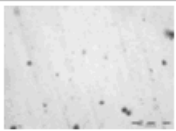
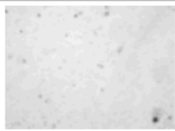
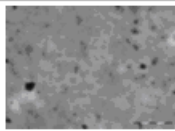
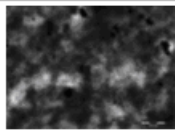
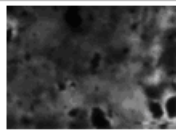
Figure 6- 16 reports the bending modulus (DMA measured) of nano-composites obtained by isothermal sonication for 60 min at 60°C, 90°C and 120°C respectively. Experimental results reveal that mechanical properties improve as dispersion temperature is increased. In fact, optical micrograph images, superimposed in figure, show the presence of coarse submicron particles of pristine nanotubes agglomerates, in the case of 60°C sonicated nanocomposite. Instead, a fine texture, as well as no evidence of micron sized agglomerates, has been observed for the highest sonication temperature (90°C and 120°C), with very rarely found nanotube agglomerates.



**Figure 6- 16: Bending modulus of nanocomposites processed by sonication at three different temperatures with a MWCNT content of 0.1 % wt**

Dispersion state and cluster morphology at the micron scale has been investigated by transmission optical microscopy. Table 6- 1 shows the micrographies of MWCNT/RTM6 samples at different nanotubes concentration (0.05 %wt, 0.1 %wt, 0.2 %wt, 0.3 %wt, 0.5 %wt) cured after sonication dispersion for 60 min at 120°C. At low nanotube content (0.05 %wt and 0.1 %wt – Table 1 a/b) samples appear homogeneous under optical microscope analysis, showing no micro-texture, so at least down to micron scale the sonication provides a dispersion of nanotube agglomerates within the hosting system. At higher concentrations (0.3, 0.5 %wt - Table 1 d/e), optical microscopy reveals not only a sub-micrometric texture but also the formation of micro-sized nanotube agglomerates. At intermediate nanotube content (0.2 %wt – Table 1 c) only a submicron scale texture is observed. As a conclusion, a nanotube network is growing due the increasing nanotube concentration within the matrix by changing the nano-loading content from 0.05 to 0.5 %wt.

**Table 6- 1: Optical microscopy of final nano-composites (Nanocyl N7000) with different CNT content: 0.05 %wt (a); 0.1 %wt (b); 0.2 %wt (c); 0.3 %wt (d); 0.5 %wt (e) MWCNT content.**

<b>MWCNT content (% w/w)</b>				
Sonication for 1hour at 120°C and cure for 1h30' at 160°C and 2h at 180°C				
<b>a</b>	<b>b</b>	<b>c</b>	<b>d</b>	<b>e</b>
				
<b>0.05 %w/w</b>	<b>0.1 %w/w</b>	<b>0.2 %w/w</b>	<b>0.3 %w/w</b>	<b>0.5 %w/w</b>

#### **6.4.2 Characterization of hybrid nano-scale hosting matrix**

The potentiality of carbon nanotubes as reinforcement for polymer matrix is primarily due to their exceptional mechanical property, very high aspect ratio and specific surface to volume ratio [9]. However, in real random carbon nanotube composites, the tubes aggregation or their networking may become a defect causing a loss of the theoretical enhancement of the mechanical properties. Percolation is a statistical topological game, which describes the formation of an infinitive cluster of contacting particles by means of their random distribution on a lattice. Moreover, even if the interparticles potential do play a role in the real organization of the nanotubes network, and then influences the real percolative content, the scaling law relating critical volume fraction,  $\phi_{St}$ , at which the

statistical percolation transition occurs, and filler aspect ratio, AR, fixes a proper upper bound:

$$\phi_{St} = 0.5 AR^{-1}$$

In line with this argument, three types of multiwalled carbon nanotubes (MWNT) with nominal aspect ratios AR=30, 55, 505 were used as received to prepare epoxy matrix composites to experimentally evaluate the effect of the tubes aspect ratio upon the reinforcement mechanism. To this aim, carbon nanotube volume loadings have been chosen within the range of statistical percolation threshold.

N7000 series from Nanocyl (AR=505) and 659258 (AR=55) and 636843 (AR=30) series from Aldrich MWNTs were dispersed into the monocomponent epoxy system RTM6 according to the dispersion process previously defined. In order to isolate the effect of the filler all tests have led at the temperature of 80°C, Figure 6- 5 reports the DMA test for the neat epoxy system considered, the RTM6 resin exhibits two transition temperature, a small transition is detected at -50°C whilst the glass transition of the overall system starts at 150 °C. The temperature test has chosen at 80°C so that any effects of the transitions would affect the measurements.

Since percolation status has been identified as a critical issue for the mechanical behaviour of the system each samples were electrically tested. Electrical measurements were performed in DC current on nanocomposite samples cut and polished on both surfaces until a mean thickness of 1±0.1mm. Electrodes consisting of 50 mm<sup>2</sup> of area circles were painted on the flat surfaces with conductive silver paint. Two-point conductivity measurements were performed on composites through the thickness direction by means of a pico-amperometer connected to a two-probe station (Signatone 1160). A voltage generator was used to apply a constant voltage of 40 V for 300 seconds.

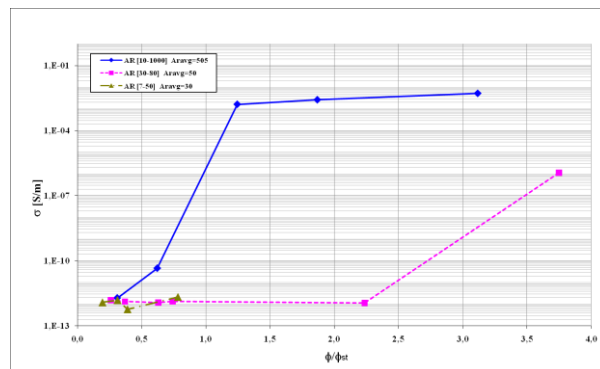


Figure 6- 17: Electrical conductivity measurement. Data are plotted against the ratio of actual filler content and the statistical critical value.

Figure 6- 17 shows the electrical measurement results, data have been reported as function of the filler content to statistical threshold ratio. It is possible to individuate for each hybrid system tested a critical threshold in some cases quite different from the statistical one which allows the definition another critical threshold for the system, depending on the system as representative of the filler status within the hosting matrix, *i.e.* the effective percolation limits for the AR 505 is at 0.06 % vol corresponding to an aspect ratio effective of 811, further details of this analysis have reported from Martone et al.[13].

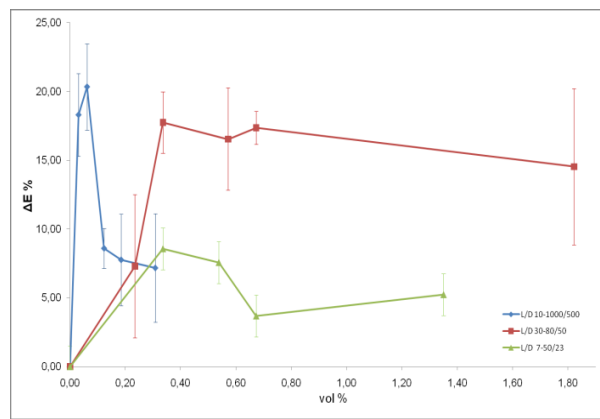


Figure 6- 18: Effect of the aspect ratio in the increment of bending modulus. At higher nanotubi content in each case a decrement in the effect of introducing nanotubes in the matrix is present.

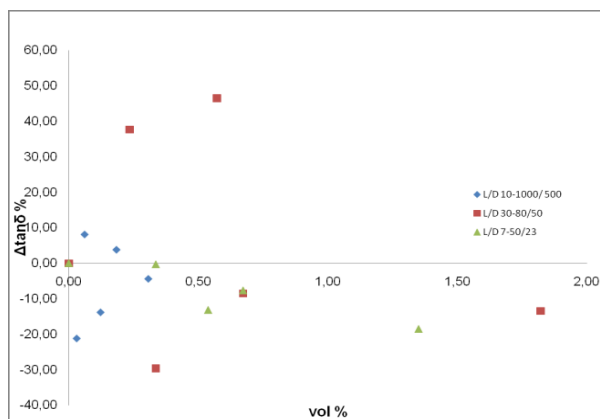


Figure 6- 19: Effect of the aspect ratio in the increment of  $\tan \delta$ . The filler with aspect ratio 50 granted a stepwise increment in  $\tan \delta$ .

In Figure 6- 18 and Figure 6- 19 DMA measurement for each type of filler have reported against the volume content within the hosting matrix.

Even if the enhancement of elastic modulus is clearly identified according to the percolation status of the system, the dissipative behaviour does not follows a trend. In fact,

for two families (AR=505, and AR=30) there is not enhancement in the damping capability of the system, although the MWNTs with aspect ratio 55 shows a stepwise behaviour in terms of  $\tan\delta$ , below percolation their improve the damping capacity of the system until the 45%, whereas for higher loading content this effect disappear.

## **6.5 Coupons for testing**

The aim of this experimental work is to identify a suitable composite architecture capable both to keep the required structural features, and improve passive damping response of the overall structure. As first step, once identified the manufacturing technology allowing the proof for each dimension scale proposed hybrid architecture, unidirectional composites were manufactured to verify if there was the global enhancement of the material response. In the case of interleaved layer, as literature report clearly the advantages of an unidirectional laminate interleaved by a damping film, angle ply composite were manufacture in order to understand if this architecture could be further refined.

### **6.5.1 Hybrid matrix- RTM6 + MWCNT Unidirectional laminates**

Since the VARTM process, considered for fabrication of coupons, requires that additived resin keep a viscosity behaviour to allows the infusion. From results obtained on the resin the nanotubes more promising for the application under study are the MWNT provided by Sigma-Aldrich characterised by a nominal aspect ratio of 55, moreover as previously verified interesting contents are below 2 %vol. (about 3 %wt).

The well dispersed states can be characterized by their reproducible profile of the rheological linear response. Increasing nanotubi concentration increases the values of effective viscosity, a study has led to verify the processability of resin mixed with carbon nanotubes at the interesting concentration. Figure 6- 20 shows the isothermal behaviour of solution containing 0.5 %wt, 1%wt, 3%wt of MWNT, in addition the measurement for the neat resin is reported as baseline.



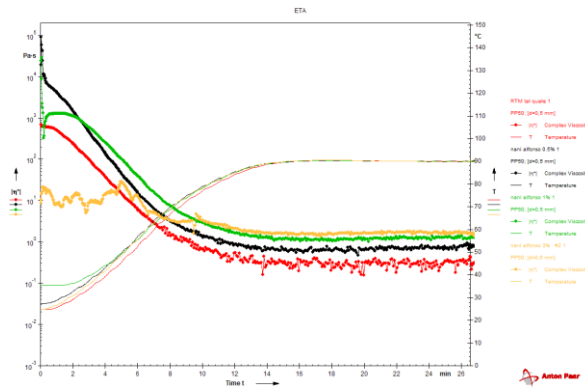


**Figure 6- 20: Viscosity measurements for the nano-loaded matrix at different nanotubes content. Hybrid system consists of the RTM6 epoxy resin mixed with MWNT having aspect ratio of 55.**

Although there is an increment in the resin viscosity the viscosity of the mixture is compatible with the infusion process, moreover in each case the hybrid resin keep this feature for the time need for the infusion process. Figure 6- 21 shows the dispersion state of MWNT within the resin at the content of 1 %wt.

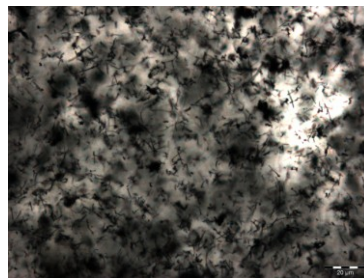


**Figure 6- 21: Optical microscopy for the hybrid 1%wt nano-composite. Image is magnified at 50X.**

Panels were fabricated using VARTM, first precalculated amounts of CNTs and resin were weighted and mixed together such as the weight fraction is the required, then the mixture is sonicated using the procedure defined in section 6.4.1. Unidirectional plates of 8 layer each measuring approximately 220mm x220mm were stacked. Once the fiber preform was infiltrated with RTM6/MWNT system it was allowed to cure 1h at 160°C and post-cure 2h at 180°C. In this study four fiber reinforced panels were fabricated – one control panel with neat resin and three panels with 0.5 %wt, 1 %wt, 3%wt CNT dispersed resin, respectively (Figure 6- 22).

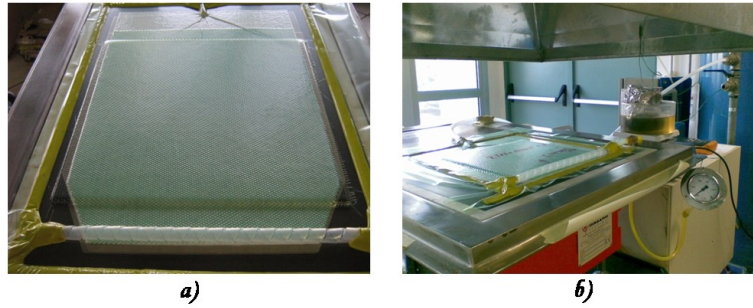


Figure 6- 22: Manufacturing of hybrid unidirectional multiscale composite.

From analysis of the nanocomposite based on the RTM6 and nanotubes characterised by nominal aspect ratio of 55, the more interesting concentration of filler within the matrix would be both 1%wt or 3%wt, the nanocomposite exhibits a stepwise behaviour at the latter contents. Although there is a quite similar enhancement in mechanical and dissipative performance of the system, as preliminary verification on the behaviour of the unidirectional composite the damping test have executed on the reference neat panel and to the 1%wt.

Samples for the further damping tests have cut from the manufactured panel with dimension of 200 mm x 180 mm, with bigger side along the fiber direction.

Damping test had performed in a conditioning chamber at different temperature from -50°C to RT, the specimen is positioned in the chamber hung up with metallic coil to create a boundary condition of free motion the space. The specimen is then excited by a shaker covering all the frequencies, for each testing temperature the experimental loss factor is the mean value over all frequencies.

In the following figures the damping measurement for the baseline plate and for the 1%wt nanocomposite have reported.

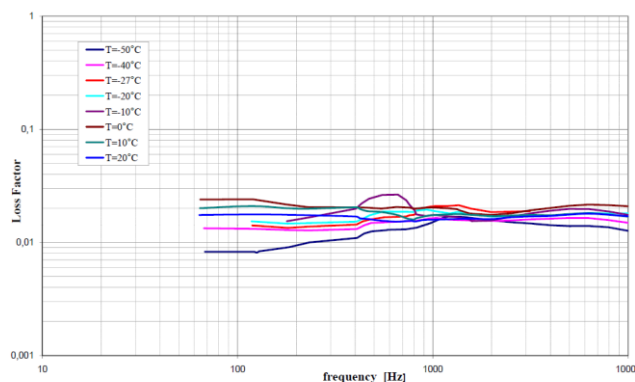


Figure 6- 23: Damping test for the unidirectional composite used as baseline.

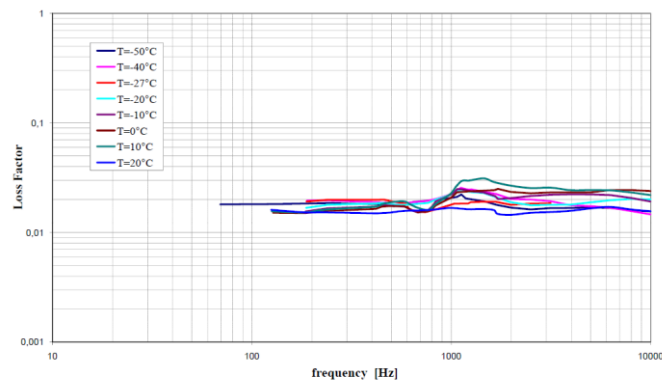


Figure 6- 24: Damping test for the unidirectional composite containing 1% wt of CNTs.

It is important to highlight that at lower temperatures there is a consistent increment in passive damping for the material, whereas at higher temperature the material response is not sensitive of the matrix hybridization.

### 6.5.2 Unidirectional laminates integrating hybrid dry preform

Hybrid carbon fiber preform with previously integrated viscoelastic fibres at two volume fraction percentage ( 5 % vol., 10 % vol.) have been used to manufacture laminate by using the RTM6 epoxy system through the vacuum infusion process. The following figures show the relevant steps in hybrid flat panel manufacturing. In addition to the hybrid laminate a plate without damping treatment was manufactured as baseline for testing phase.

The Figure 6- 25 a) shows the stacking of the hybrid laminae upon the tool, in the b) and c) are shown the vacuum bag preparation and the infusion process. Figure 6- 25 d), e) and f) report the curing phase of coupons, the demoulding phase and the final composite plate, respectively.

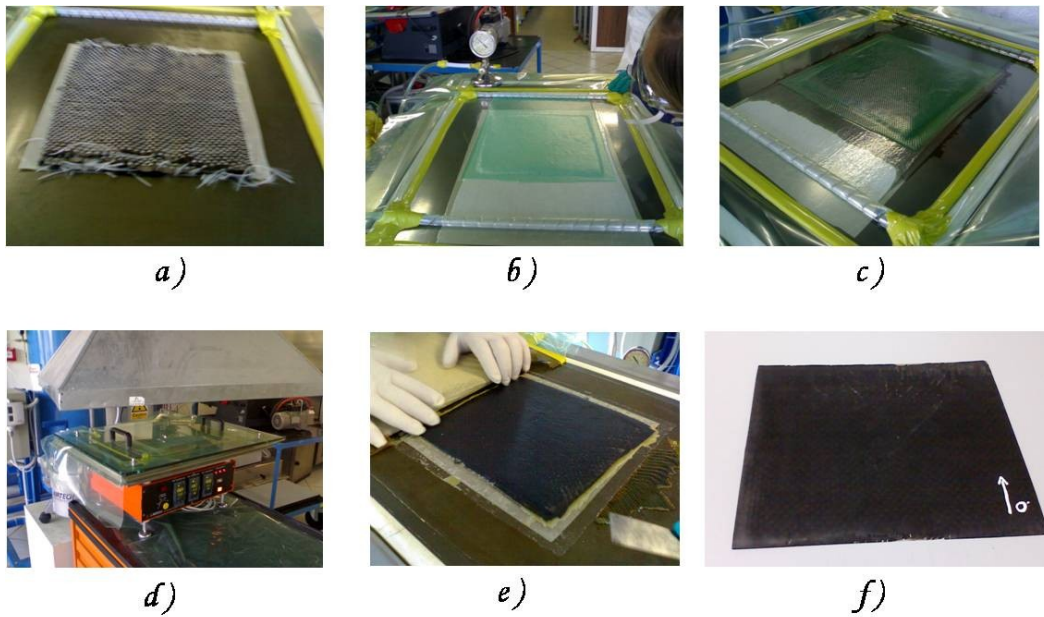


Figure 6- 25: Composite manufacturing via vacuum infusion process. The relevant phases of the process are: the stacking upon the tool a), vacuum bag preparation b), resin infusion c), cure of the system, d) demoulding of composite plate.

Critical items in the manufacturing of the hybrid dry preform composite, are related to the viscoelastic fibres behaviour within the dry preform.

Before the infusion viscoelastic fibres could introduce a shrinkage phenomenon in the preform for effect of a excessive strains induced by the weaving, moreover a similar consequence could be brought out when mould is heated.

Micrographs confirm that the viscoelastic fibres resists to the manufacturing process, even if, perhaps due to cutting of preform or to the stacking phase Lycra fibres seems to became stretched, Figure 6- 26 shows the carbon tow and the contiguous viscoelastic fibres.

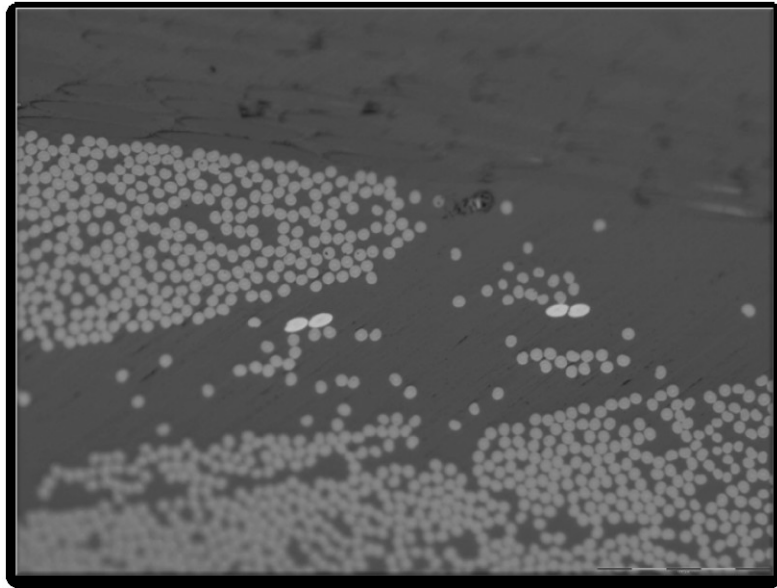


Figure 6- 26: Micrograph of hybrid laminate including 5 % vol. of viscoelastic fibres, picture is magnified at 20X. The thermoplastic elastomeric fibres are visible contiguous to carbon tow according to the textile architecture defined.

The hybrid preform with 5 percent in volume of viscoelastic fibres maintains its cohesion, unfortunately preforms with 10 percent in volume are extremely sensible to the thermal effects Figure 6- 27 a), in that case for the manufacturing of the composite plate the vacuum bag required to be prepared upon a cold tool. Although this expedient in resin infusion final composite had some regions where hybrid tow have moved away Figure 6- 27, rationale for such finding is the effect of hot flow during infusion process.

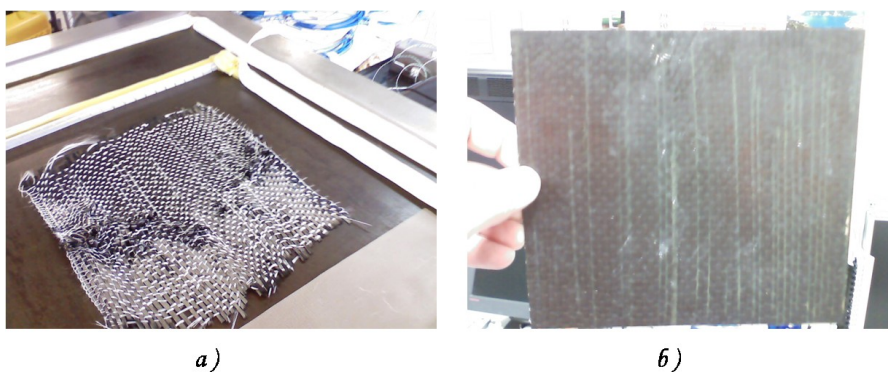


Figure 6- 27: Hybrid dry preform containing 10 % vol. of viscoelastic fibres exhibits important manufacturing problems. a) shrinkage due to the contact with the heat tool b) composite plate after demoulding,

Dynamical mechanical measurement were carried out using a TA DTMA Q800 in three point bending testing mode, with 50 mm span between the supports. The temperature scan

measurement were performed over the temperature range of -50 °C to 180 °C with heating rate of 5.0 °C/min and constant frequency of 1.0 Hz.

The following pictures reports dynamical mechanical tests for the unidirectional composites. In Figure 6- 28 and Figure 6- 29 elastic modulus and  $\tan\delta$  for unidirectional composite made of the neat dry preform and RTM6 resin were reported, this data will be used as baseline in further investigations.

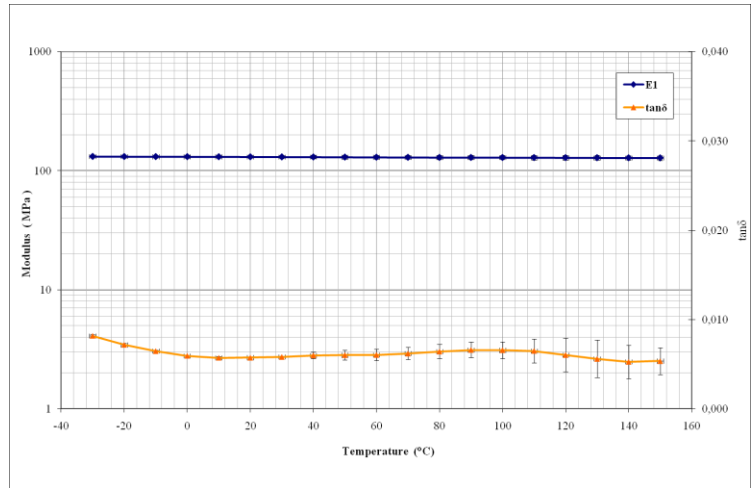


Figure 6- 28: DMA analysis of TCU260+RTM6 composites, unidirectional 0° samples

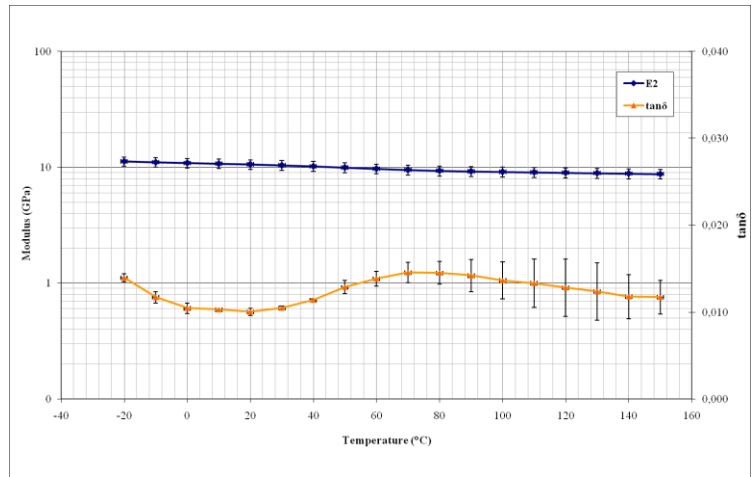


Figure 6- 29: DMA analysis of TCU260+RTM6 composites, unidirectional 90° samples

In the following Figure 6- 30 and Figure 6- 31 experimental data for the composited fabricated with the hybrid dry preform including 5 volume percent of viscoelastic fibres.

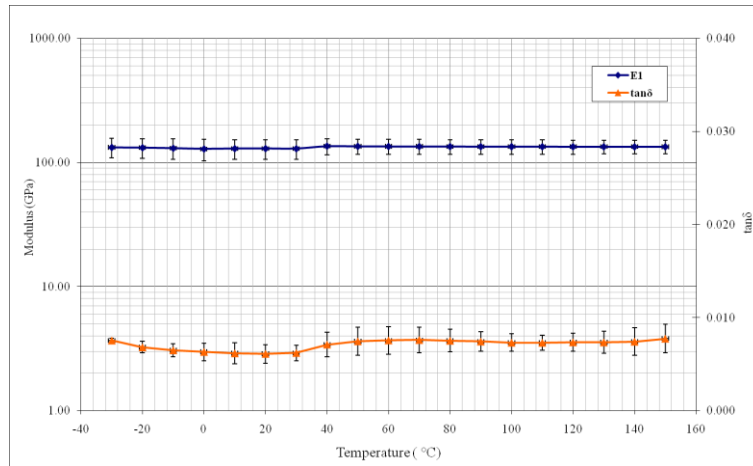


Figure 6- 30: DMA analysis of Hybrid 5%+RTM6 composites, Unidirectional 0° samples.

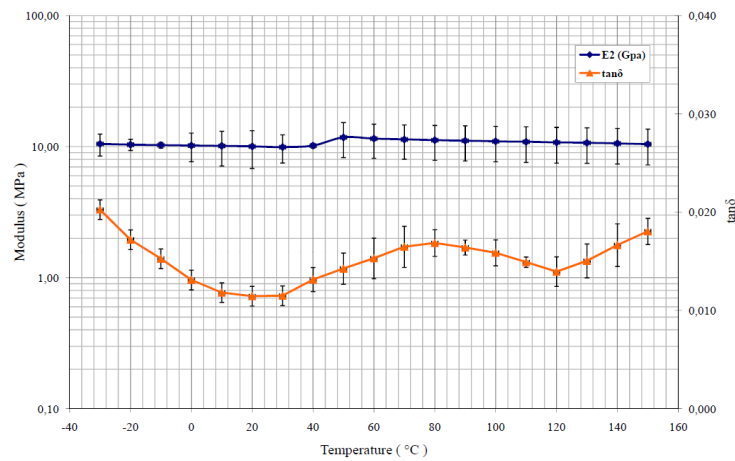


Figure 6- 31: DMA analysis of Hybrid 5% +RTM6 composites, Unidirectional 90° samples.

Whereas in the Figure 6- 32 and Figure 6- 33 experimental data for composites made with the 10 volume percent hybrid dry preform have reported.

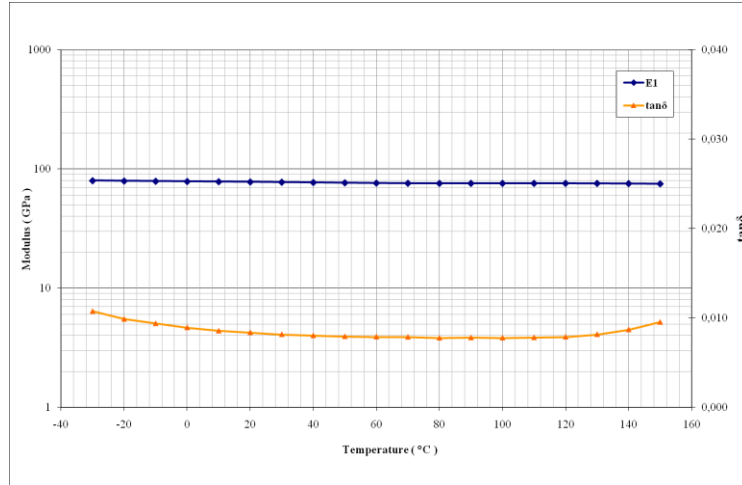


Figure 6- 32: DMA analysis of Hybrid 10%+RTM6 composites, unidirectional 0° samples

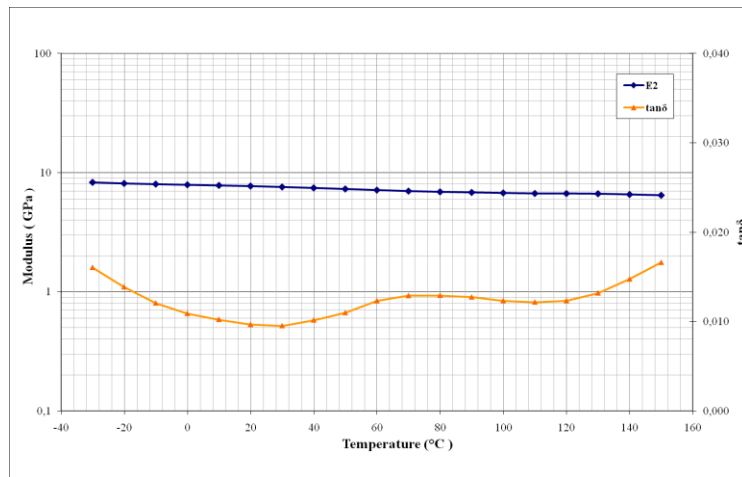


Figure 6- 33: DMA analysis of Hybrid 10%+RTM6 composites, unidirectional 0° samples

### 6.5.3 Hybrid laminates- Angle ply laminates embedding viscoelastic sheets

The capacity of unidirectional laminates with interleaved viscoelastic layer has been proved by a number of literature works, in chapter IV a review of the more interesting activities has been provided. As observed the main criticality related to the use of a softer layer in the stacking is the effect of interlaminar stresses that could promote material failure. Another aspect is the role that laminate stacking exercises in the damping capacity of a layered material. Combining the effects of the damping layer on the raising up of interlaminar stresses and consequently the damping with the tuning of the interlaminar shear stress due to the stacking sequence, hybrid laminates including viscoelastic layer have fabricated in



order to individuate an optimum configuration able to keep mechanical property and able to increment passive damping feature.

Four composite plates were fabricated by VARTM process, three hybrid laminates where viscoelastic layers are positioned at centre, symmetrically moved from middle plane of one layer, moved of two layer, as baseline for the investigation were fabricated a layer without damping treatments. The base stacking sequence used is  $(0/90/0)_s$ , viscoelastic material used for this investigation was the Mobilon provided by Nisshimbo available as adhesive film of controlled thickness. Figure 6- 34 shows manufacturing process for the hybrid plates.

The symmetric balanced laminates were fabricated with dimension of 220 mm x 220 mm, viscoelastic sheet were cut in sheet of 200 mm x 200 mm and located at the centre of laminate. Each hybrid plate contain the same amount of viscoelastic material, the configuration with the layer at middle plane has an only sheet of 200  $\mu\text{m}$ , whereas in other configurations there are two sheet of 100  $\mu\text{m}$ .

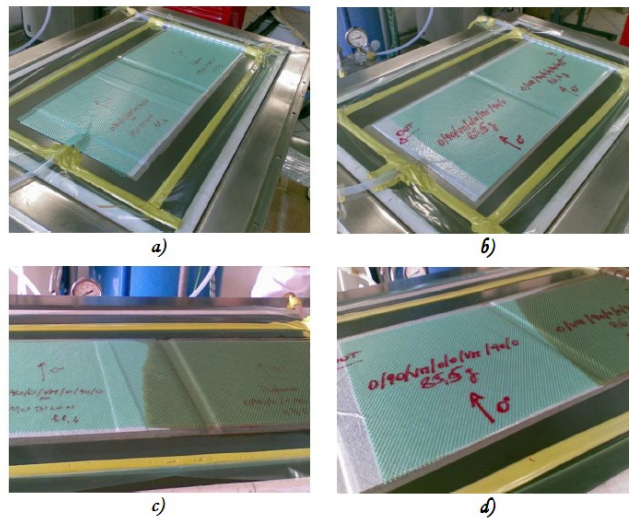


**Figure 6- 34: Manufacturing of hybrid interleaved layer architecture composites. Baseline plate and laminate with the viscoelastic layer at the middle C0 have been fabricated together a), e). The hybrid laminates with viscoelastic layer moved away from middle plane have fabricated below a common vacuum bag.**

The following table describes the configuration of laminates fabricated.

**Table 6- 2: Interleaved layer fabricated panels**

Reference	$(0/90/0)_{\text{sym}}$
C0-middle plane	$(0/90/0/\text{VM})_{\text{sym}}$
C1-middle plane +1	$(0/90/\text{VM}/0)_{\text{sym}}$
C2-middle plane +2	$(0/\text{VM}/90/0)_{\text{sym}}$

Specimens cut from the manufactured plates were tested by Dynamical Mechanical Analyzer, in three point bending mode. Span distance in the test was set to 50 mm, the test has led at constant frequency of 1 Hz over the temperature range of -40°C to 160°C at constant temperature rate of 5 °C/min. Following figures reports test results.

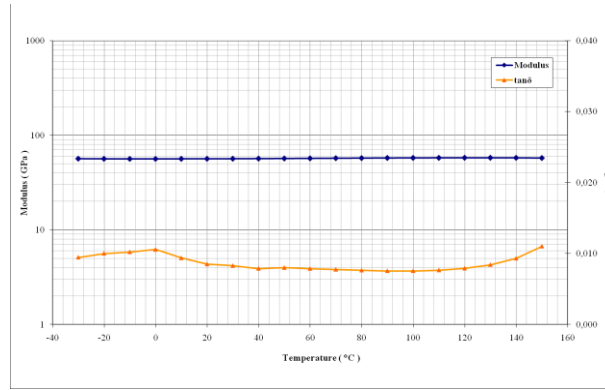


Figure 6- 35: DMA test for the reference angle ply laminate

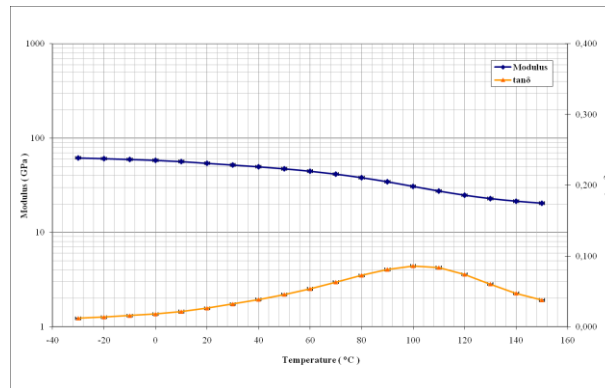


Figure 6- 36: DMA test for the interleaved layer configuration

The test on the C0 configuration, where the viscoelastic sheet is arranged in correspondence of the middle plane, indicates that laminate passive damping is greatly improved, but it is evident the decrease in bending modulus.

In the case of C1 or C2 there is not relevant variation from the reference laminate, rationale for this behaviour is the fact that in each case the viscoelastic layer position does not reach a region with high interlaminar stresses, moreover the sheet (0.10 mm) are too thin to trigger the high strain required for increment the energy stored by it selves.

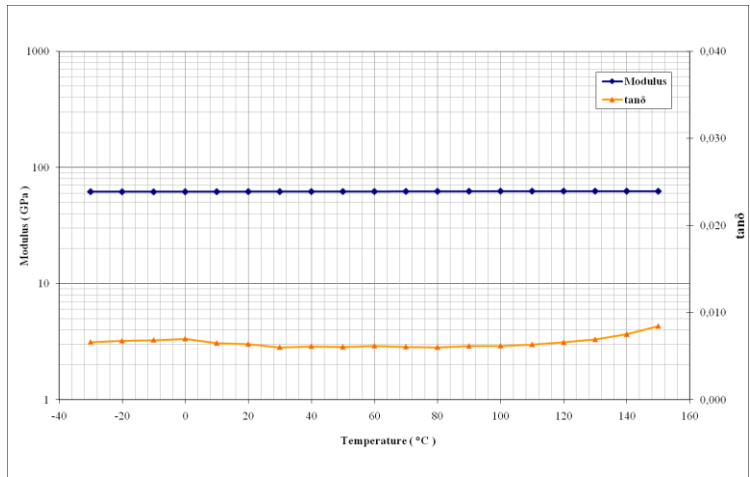


Figure 6- 37: DMA test for the C1 configuration

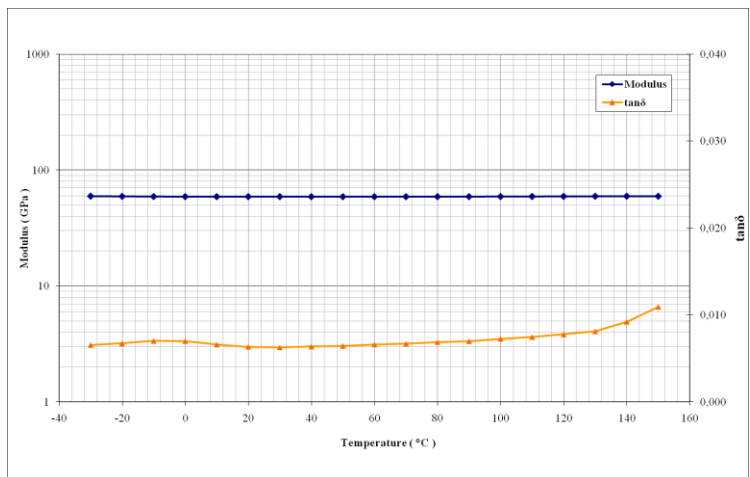


Figure 6- 38: DMA test for the C2 configurations

## 6.6 Conclusions and Discussions

In this chapter the experimental analysis of the proposed hybrid architecture have proposed. For each architecture proposed an unidirectional coupon has tested to verify the increment in loss factor.

In each case a valuable increment in passive damping were measured, mainly at the requirement temperature, i.e. the cruise condition in the case of an aeronautical application. Both the interleaved layer and the hybrid dry preform lead to a loss in mechanical performances for the considered material, although the material damping is enhanced at each testing temperature.

In the case of nanoloaded matrix composites, mechanical performances are kept over all test condition, but the enhancement in material damping is sensible only at temperatures below zero degrees.

### 6.6.1 Macro-scale analysis of hybrid composites.

The experimental data on the interleaved architecture confirm that this solution allows to a strong increment in material loss factor, however a sensible effect is recorded in term of material stiffness.

The most efficient configuration for damping enhancement is discovered to be the laminate with a viscoelastic layer at middle plane. In a laminate beam the shear stress distribution is a curve formed by arcs of parabola with the boundary condition of to be zero at laminate faces and reaches its maximum value in correspondence of the middle plane. The strong increment in damping performance measured indicates that shear stresses induce a great deformation in the viscoelastic layer which allows to store an higher energy and thus an increase in the dissipated energy.

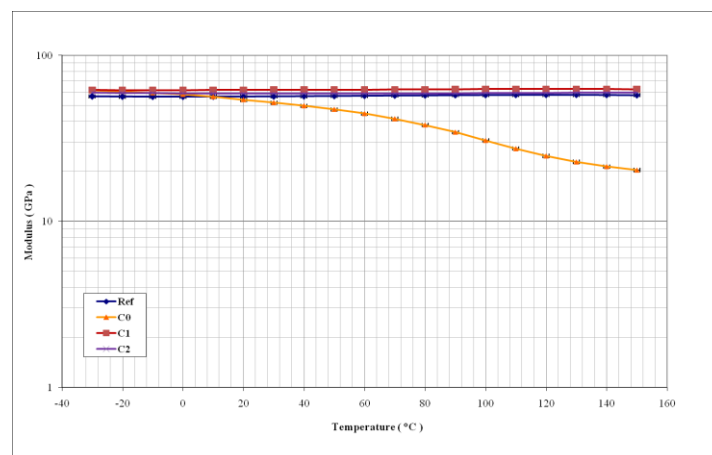


Figure 6- 39: Comparison of mechanical data for interleaved layer architectures

The C0 configuration is the most suitable for temperatures well below zero degree, in fact at the standard temperature of  $-30^{\circ}\text{C}$  an increasing of about 25% in material damping is measured, this enhancement is magnified increasing temperatures. Unfortunately approaching to room temperature coupling to the increment of material damping capacity the bending modulus progressively decrease, at room temperature 20% in mechanical performance is lost by this phenomenon.

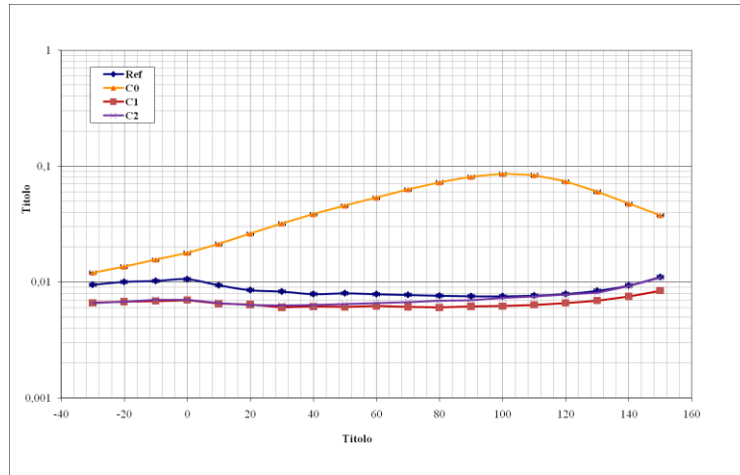


Figure 6- 40: Comparison of dissipative data for interleaved layer architectures

Other configurations, instead does not reveal any variation in material performance, this could be attribute to two main causes, the sheet are thinner enough to do not excessively deforms and away from high shear stress.

Furthermore the use of this architecture may require a modification in the case of automated production process due to the stacking of viscoelastic sheet within dry preform before the infusion.

### 6.6.2 Micro-scale analysis of hybrid composites.

In the following figures are highlighted experimental data extrapolated from tests on the hybrid preform composites at the temperature of  $-30^{\circ}\text{C}$ , actually requirements for damping performance for aeronautical application are formulated for the cruise phase.

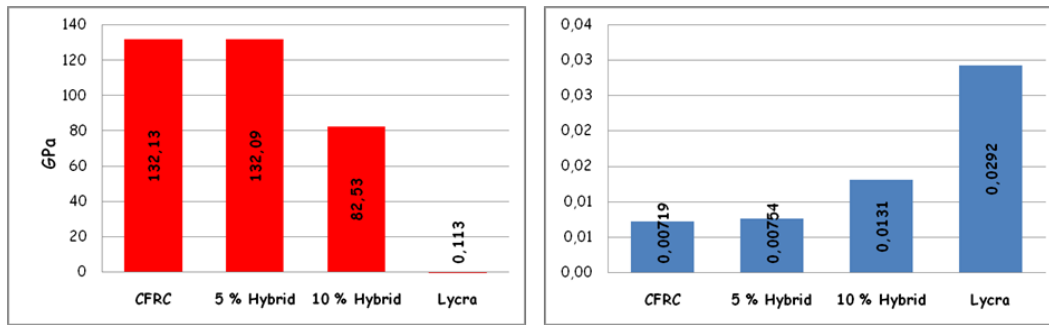


Figure 6- 41: Comparison of the mechanical and the dynamic properties of the hybrid unidirectional composites. The data have been extrapolated from previous tests at the temperature of -30 °C in fiber direction.

The 5 % hybrid preform performed a negligible effect in fiber direction, but in transverse direction a 20% increment has obtained over the decreasing in transverse elastic modulus. The 10 % hybrid preform had a strong decrease in material stiffness.

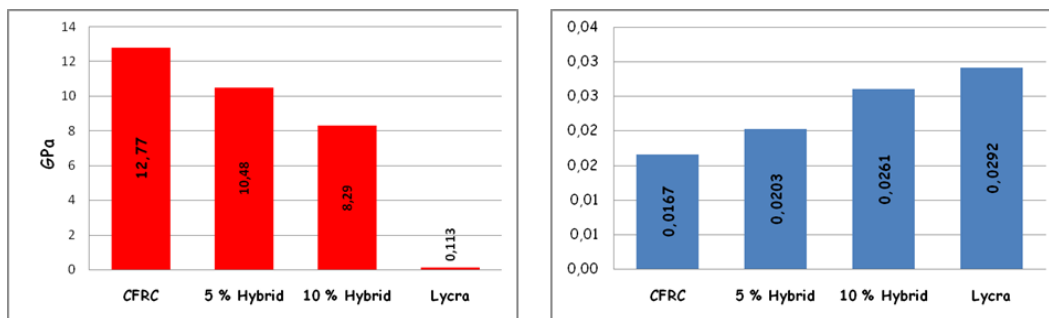


Figure 6- 42: Comparison of the mechanical and the dynamic properties of the hybrid unidirectional composites. The data have been extrapolated from previous tests at the temperature of -30 °C orthogonal to fiber direction.

At the temperature of -30 °C an increment of damping capacity in the orthogonal to fiber direction of 60 % has been reached in the case of 10 % specimens even if this lead to a loss in mechanical performances of the final composite. In the case of 5 % specimens the increase of the loss capacity is of 20 % and in the latter case the bending modulus in fiber direction has been kept to the reference value.

### 6.6.3 Nano-scale analysis of hybrid composites

The Figure 6- 43 shows the effective reinforcement modulus,  $E_{\eta}$ , as a function of the volumetric filler content normalised to the electrical percolation threshold. Mechanical

reinforcement data have been redrawn with reference to the effective mechanical modulus of the reinforcing phase,  $E_{\eta}$ , according to the following equation:

$$E_{\eta} = \frac{E_{\text{composite}} - E_{\text{matrix}}}{\phi} - E_{\text{matrix}}$$

For all filler typologies the effective filler modulus,  $E_{\eta}$  is a monotonic decreasing function of the content.  $E_{\eta}$  is characterised by two limiting behaviours, both aspect ratio dependent, whose transition region coincides with the development of the network of the nanotubes within the matrix. Well below the percolation threshold, the carbon nanotubes contribute to the composites stiffness with highest  $E_{\eta}$ , with effective modulus that varies with the aspect ratio, whereas the effective dramatically decreases as the filler content increases.

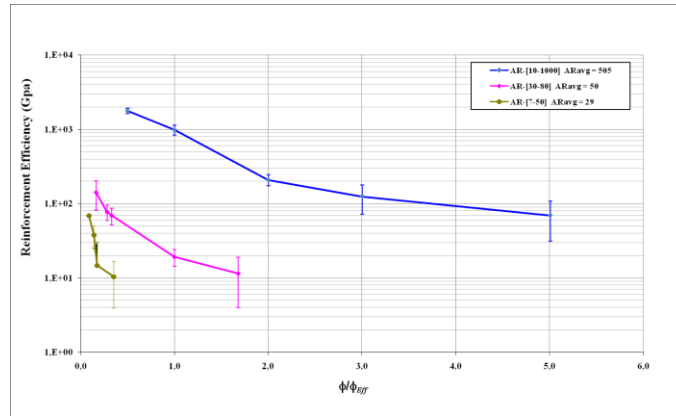
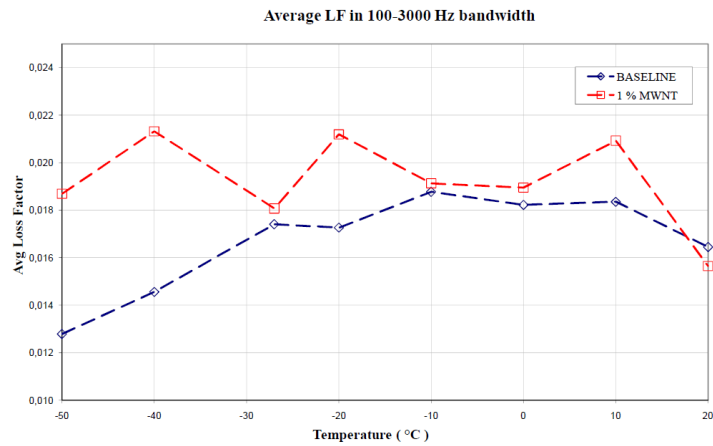


Figure 6- 43: Effective reinforcement modulus,  $E_{\eta}$ , as a function of normalised volume content of nanotubes for the different aspect ratios fillers.

To predict the material properties of multiscale composites, a three step micromechanics would be used. First mechanical properties of the nano-composite is evaluated, then the classical micromechanics for long fiber composites lead to the final properties of the hybrid lamina. In the following table the prediction for the mechanical properties of the 1%wt composite have reported.

Table 6- 3:Multi-scale composite properties for 1%wt plate

	Dry preform		MWNT+RTM6 @ RT			Composite			
Preform	E	231.0	GPa	E	2.89	GPa	$E_1$	139.8	GPa
volume	$v_f$	0.30		$v_f$	0.38		$E_2$	7.09	GPa
content	$\rho_f$	1790	kg/m <sup>3</sup>	$\rho_r$	1140	kg/m <sup>3</sup>	$v_{12}$	0.33	
	0.60	G	88.85	GPa	G	1.05	$G_{12}$	2.57	GPa
							$\rho$	1530	kg/m <sup>3</sup>



**Figure 6- 44: Damping test for unidirectional hybrid multi scale unidirectional composite.**

Figure 6- 44 reports the comparison for the averaged loss factor for the baseline and the 1% nano-loaded unidirectional composites over the temperature of test.

In the range of interest for aeronautical application ( from -20 °C to -40 °C) the use of nanoloading lead to a strong increment in dissipative material property, in fact in this range there is a gain of 30%, moreover the use of a filler as carbon nanotubes, capable to increment the elastic modulus, allows to acquire a neat increment of damping performance without loss in mechanical performances of the overall structure.



## 6.7 References

- [1] Campbell FC, 2006. Manufacturing Technology for Aerospace Structural Materials. *Elsevier*.
- [2] Tong L, Mouritz AP, Bannister MK, 2002. 3D Fiber reinforced polymer composites. *Elsevier*
- [3] <http://www.hexcel.com/.../HEXCELRTM64PPA4.pdf>
- [4] Martone A, Zarrelli M, Antonucci V, Giordano M, 2009. Manufacturing and testing of an hybrid composite integrating viscoelastic fibres. *Proceeding of ICCM 17<sup>th</sup>-International Conference on Composite Materials*
- [5] [http://www.invista.com/page\\_product\\_index\\_en.shtml](http://www.invista.com/page_product_index_en.shtml)
- [6] [http://www.nisshinbo-chem.co.jp/english/products/tpu\\_mobilon/mobilon\\_film.html](http://www.nisshinbo-chem.co.jp/english/products/tpu_mobilon/mobilon_film.html)
- [7] Suhr J, Koraktar N, Keblinski P, Ajayan P, 2005. Viscoelasticity in carbon nanotube composites. *Nature Materials Vol. 4*.
- [8] Rajoria H, Jalili N, 2005. Passive vibration damping enhancement using carbon nanotube-epoxy reinforced composites. *Composite Science and Technology 65*.
- [9] Thostenson ET, Li CY and Chou TW, 2005. Nanocomposites in context. *Composite Science and Technology 65*.
- [10] Hernández-Pérez A, Avilés F, May-Pat A, Valadez-González , Herrera-Franco PJ, Bartolo-Pérez P, 2008. Effective properties of multiwalled carbon nanotube/epoxy composites using two different tubes. *Composite Science and Technology 68*.
- [11] Formicola C, Martone A, Zarrelli M, Giordano M, 2008. Dispersion of Carbon Nanotubes in a mono-component epoxy system. *Proceeding of AIDC 2008*.
- [12] Formicola C, Martone A, Zarrelli M, Giordano M, 2009. Reinforcement efficiency of multi-walled carbon nanotube/epoxy nanocomposite. Submitted to *Composite Science and Technology*.
- [13] Martone A, Formicola C, Zarrelli M, Giordano M, 2009. The effect of the aspect ratio of carbon nanotubes on their effective reinforcement modulus in an epoxy matrix. Submitted to *Applied Physics Letters*.
- [14] Kim M, Park YB, Okoli O, Zhang C, 2009. Processing, characterization and modelling of carbon nanotube-reinforced multiscale composites. *Composite Science and Technology 69*.

# 7

## Hybrid composite Stiffened Plate

### 7.1 Summary

Among the hybrid architectures examined in the course of this study the more promising which is, at same time, capable of enhancing the damping response of a composite structure and withstand its mechanical performances, has resulted the “multiscale” laminate.

A multiscale laminate is a fiber reinforced polymer modified with CNTs, is indicated as “*multiscale*” as they are reinforced with microscale fibres and nanoscale nanotubes. High energy sonication has been widely used to disperse the CNT load in the resin before the infusion, however more recently calendaring has gained popularity as a means to disperse CNTs due to its efficiency and scalability which make it the suitable for high volume and high rate production.

This chapter addressed the design and the manufacturing of typical composite structures for aeronautical application. A stiffened composite plate is manufactured by using VARTM process and acoustical tests performed; large scale panel was also manufactured to mechanical characterize the hybrid laminate.

## 7.2 Manufacturing and testing of multi-scale plane plate

In chapter VI, the comparison of the obtained experimental data between the considered hybrid material architectures has indicate as most valuable configuration the hybrid multiscale system. In fact, at low temperatures range (-50 °C to 0°C), which are typical cruise condition for a commercial aircraft, this architecture warrants an improvement for damping features, without loss in mechanical performances.

In chapter VI only the material performance at coupons level and unidirectional layup has been examined. In order to verify if the proposed solution maintains its special features at component level Angle ply composites were manufactured and statically tested. This chapter present the experimental results obtained on hybrid “multiscale” angle ply composite specimens.

### 7.2.1 Material architecture

According to the study performed on carbon nanotube effects on damping performances it has been resulted that nanocomposites loaded with low aspect ratio filler can improve their passive damping feature, therefore confirming the numerical study presented in chapter V. Furthermore, the CNT characterised by aspect ratio of 50 (nominal property are reported in Table 7- 1) determine an improvement of the overall material damping.

**Table 7- 1: Properties of CNTs used**

Aldrich – 659258			
	Min	Max	Average
<b>L [μm]</b>	<b>5.0</b>	<b>9.0</b>	<b>7.0</b>
<b>D [nm]</b>	<b>170</b>	<b>110</b>	<b>140</b>
<b>L/D</b>	<b>29.4</b>	<b>81.8</b>	<b>50</b>
<b>ρ [g/mL]</b>		<b>1.7</b>	

The study on nanocomposites based on the multiwalled carbon nanotubes Aldrich 659258 reveals a stepwise behaviour for this typology of hybrid material. For loading below the 1% weight, the effects on  $\tan\delta$  is negligible, while, at concentration above this limit, a remarkable increment of about 35% was experienced. It was also noted that an increase in nanotubes content into the liquid resin will dramatically arise the viscosity affecting its potential usage for the infusion processes.

To strike a compromise between the requirement of improving material damping and the necessity of keep low the system viscosity, nanotubes content was fixed at 1% weight, as

this percentage could represent an optimal balance between the passive damping enhancement of the system, along with an increment in elastic modulus too, and the system viscosity at a level suitable for the liquid infusion technology. Figure 7- 1 shows the viscosity behaviour of the nanoloaded system for effect of increasing temperature, the system reaches it minimum viscosity at the temperature of 120°C, and gelation phenomenon starts at 160°C after few minutes.

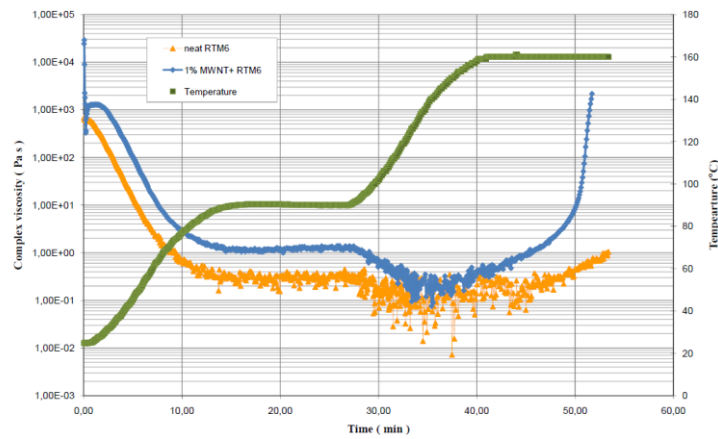


**Figure 7- 1: Complex viscosity measurement for the 1% CNTs+ RTM6 system. The isothermal measure at the infusion temperature of 90°C shows the increment of the system viscosity**

The manufacturing process of multiscale composites is divided in two separated processes; first, the amount of needed carbon nanotubes is dispersed into the resin according to the process described in the chapter VI, then the composite plate is fabricated by VARTM process. Although the minimum value for system viscosity at 120°C, the resin infusion temperature was set to 90°C, rationale for this choose is that at 120°C resin system could start its cure if the infusion time is elevated, this solution was used taking into account the possible stage of infusing a bigger sized component, in addition the high volume of resin could create a mass effect on the system making difficult the control on the resin temperature during the infusion.

For mechanical characterization two composite plate were manufactured, one used as baseline has been infused with pristine RTM6 and the second with the nanoloaded resin. Figure 7- 2 shows the main phases of the manufacturing process. Firstly the reinforcement preforms are stacked upon the preheated tool, *a)* including the peel ply and *b)*, the distribution, package then the vacuum bag is tightened by vacuum application *c)*. Later the resin system is infused and the plate is cured 1 hour at 160°C, the plates were subject to a post-curing phase of 2 hours at 180°C.

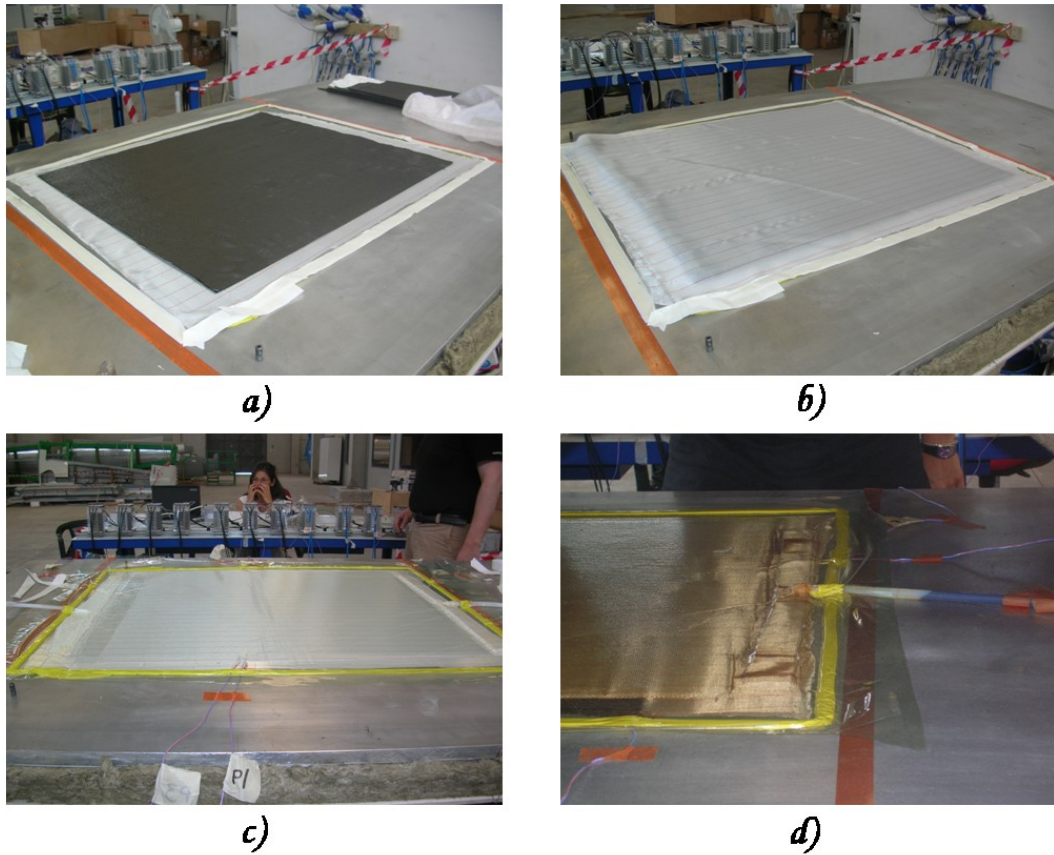


Figure 7- 2: Vacuum bag preparation. a) the reinforcement preform is stacked upon the tool, b) pellply application, c) vacuum bag application, d) the plate after the curing process

The two manufactured laminate plate are described in the Table 7- 2; laminates stacking sequence was defined so that the final composite would be symmetric and balanced. Since this material would be used for the final component and knowing how laminate lay-out influences the passive damping behaviour, the stacking sequence is chosen with central layers oriented at  $45^\circ$ , solution that increment the interlaminar stresses and consequently the material damping, the laminate stacking sequence is set to be  $(0/45/90/-45)_{sym}$ , the dimension of the final plane plates was defined so that from each plate, 5 different specimens for each type of mechanical test could be available.

Table 7- 2: Manufactured hybrid plates

	Size	Lay-up	Preform	Resin system
Reference Plate	740x630 mm	$[0/45/90/-45]_s$	HTA-G1157	Hexcel RTM6
Multiscale Composite	740x630 mm	$[0/45/90/-45]_s$	HTA-G1157	Hexcel RTM6 +1% MWCNT

From manufactured plates were cut five typology of specimens to be used for each mechanical test configuration Figure 7- 3.

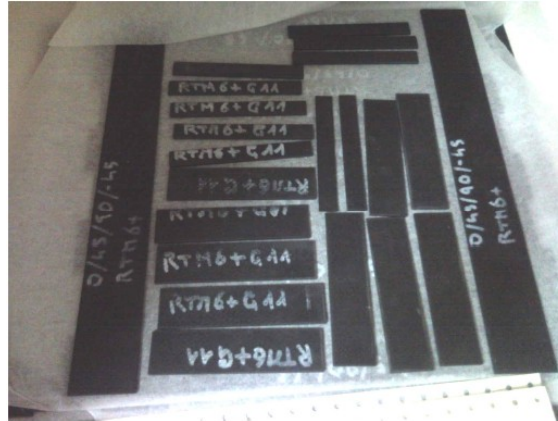
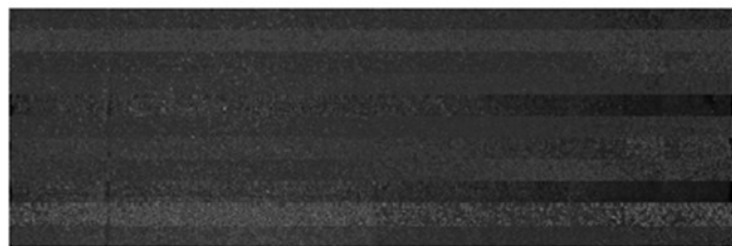
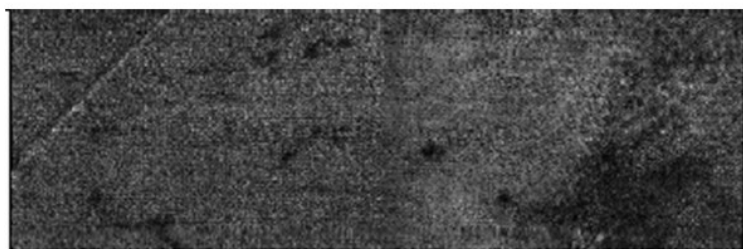


Figure 7- 3: Specimens for mechanical testing

The integrity of specimens cut from the manufactured plate to performed the mechanical tests was verified by the ultrasonic NDT technique; in fact in some cases the cutting phase could introduce delamination within specimens. Figure 7- 4 shows two images from ultrasonic scanner; figure 7-4 a) represents an image of the plate made by neat resin, the ultrasonic investigation confirms that plates are uniformly in thickness and the global integrity of material is preserved, even if there are small delaminations at plate edges.



a)



b)

Figure 7- 4: Ultrasonic analysis of coupons before testing. a) scanning on the fiber reinforced plate manufactured as baseline in testing, b) scanning on the multiscale fiber reinforced plate

Figure 7- 4 b) reports the ultrasonic scan for the multiscale composite, also in this case the plate integrity is confirmed, however some gaps were detected on the right side of the plate. The hybrid plates presents some delaminations at the edges as well as detected for the baseline plate. In addition to samples needed for mechanical test, two plates for the damping analysis have been prepared in the dimension of 200mm x 600mm corresponding to free space from stringers for the final stiffened plate.

### 7.2.2 Mechanical testing

In this paragraph mechanical test for the hybrid composites described in the previous section are reported. Mechanical tests were defined in order to have a complete mechanical characterization of the material and to investigate the effect of carbon nanotubes dispersed into the resin system. For a complete mechanical description of a composite material the tensile, the compression and the bending behaviour are requested, in addition the interlaminar strength feature is examined.

All the test have been performed with the Instron 8800 system, with load cells of 100 kN (for tensile and compression tests) and 10 kN (for bending tests), for each test fixtures requested for the corresponding standard have been employed [27]-[30].

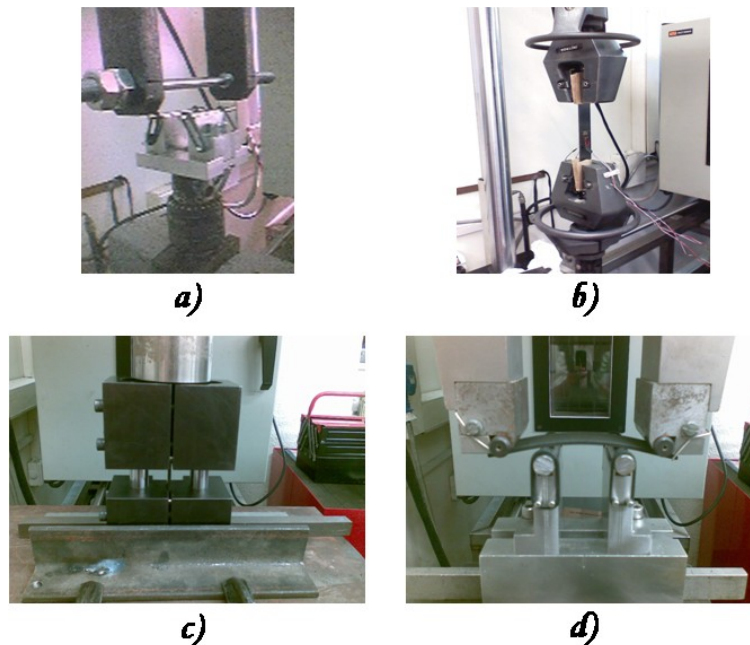
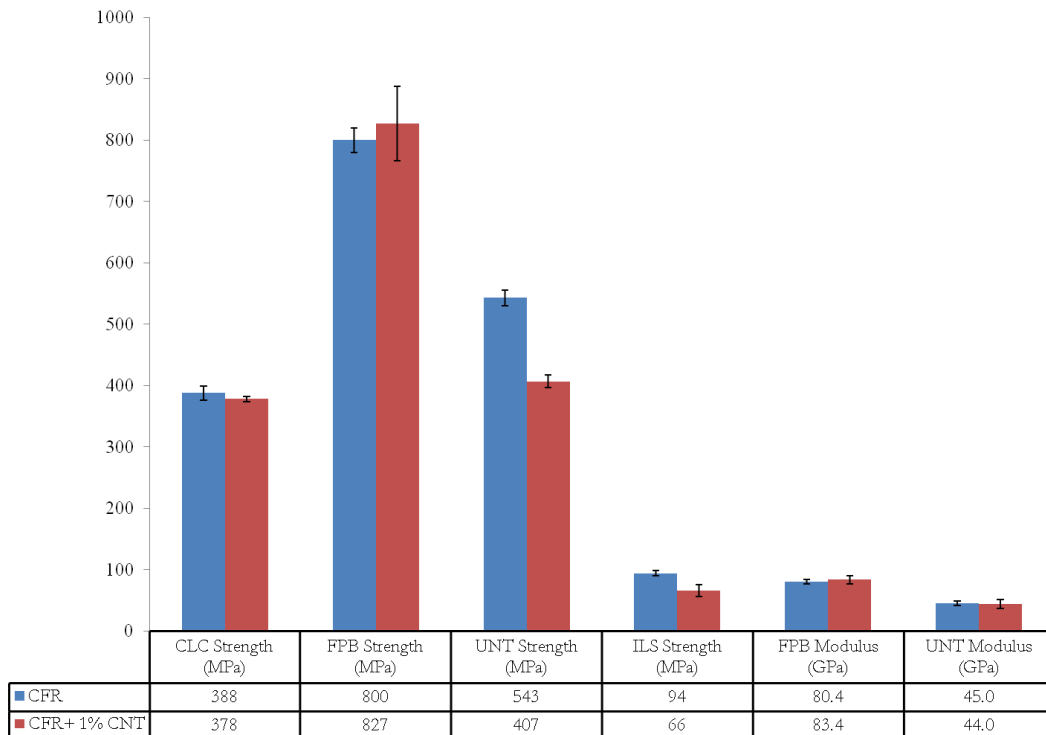


Figure 7- 5: Mechanical test set-up. a) Short beam test fixture (SBS), b) Un-notched tensile fixture (UNT), c) Uniaxial compression fixture (CLC), d) Four point bending fixture (FPB).

In, Figure 7- 6, mechanical test results have been reported comparing the two different neat and nanoloaded matrix. The presence of carbon nanotubes in the matrix does not influence the mechanical performance in term of elastic modulus, in fact tensile modulus and bending modulus for both configuration are quite similar taking into account standard deviation.



**Figure 7- 6: Mechanical test results. Loading the matrix by carbon nanotubes does not modify sensibly the mechanical properties of the laminate, only tensile and interlaminar strength decreases.**

As well as the elastic modulus flexure strength and the compression strength are comparable, in the case of four point bending the standard deviation for the measure of the multiscale composite includes the value measured for “neat” composite, moreover the deviation from average value is greater than neat measure; analogues considerations could be drawn for the compression strength.

Instead, the effects of nanotubes is evident on the tensile strength feature were the material loss over the 20% of its strength. Another critical performance is the interlaminar shear strength which is decreased by the nanotubes introduction, in that case besides the loss in the mechanical performace of the material, there a change in the failure mode: the “neat” composite fails in flexure, the internal fiber breaks in compression mode, whereas the “multiscale” composite fails due to the inelastic deformation.



## 7.3 Design and Manufacturing of Stiffened plate

Aim of this chapter is to verify the feasibility on large scale component for the optimal defined material architecture. The technology chosen for the fabrication remains the VARTM process thanks to its adaptability on possible geometries and, as mentioned before, the capability to process easily the hybrid material. In fact by VARTM it is possible to infuse modified resin, i.e. pre-processed by the addition of carbon nanotubes, or to infuse an hybrid preform or preform including viscoelastic material sheet.

In this paragraph, is reported the preliminary definition of a large scale composite component, and the manufacturing process. As mentioned in the previous paragraph the hybrid solution considered is the “multiscale” composite which consists in a fiber reinforced composite with the epoxy matrix is filled by properly chosen carbon nanotubes. The defined solution allows to avoid relevant modifies to manufacturing process, and the final composite has been verified to improve passive damping withstanding its mechanical performances. Paragraph 7.2 reports the mechanical characterization of a symmetric and balanced laminated , stacking sequence is  $(0/45/90/-45)_{sym}$ , based upon this architecture where the matrix load is 1% of the overall resin weight, the addition of such a small quantity of filler influences only the material strength and the interlaminar strength, whereas the elastic modulus does not changes.

### 7.3.1 Large scale component specification

The most important structural component of an aircraft, namely the wings, the fuselage and the empennage, based on stress analysis can be considered as a bending beam. In particular in the case of a modern fuselage a key structural component are the stiffened plates constituting a fuselage barrel.

The simplest structural component valuable for aeronautical application undoubtedly is a stiffened plate, in fact its mechanical performance is primary for the structure, moreover this components has the further function of insulating the internal cabin from external noise and vibration. The basic large scale considered to verify if the material architecture respects all the requirements at the industrial scale is a stiffened plane plate.

A plane plate was preferred since the most important structural properties is the bending strength which could be verified even on the plane structure, however the curved plate could be fabricated following the same process the only difference is the need of a curved

tool. The primary design load for an integrally stiffened panel is the compression axial load [31]. For preliminary design purpose, the primary axial load could be used for panel sizing. Figure 7- 7 reports the stiffened plate specifications. The plate dimensions are 1370 mm x 720 mm, the laminate stacking sequence is (0/45/90/-45)sym, each lamina consist of Hexcell G1157 dry preform with nominal thickness of 0.300 mm that is a laminate nominal final thickness of 2.40 mm.

Five “L-geometry” stiffeners have used for strengthen the plate, each stiffener has dimensions of 40mm x 40 mm with laminate stacking sequence of (0/45/0/90/-45)sym; an additive lamina oriented on the axial load direction is inserted to increment the overall buckling stiffness.

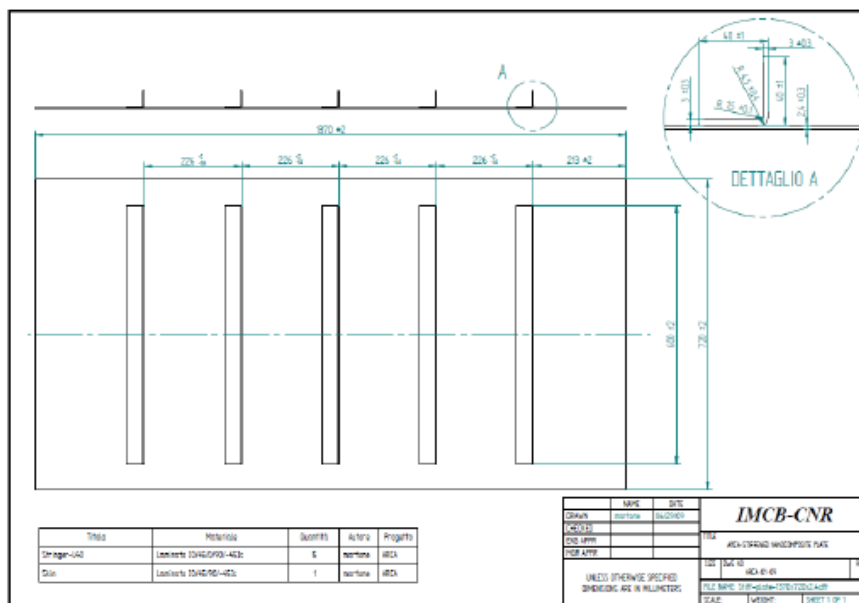


Figure 7- 7: Composite stiffened plate specifications

A preliminary prediction of the critical load could be executed by considering the equivalent isotropic solid to the composite shell, this value could not describe efficiently the mechanical behaviour of the composite plate but could indicate a first failure load qualitative estimation for the considered plate.

The effective width of skin is the portion supported by a stringer in a skin-stringer construction that does not buckle when subject to axial compression load. The collapsing load for a stiffened plate could be evaluated as sum of the critical loads for each stiffeners

$$P_c = \sigma_c [n A_c + (n - 1) 2 c t]$$

Where  $A_c$  is the section of the stringers,  $c$  the effective width,  $t$  the plate thickness.

The critical stress for each stringer is evaluated by an iterative procedure where the effective width is guessed starting from the Von Karman expression

$$c = 0.95 t \sqrt{\frac{E}{\sigma_r}}$$

at each iteration the critical Euler stress as buckling value for stringers, as measured the tensile modulus it is assumed as 45 GPa. The von Karman law requires as tension the limit of material linear behaviour, since composites have a linear behaviour until the failure as limiting stress is assumed 400 MPa.

In the next step, effective width is evaluated according to the following formula:

$$c = \frac{b}{4} \left( 1 + \frac{\sigma_c}{\sigma_r} \right)$$

In the present case a compressive preliminary load of 17300 daN is expected, although this value it is an estimation of the first ply failure load and probably the panel could carry on a greater load, the stiffener section is incremented in order to sustain at least a load of 24000 daN. The final dimension for stringer section was thus assumed to be 150 mm x 40 mm.

It may be remarked that this is only a preliminary evaluation of the compression load in fact composites mechanical behaviour depends on interlaminar stresses distribution the axial load could be non separated by the shear effects within material. Furthermore the analysis of a bending stiffened plate could be led following the same principles but the compressed section could be separated from section under axial tensile load.

### 7.3.2 Manufacturing

A three step manufacturing procedure was followed for manufacturing the hybrid stiffened composite plate. First the required amount of carbon nanotubes are dispersed within the hosting Hexcell RTM6 resin. The dry preforms cut according to material lay-out are stacked upon the preheated tool and infused. At the end stringers are bonded to the structure. The Figure 7- 8 shows the tool in its components, a stringer is manufactured monolithically with the base panel.

A critical factor for the infusion process is the temperature control, in fact both the resin progress within the preform and the curing phase are dependent on the tool temperature, as viscosity changes in reason of the temperature which the resin system is hold, Figure 7- 1. The tool is heated by a series of electrical resistances automatically controlled by an

homemade system, the system consists in a series of solid state power relays and modular controllers colligated to a computer which aid to monitoring the tool status, Figure 7- 9 a). Figure 7- 9 b) shows the disposition of thermocouples upon the tool, red highlighted marker indicates the sensor mounted on the tool, which have a drive function in the system, the green highlighted marker indicate sensor measuring the system temperature positioned above the vacuum bag.

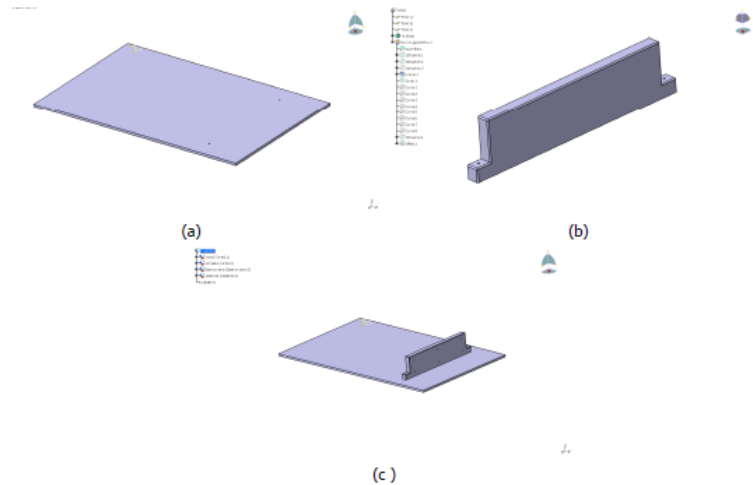


Figure 7- 8: Tool parts assembly

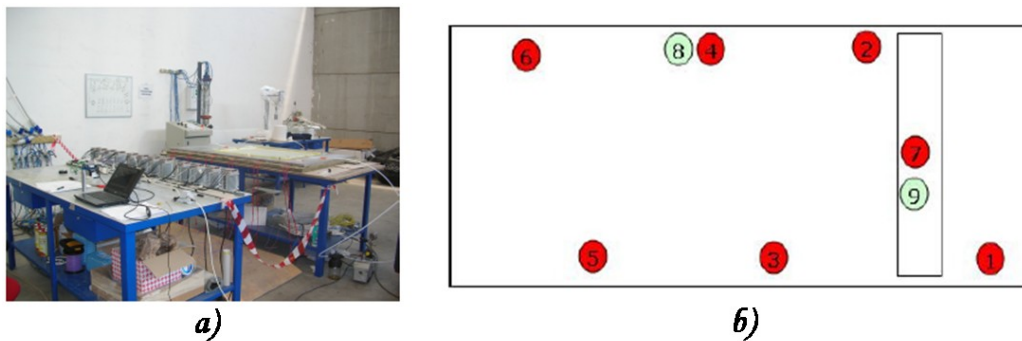


Figure 7- 9: Tool control system. a) A series of electrical resistances control the temperature, b) Thermocouples “J” monitor the tool temperature during the infusion process.

Figure 7- 10 illustrates the manufacturing phase for the second step of the process. The dry preforms are stacked upon the tool, a), the vacuum bag is and air vent arranged, b), then the nanoloaded resin is infused in the preform, c), and after the curing cycle the plate is demoulded, d). According to resin supplier instructions the curing cycle is in two step , the cure 1,30 hours at 160°C and the post-cure 2 hours at 180°C.

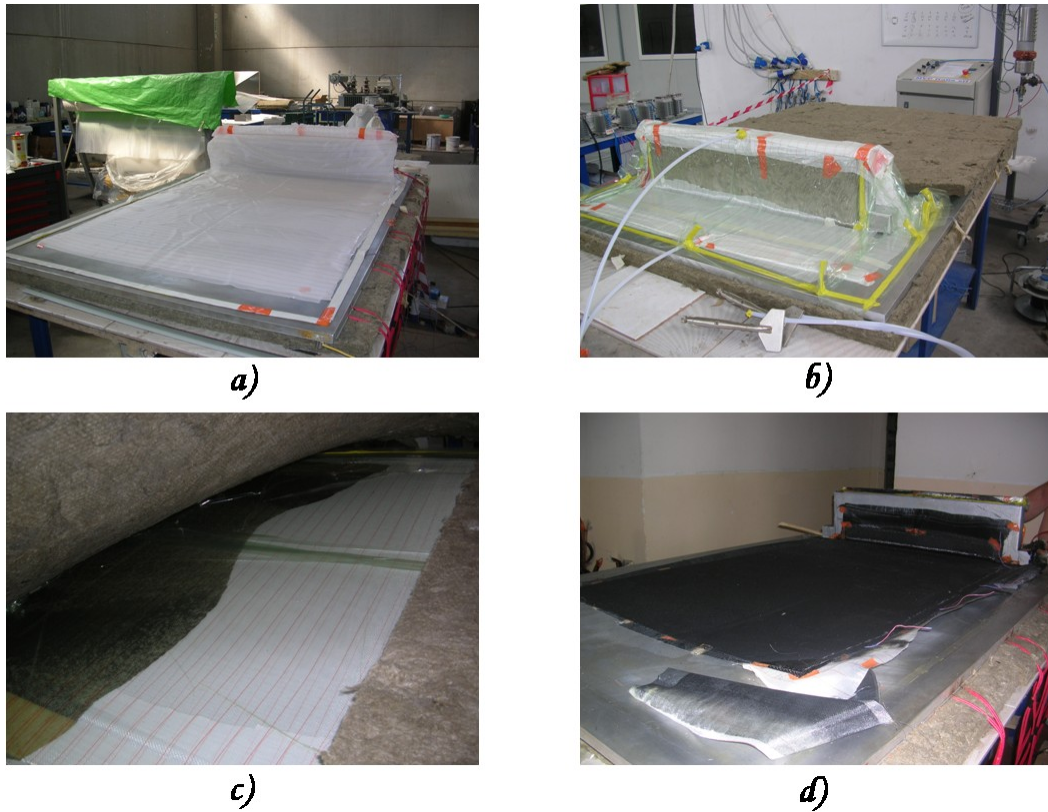


Figure 7-10: Manufacturing of the hybrid stiffened plate. a) stacking of the preform upon the tool, b) vacuum bag, c) resin progression within bag, d) final composite.

The base plate was fabricated with only one stiffener monolithic with the panels, other stiffener were manufactured on angular tool, as shown by the Figure 7- 11.

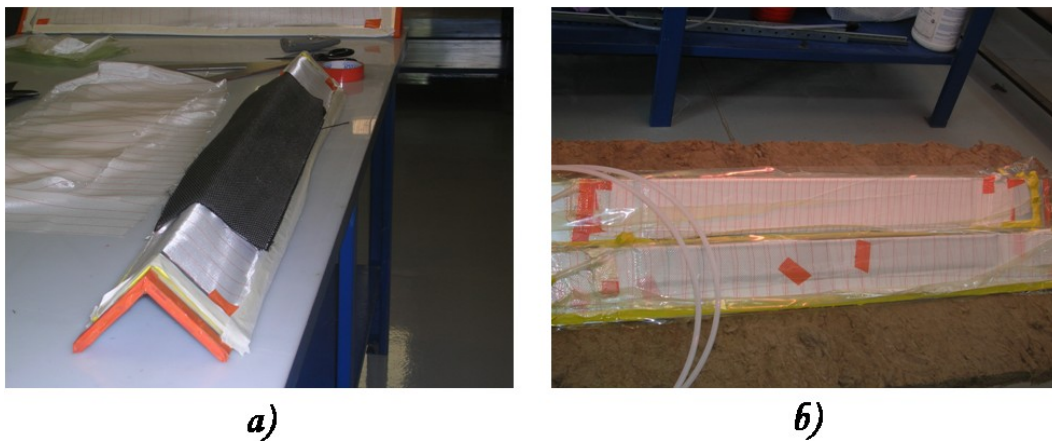


Figure 7- 11: Stringers manufacturing. a) Stacking of the preform, b) Vacuum bag

The stringers and the composite plate, finally, were bonded by the epoxy adhesive ARALDITE® 2011, under a negative pressure (-0.6 bar) applied by a vacuum bag and cured at room temperature for 24 hours.

Two composite plates have fabricated, one where the matrix is the neat RTM6 as baseline for testing, and another with nanoloaded resin as final sample.

The followings figures 7-12 and 7-13 shows the final plates, non hybrid and hybrid multiscale respectively.



Figure 7- 12: Final stiffened composite plate- baseline plate



Figure 7- 13: Final *multiscale* composite plate

## 7.4 Conclusions

The work described in this chapter relates to the scaling up technology for an industrial application of the study conducted on the damping properties of composites.

For verifying the feasibility of the hybridization technology proposed a simple but realistic component was chosen as prototype. Stiffened plate represents the base element for the main aeronautical components, as well as the wings, the fuselage and the empennage.

Since in most cases load condition is dominated by the compression phenomenon the sizing load for a stiffened plates is the axial compression.

The study addressed to examine the design according to an approach bottom-up, starting from each composite material constituents until the final laminate predicting its engineering constants, the final composite structure could be examined. Parallel to the static behaviour the damping behaviour of the composite material was studied, and the damping constant for each dimensional scales were identified.

The final design proposed tool allows a multidisciplinary analysis for hybrid materials which include special damping features.

Experimentally after the efficiency in damping enhancement due to the dispersion of carbon nanotubes in the resin system has been verified, the concept was applied to larger scale structures. Knowing that laminate passive damping is function of the material stacking sequence, in particular the lay-out arrangement could promote the raise of interlaminar stresses in bending structures improving the laminate damping. Before the design of a structural component, a plate with the selected architecture was manufactured and mechanically tested, in addition samples for further damping characterization were manufacturing.

Verified that the pre-process of the resin does not compromise the mechanical behaviour of the composite material, a simple composite structure was designed, the mechanical requirement to be satisfied is the capability to sustain at least 24000 daN typical compressive load for a stiffened plate for a commercial aircraft for long range missions.

The proper sizing of the component accounting for damage tolerance and post-buckling behaviour is beyond the aim of this study, so a preliminary sizing was done considering the equivalent material to the laminate by the engineering constants and the concept of effective width. The stringer geometry was chosen according to the simplicity of the tool because the aim is to prove the scaling up feasibility of the process, the final geometry is angular wide 150 mm and pitch of 40 mm.

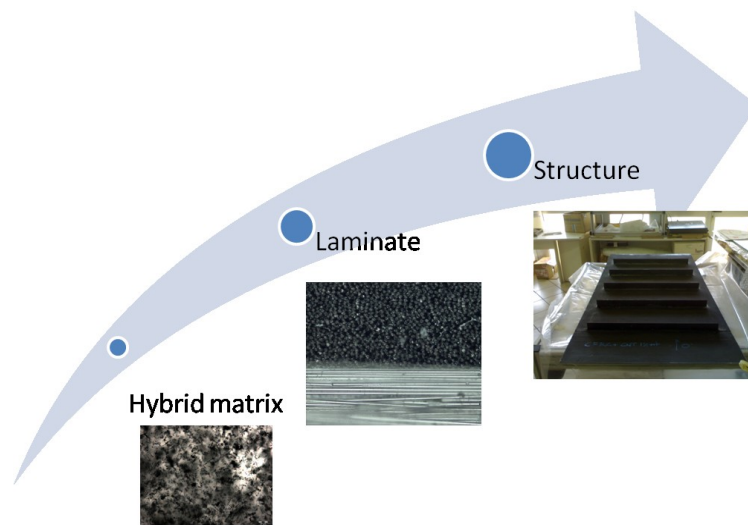


**Figure 7- 14: Multilevel composite structure**

The figure 7-14 shows the through the scale approach followed in the design of the final structure. Furthermore for each dimensional level has theoretical study with the aim of individuate or formulate where is not already available in literature, i.e. damping of carbon nanotubes, was conducted.

The proposed approach allows to cover both the requirement path, from final structure to material properties, and the multiscale design path, starting from constituents to the final composite structure. In addition the analysis could be entered at each intermediate level for propose other material features to take into account.

As future work acoustical test and buckling on the composite stiffened plate would be execute and the final correlation of data.



## 7.5 References

- [26]Campbell FC, 2006. Manufacturing Technology for Aerospace Structural Materials. *Elsevier*.
- [27]ASTM D3039. Standard test method for Tensile properties of polymer matrix composite materials. *ASTM International*.
- [28]ASTM D6272. Standard test method for Flexural properties of unreinforced and reinforced plastics and electrical insulating material by four point bending. *ASTM International*.
- [29]ASTM D6641. Standard test method for Determining the compressive properties of polymer matrix composite laminates using a combined loading compression (CLC) test fixture. *ASTM International*.
- [30]ASTM D2344. Standard test method for Short beam strength of polymer matrix composite materials and their laminates. *ASTM International*.
- [31]Niu CYM, 1992. Composite airframe structures—practical design information and data. *Hong Kong Conmilit Press*.
- [32]Herencia JE, Weaver PM, Friswell MI, 2008. Optimization of anisotropic composite panels with T-shaped stiffeners including transverse shear effects and out-of-plane loading. *Structure Multidisciplinary Optimization* 37.

# Conclusions

## 8.1 Final discussion

The current design technique is characterised by a sequential methodology, where structure optimization is primarily done with respect to the stiffness and the strength. The fulfilment of relevant functional requirements such as the thermal and the acoustical insulation is later addressed with weight penalties for the structure. Current state of the art of damping treatments uses viscoelastic polymer-based damping tapes, bonded externally to the vibrating structure, however these techniques incur significant weight and volume penalty.

An alternative to externally bonded damping tapes can be to engineer the damping properties into the material, a promising composite architecture embed a layer of viscoelastic material within the laminate. This research focused on the study of hybrid composite architectures able to enhance the material dissipative behaviour, nevertheless material may maintain its structural function.

The design of a typical aeronautical structure, such as a stiffened composite plate, represents a multi-disciplinary problem. The key features which a stiffness plate has to obey are the primary structural function, the vibroacoustic and the thermal requirements.

In this dissertation a study about the optimal material architecture has carried out accounting as design variables the damping and mechanical performances.

Through the study of damping mechanism at each dimensional scale three hybrid configuration were considered for improve the laminate damping, analytical study, confirmed by the experimental activities, identify as the most promising the pre-processing of composite hosting matrix by embedding low aspect ratio carbon nanotubes.

## 8.2 Contributions

In this dissertation the analysis of passive damping of composite materials were examined accounting the multiscale behaviour of composite structure. The work covered two main aspects. The numerical description of damping mechanism for composite materials by a “through-the-scale” analysis allows to propose hybrid architecture able to improve damping performance of the final composite. Experimentally the proposed architecture were manufactured and tested.

- The passive damping behaviour for a composite material was studied at each characteristic dimensional scale, in particular the homogenization of the composite properties was obtained through the definition of constitutive matrices describing the elastic and dissipative material behaviour, a composite laminate could be decomposed in its sub-components, the layers, and finally in their constituents, reinforcing fibres and hosting matrix.
- A hierarchical procedure for the evaluation of a multiscale hybrid composite is proposed. Starting from the lowest scale the hosting matrix filled by nanoloadings, the hybridization process raise up by means of the homogenised matrices at each level.
- An analytical design tool is proposed for the analysis of multi-functional materials that integrates high damping performances. The final damping of the examined structure will depends not only on the composite material architecture but even on the boundary condition influencing the energy component allocation within the structure.
- Composite material could be describe by its equivalent material by the engineering constant calculation, in line with this practise the equivalent dissipative material constants could be calculated, in particular by applying to simple structural elements boundary condition which induce only one energy component, the predicted loss factor is the damping constants associated to this component of equivalent material.
- The manufacturing technology selected for the experimental analysis is the Vacuum Assisted Resin Transfer Moulding, such as manufacturing process allows the fabrication of samples which components could be pre-processed before the infusion.

- Interleaved composites were manufactured by embedding Mobilon<sup>®</sup> sheets as a layer within the laminate, the passive damping is strongly improved, however the mechanical performance exhibits a great decrease.
- The manufacturing of hybrid preform was performed by a standard loom, viscoelastic fibres were arranged along carbon tow in the weaving creel. Two hybrid preform were manufactured, containing 5%vol and 10%vol. Composites manufactured with this preforms showed an enhancement on passive damping performance, but a detrimental effect was measured on the mechanical performances.
- The manufacturing of multiscale composites introduce a number of research item, first the state of dispersion of nano-filler within the hosting matrix, the definition of the filler content, the filler aspect ratio and the feasibility of the infusion process. The most efficient technique for the dispersion of carbon nanotubes is the ultrasonication. A sonication procedure, accounting the viscosity and curing behaviour of the epoxy system used, was developed.
- A study on the behaviour of carbon nanotubes based nanocomposites was conducted with the aim of understand the mechanical and dissipative behaviour of certain nanocomposites. The most important property identified for the optimal dispersion state within the hosting system is that filler would not exceed a physical threshold indicated as statistical percolation, above this content fillers tend to clustering then mechanical and dissipative features of the system decrement. In addition the filler aspect ratio (AR), apart from influencing on the statistical threshold, affects the damping performance, in fact filler choice could be tailored in function of the aspect ratio since high ARs promote mechanical enhancement while low AR enhance damping.
- Unidirectional “multiscale” composites exhibits the best performances, in fact in any case a decrement in mechanical performances was measured, moreover damping test for this composites indicated an increment in loss factor of about 40% at the interesting temperature for aeronautical applications.

The most promising architecture from tested was the multiscale composite material, which was selected for the manufacturing of the stiffened plate. This solution appears extremely suitable for industrial large scale application.

The stiffened plate was assumed plane, in fact the curvature would not add difficult to the argument, but requires only a more complex tool beyond the aim of this study.

In addition a plane plate of the composite employed was manufactured for mechanical characterization. Mechanical tests confirmed that the hybridization process of the composite does not decrease mechanical features. For a complete dynamic and acoustical characterization coupons for damping and transmission loss tests were manufactured.

Finally the stiffened plate will be acoustically tested and its buckling load will be measured. For baseline in the experimental analysis a stiffened plate without nanofiller was manufactured.

### **8.3 Future Work**

As described in previous sections, both experimental and computational efforts have been presented in the dissertation research. However, limited by the current manufacturing challenge and modelling challenges, there are still some limitations for the research.

- The mechanical behaviour of nanocomposites is based on short fiber modelling, but this kind of filler required more dedicated numerical tool. The carbon nanotubes have dimension comparable with the epoxy chain in the resin, in addition the re-aggregation above statistical threshold is a phenomenon not clearly defined.
- Although the ultrasonication is the better dispersion technique, its application is appropriate only for laboratory application. For large scale composite manufacturing needing higher resin volumes a more suitable dispersion technique may be individuated. A solution that is gaining popularity is the calendaring process, in this the nanofiller is dispersed within the laminate by high shear rates induced by rotating cylinders.
- The developed tool integrate only the mechanical analysis of composite materials in linear regime and the damping analysis, the introduction of more analytical tool, such as the fracture analysis, would improve the multidisciplinary analysis of final composites component

## 8.4 Academic publications

- [1] A.Martone, M.Giordano, “Multiscale modelling of hybrid structural composites with integrated damping features”-IV International Conference on Times of Polymers & Composites (TOP2008)
- [2] C. Formicola, A. Martone, M. Zarrelli, M.Giordano, “Dispersion of carbon nanotubes in a monocomponent epoxy system”-AIDIC 2008 Workshop on Nanomaterials Production Characterization and Their Industrial Application
- [3] A. Martone, C. Formicola, M. Zarrelli, M. Giordano, “Structural Damping Efficiency in Carbon Nanotubes/Monomponent Epoxy Nanocomposites” - AIDIC 2008 Workshop on Nanomaterials Production Characterization and Their Industrial Applications
- [4] A. Martone, M.Giordano, “Manufacturing and testing of a novel hybrid advanced composite laminate with increased damping performances” –Hybrid Materials 2009 First International Conference on Multifunctional Hybrid and Nanomaterial, Tours (France)
- [5] M. Giordano, V. Antonucci, M. Zarrelli, C. Formicola, A. Martone, G. Faiella, “Functional and structural properties of epoxy/nanotube composites” – EUROFILLER 2009, From macro to nanofillers for structural and functional polymer materials, Alessandria (TO)
- [6] C. Formicola, A. Martone, M. Zarrelli and M. Giordano, “Reinforcement Effect of Multi-Walled Carbon nanotube in sonicated monocomponent epoxy matrix nanocomposite” – ICCM17, 17th International Conference on Composite Materials, Edinburgh (UK)
- [7] A. Martone, M.Zarrelli, V.Antonucci, M. Giordano, “Manufacturing and testing of an hybrid composite integrating viscoelastic fibres” –ICCM17, 17th International Conference on Composite Materials, Edinburgh (UK)
- [8] C. Formicola, A. Martone, M. Zarrelli and M. Giordano, “Influence of dispersion and concentration of multi walled carbon nanotubes on the mechanical properties of monocomponent epoxy resin” –ICCM17, 17th International Conference on Composite Materials, Edinburgh (UK)
- [9] C. Formicola, A. Martone, M. Zarrelli and M. Giordano, “Reinforcing efficiency of different aspect ratio Carbon Nanotube/Epoxy composites” –CNTComp 09, 4th International Conference on Carbon Based Nanocomposites, Hamburg (Germany)